THE IMPACT OF SURFACE TEXTURE AND WIND ON CONVECTIVE HEAT
TRANSFER FROM BUILDING FAÇADES

A THESIS SUBMITTED TO
THE GRADUATE SCHOOL OF NATURAL AND APPLIED SCIENCES
OF
MIDDLE EAST TECHNICAL UNIVERSITY

BY

NECİL ÖZTÜREL

IN PARTIAL FULLFILMENT OF THE REQUIREMENTS
FOR
THE DEGREE OF DOCTOR OF PHILOSOPHY
IN
BUILDING SCIENCE IN ARCHITECTURE

SEPTEMBER 2013

Approval of the thesis:

THE IMPACT OF SURFACE TEXTURE AND WIND ON CONVECTIVE HEAT TRANSFER FROM BUILDING FAÇADES

submitted by **NECİL ÖZTÜREL** in partial fulfillment of the requirements for the degree of **Doctor of Philosophy in Department of Architecture, Middle East Technical University** by,

Prof. Dr. Canan Özgen
Dean, **Graduate School of Natural and Applied Sciences**   _____

Assoc. Prof. Dr. Güven Arif Sargın
Head of Department, **Architecture**   _____

Assoc. Prof. Dr. Soofia Tahira EliasOzkan
Supervisor, **Dept. of Architecture**   _____

Examining Committee Members:

Prof. Dr. Gülser Çelebi
Dept. of Architecture, Gazi University   _____

Assoc. Prof. Dr. Soofia Tahira Elias Ozkan
Dept. of Architecture, METU   _____

Prof. Dr. Vacit İmamoğlu
Dept. of Architecture, METU   _____

Prof. Dr. İbrahim Günal
Dept. of Physics, METU   _____

Assoc. Prof. Dr. Oğuz Uzol
Dept. of Aerospace Engineering, METU   _____

Date: 11 September 2013

I hereby declare that all information in this document has been obtained and presented in accordance with academic riles and ethical conduct. I also declare that, as required by these rules and conduct, I have fully cited and referenced all material and results that are not original to this work.

Name, Last Name : NECİL ÖZTÜREL

Signature   :

ABSTRACT

THE IMPACT OF SURFACE TEXTURE AND WIND ON CONVECTIVE HEAT TRANSFER FROM BUILDING FAÇADES

Öztürel, Necil

Ph.D., in Building Science, Department of Architecture
Supervisor: Assoc. Prof. Dr. Soofia Tahira Elias Ozkan

September 2013, 121 pages

In this study, the impact of the surface texture of finishing materials and wind conditions on heat loss from the building's facade are investigated. Three sets of samples (Set A, B and C) are tested and observed under varying wind speeds and varying wind angles in a wind tunnel. Both Sets A and B are composed of seven samples each, all having different surface textures. Set A samples were prepared from gypsum plaster and Set B samples from cement plaster mix. Set C consists of five different samples of conventional building materials (porcelain coated clay tile, travertine, marble, andesite and acrylic resin based composite siding material) with proprietary surface textures. Findings of the experiments are used in calculations within the introduced mathematical model where Roughness Index (RI) values for the sample surface textures are integrated and a set of convective heat transfer coefficient (h) and time constant (τ) values are presented for each sample. Correlation of these h values with the wind speed is investigated. It is found that variation in surface texture results in substantial deviations in h for varying wind profiles. The effect of surface texture of abovementioned materials and wind on h and τ is presented in comparative reference tables that can be used in further calculations of building energy fluxes.

Keywords: Surface Texture, Building Materials, Wind, Convective Heat Transfer Coefficient, Time Constant

ÖZ

YÜZEY DOKUSU VE RÜZGARIN BİNA CEPHELERİNDE KONVEKTİF ISI TRANSFERİ ÜZERİNDEKİ ETKİSİ

Öztürel, Necil

Doktora, Yapı Bilimleri, Mimarlık Bölümü
Tez Yöneticisi: Doç. Dr. Soofia Tahira Elias Ozkan

Eylül 2013, 121 sayfa

Bu çalışmada, bina cephelerinde kullanılan yapı malzemelerinin yüzey dokusu ve rüzgarın ısı kayıplarına etkileri incelenmektedir. Üç örnek seti (Set A, B ve C) farklı rüzgar hızı ve rüzgar açıları ile bir rüzgar tünelinde test edilmiş ve gözlenmiştir. A ve B örnek setlerinin her biri farklı yüzey dokuları olan yedi örnekten oluşmaktadır. A Seti örnekleri alçıdan, B seti örnekleri ise çimento sıvasından hazırlanmıştır. C seti örnekleri gerçek hayatta bina cephesine uygulandıkları halleri ve imal edildikleri yüzey dokuları ile beş farklı yapı malzemesi örneğinden oluşmaktadır (porselen kaplamalı kil karo, traverten, mermer, andezit ve akrilik reçine esaslı kompozit kaplama malzemesi). Deneylerin bulguları, örnek yüzeylerin Pürüzlülük İndeksi (*RI*) değerlerinin entegre olduğu bir matematik model ile hesaplamalarda kullanılarak her bir örnek için konvektif ısı taşınım katsayısı (*h*) ve zaman sabiti (τ) değerleri bulunmuştur. Bulunan *h* değerleri ile kullanılan farklı rüzgar hızları arasındaki korelasyon incelenmiştir. Farklı yüzey dokularının *h* değerlerinde değişen rüzgar profilleri için önemli değişikliklere sebep olduğu saptanmıştır. Yukarıda belirtilen yapı malzemelerin yüzey dokularının *h* üzerindeki etkisi, bina enerji akışlarının hesaplanmasında kullanılabilecek karşılaştırmalı referans tablolar ile sunulmuştur.

Anahtar Kelimeler: Yüzey Dokusu, Yapı Malzemesi, Rüzgar, Konvektif Isı Taşınım Katsayısı, Zaman Sabiti

To My Beloved Wife and Son

ACKNOWLEDGEMENTS

TABLE OF CONTENTS

LIST OF TABLES

LIST OF FIGURES

FIGURES

LIST OF ABBREVIATIONS

A_s	Surface Area
$A_{textured}$	Surface Area of the Textured Body
$A_{uniform}$	Surface Area of the Uniform Base of the Body Without Texture
ANSI	American National Standards Institute
c	Specific Heat
CFD	Computational Fluid Dynamics
CHTC	Convective Heat Transfer Coefficient
CSF	Concrete Surface Profiles
GPS	Geometrical Product Specification
h	Convective Heat Transfer Coefficient
$H_{uniform}$	Height of the Uniform Body
$H_{textured}$	Height of the Textured Body
ISO	International Organization for Standardization
LRA	Laser Roughness Analyzer
PDL	Processing Digital Images
ρ	Density
RI	Roughness Index
RUZGEM	Rüzgar Enerjisi Teknolojileri Araştırma ve Uygulama Merkezi
τ	Thermal Constant
T	Surface Temperature
T_∞	Ambient Temperature
V	Volume

CHAPTER 1

INTRODUCTION

The overall heat loss of a building is directly effected by the wind characteristics and the surface texture of the building materials that are being used at the building facades. The purpose of this thesis is to reveal the behavior of the overall heat loss of a building by evaluating the effects of the wind and the surface texture of the building materials. To accomplish this, in this thesis materials that are used in building facades that are having characteristic surface textures are tested under wind with direction and speed being changed in a wind tunnel simulation.

In this chapter, the motivation for studying the effects of wind in heat loss of a building as being dependent on the material and texture are presented in Section 1.1. Respectively, Section 1.2 aims in conducting this research in correlation with the arguments are summarized. Then, the experimental procedure is overviewed in Section 1.3. Finally, this chapter concludes by presenting the disposition of this thesis in Section 1.4.

1.1. Argument

Thermal performance of a building is strongly influenced by the microclimate that surrounds it as an envelope. The variables of this microclimate include the surrounding ambient air temperature, solar radiation and wind flow (Lunde, 1980). Therefore, in design of built environment, building facade structure, which roughly defines the outlook of a building, is effected by these variables. In parallel, wind has a non-negligible fundamental influence and importance on the thermal performance and heat losses of the building.

Notably thermal comfort of a building is also effected from heat losses. The research on thermal comfort, which analyses and relates design of buildings on physical and psychological impacts on its occupants regarding the thermal mechanics of the structure, is one of the major concerns of building science. Thus, in this thesis representations of thermal mechanics of buildings will be investigated from a broader perspective, where its narrower implications on the occupants are left beyond the scope. Although, existing models of the literature on thermal comfort provide an essential ground for studying factors that effect thermal comfort of the environment in terms of thermal sensations, they cannot account for the direct relation between thermal mechanics of the building and thermal comfort of individuals (Cheng et al., 2012 p.20). Hence, the argument, which will be presented here, is related with thermal comfort in a broader sense, yet in this scope the research of this thesis is not limited with localized parameters that are involved in thermal comfort models.

Before elaborating these effects that are related with wind it is essential to overview how total energy of a building is defined so that the argument related with possible

contributions of wind effect on thermal performance can become clear. Total energy of a building can be described over the energy that is gained and the energy that is lost. A building can usually gain energy through the building heating system as it generates heat and also through exposition to natural energy sources such as the solar energy (Duffie & Beckman, 2006). Regarding the total energy of a building, these two means of energy gain can be explicitly controlled. Specifically, first component can be easily controlled by conventional methods that are provided by modern heating systems. Likewise, energy gained from the sun can be controlled through some of the design parameters of the building such as orientation of the building and the walls relative to the sun, preference of using shadings, type and size of the windows and the structure and type of the material that is being used for the glazing.

For a building, energy loss is mainly through conduction, radiation, ventilation and infiltration (Duffie & Beckman, 2006). Heat loss from a building to exterior by conduction is the heat transfer through the building materials that are in touch with each other. Secondly, a body that is heated radiates energy as in the form of electromagnetic waves, thus when the concept is applied to buildings' thermal mechanism it is said to radiate heat. On the other hand, infiltration is usually caused by the leakage of indoor air through the doors and fenestration structures to outdoor. On the purpose of refreshing indoor air for comfort purposes ventilation is used. Ventilation may cause exhaust of some portion of the indoor air to exterior and intake of outdoor air within the building. This process of ventilation and infiltration results with heat loss through the outgoing indoor air. All these factors that are used in defining a buildings thermal performance for both energy gain and loss are studied all together and each and every factor contributes to the overall energy balance as a coefficient.

Although energy gain can be controlled as it is specified above, preservation of the energy is mainly dependent on controlling its loss. In this thesis it will be argued that one of the important factors that is dominant in the heat losses of a building is the material used at the building facades. This is because the surface structure of the facade materials, which can be broadly referred as the '*surface texture*', plays a direct role on the building heat loss. Herein, surface texture is argued to be contributing to the preservation of the energy, since it is the layer of the building that is being directly exposed to the outer environment. One of the major environmental factors that have a considerable influence on the outer shell boundary layer of the building is the wind. As being said, the surface texture of the building materials used as the building facade is directly expected to effect the overall heat loss of the building. Hence, it is plausible to work out the details of the relation between the choice of surface texture and the wind to investigate their effects on heat losses of a building.

Accordingly, surface texture and wind should be treated together. In general, there are two possible ways to analyze the interaction between wind and the surface texture of a building facade with the overall heat loss of the building. One is the numerical approach, and the other is the experimental. Numerical approach can be achieved through computerized mathematical simulations (Grimmond et al., 2011; Liu et al., 2013; Qu et al., 2012), whereas experimental approach can be conducted through a wind tunnel simulation (Nottrott et al., 2011; Rowley et al., 1930; Rowley & Eckley, 1932; Smith, 2010).

Previous findings of the research on the field from both approaches also mainly underline the need of further examination on wind effects and surface texture to come up with a more detailed definition for the wind coefficient that is utilized in studying

the energy balance of buildings. The need for extensive data in order to obtain more precise convection coefficients that define the surface to outer air heat loss flux through convection is emphasized by Nottrott, Onomura, Inagaki, Kanda and Kleissl (2011, p. 3137). Also, Palyvos (2008, p. 807) extends this statement by proposing the need for further real experimental data and research on wind effect coefficient in order to assure that it will be generalized and error-free. Furthermore, Mirsadeghi, Costola, Blocken and Hensen (2013, p. 32) points out that surface texture is one of those factors on building heat loss among others such as sheltering, convection, building dimensions that is required to be worked on in further depth.

Specifically, the surface texture (being whether plane or rough) used for the building facade affects the convection layer that is adjacent to the surface. Therefore, it is expected to reduce the overall heat loss of a building by considerable amounts once the appropriate surface texture is selected for a building also taking the wind characteristics of the location. That is to say, effects of the wind on the heat loss of a building changes depending on the nature of the surface texture of the building material. Using the same material for the building facade, but changing the surface texture only from plane to rough (or reverse), the heat loss of the building under wind is expected to vary in a significant amount.

This specific relation between surface texture and preservation of heat loss through selection of the suitable material with relevant surface texture for building facade have also been presented to be potentially improving the conservation of energy within the building (Mirsadeghi et al., 2013 p. 29). For instance, numeric studies illustrate that choosing the material with proper surface texture roughness can hypothetically effect heat loss for amounts varying between 6 - 10 %. Other than that, this effect is observed to be rising up to 15 % when these hypotheses for urban outset are tested on computational simulations (Liu et al., 2013 p. 224). Hence, still these results have to be tested on an experimental environment in order to enhance the details of the behaviors of different types of surface textures under wind so that the effect of surface texture on heat losses can be demonstrated under windy conditions.

Moreover, choice of a particular surface texture is generally a matter of architectural design choice where perceptual aspect of surface material that is being used for surface of a building facade comes in play in accompaniment with aesthetic concerns such as coherence of the surface texture of the material being used in a buildings' facade with the environment that it is being constructed into (García et al., 2006 p. 121). Formally, although there is a severe variation in defining surface texture within the literature it is generally studied under two main classifications as being the micro-texture (variation in roughness between 1 μm - 0.5 mm) and macro-texture (variation in waviness between 0.5 mm – 50 mm), such a classification cannot account for the behavior of patterns on surface texture under wind (Santos & Júlio, 2013 p. 914). Therefore, it must be noted that an experimental research on the effect of surface textures with varying roughness and patterns on heat loss under wind will be valuable for filling these gaps of the domain, which will also be studied in this thesis.

Hereby, it is also crucial to further clarify what is meant by variation in surface texture within the context of this thesis in order to fully understand the effect under investigation and the methods that are employ to measure the variation among distinct textures. Surface texture as it is worked on in the literature is an umbrella concept that cannot be measured and quantified (Chi et al., 2005 p. 2). The geometrical specification of the surface is dependent on some of the characteristics that can define an overall profile for evaluating and measuring it implicitly. These intrinsic

characteristics are roughness, waviness and lay (or form). However, these characteristics of surface texture can be abstracted for different scales (such as metrology, topology, micro-level scale for studying surface finishing) and they will still be explanatory. Specifically, when describing building surface structure the scale that is used to define these characteristic becomes rather useless, since they will be either undershooting or overshooting the metrics of the scale that will be applicable for building face structure. Therefore, by its very nature the research that is conducted with this thesis is an exploratory one, since scale of the metrics for these surface texture feature characteristics lay in a mid-level.

Usually, in order to select and use an appropriate texture at the building facade no additional investment is required. Since only the surface would be treated once initially, the same material is only used with the desired surface texture. In most real life situations the savings in terms of heat loss that can be achieved by altering surface material of a building facade is neglected. Regarding the present wind data and announced wind maps (such as Meteoroloji Genel Müdürlüğü, 2002) architects and designers can benefit from these readily available references on local wind conditions to decide on the suitable surface material with desired texture to achieve efficient thermal performance on their designed buildings.

1.2. Objective

Regarding the argument and the gaps in the current knowledge that is presented in the previous section, it can be put forth that the relationship between the surface texture (variation in both roughness and patterns) of the material used for buildings' facade under wind and heat loss must be further examined. In accordance, aim and purpose of this thesis can be summarized as follows:

- To observe and determine the effect of surface texture, wind speed and wind direction (wind angle; the angle that the wind intercepts the surface) on heat loss under wind independently from the material type that is being used.
- To compare and contrast the effect of surface texture, wind speed and wind direction on heat loss under wind for different conventional building facade materials.
- To investigate the effect of several patterns (other than roughness) used on surface texture on heat loss under wind in a material independent manner and also for materials used at the building facades.
- To examine the collected data in order to detect possible significant differentiations between surface textures (depending on their roughness and/or patterns). This includes examining whether certain groupings for heat loss behaviors occur between textures.
- To gather a collection of experimental data for the heat loss behaviors of conventional building material samples.

1.3. Procedure

This thesis is designed to determine the effects of surface texture of the building materials under several wind speeds and directions on the heat loss of the building. The experimental framework is composed of a series of wind tunnel experiments. Through these experiments surface temperature, ambient temperature and ambient humidity is recorded where wind speeds and wind angles are set to the desired values for each specific experiment. Heated material samples are tested under different wind

speeds and varying wind angles while being left for cooling on a sample holder in the test chamber of the wind tunnel. An experimental setup is established by the integration of a blow type wind tunnel, data acquisition system, K-type thermocouple sensors and a PC. The experimental setup is located in RUZGEM Aerospace in Middle East Technical University and all experiments are conducted with this setup throughout June 2013.

Three sets of experiments are performed. First set of experiments are completed with samples having different surface textures that are made of the same material (gypsum) in order to have material independency in tests. Second set is conducted with samples of a different material (cement plaster mix) than the first set which has different surface textures but same as those of the first set. Third set is performed with conventional building material samples that are available on the market (porcelain coated clay tile, natural stone-travertine, natural stone-marble, natural stone-andesite and acrylic based composite siding material).

The reason why there are three sets of experiments is (a) it is first aimed to test the effect of surface texture while material type is being kept unchanged; (b) it is aimed to test applicability of the effects that are found for specific textures while material type also changes; and (c) it is aimed to test whether those effects that are found for selected surface textures that are used in previous two tests are also extendible for building materials that are frequently used in the market. Notably, all materials are not suitable for crafting various surface textures on them because of their physical disposition, therefore first set of experiments only use samples that are made from gypsum mix, since it is easy to shape and work with it. Accordingly, one of the most frequently used building material on the market that also can be easily crafted is cement plaster mix, thus it is the one that is selected for the second set of experiments. All other frequently used conventional building materials that are aimed to be tested can limitedly be crafted, hence they are grouped in the third set of experiments while being tested as they are manufactured.

Through all three sets of experiments first the wind speed is changed for predefined values and wind direction is kept constant. Then, wind direction is changed while wind speed is kept constant. In the evaluation of the surface texture effects and the heat transfer through the material, one of the main parameters is the surface temperature and changes of surface temperature under wind. This is because the energy flow through the building material is to be detected. For all test cases in all experiment sets samples are heated up to a predefined temperature and surface temperature of the sample is recorded by using four K-type thermocouples while it is being exposed to a wind with a predefined speed and direction until surface temperature of the sample reaches ambient temperature. Therefore, change in surface temperature and its rate of change is the metric for comparing the main effect. Lastly, empirical results that are obtained from all three set of experiments are analyzed to conclude on their temperature decrease trends.

1.4. Disposition

This thesis consists of five chapters including the introduction, which presents the argument of the thesis with support from the literature that entails significance of it, the aim and objectives of the study and a brief overview of the procedure that is adopted in experimentation. Following chapters of this thesis are organized as follows;

Chapter 2 overviews the relevant literature on characterization of what texture is and how it is defined, models on convective heat transfer and heat loss that are yield by previous numeric and experimental research.

Chapter 3 includes the methodology that is being utilized in experimentation and the set of experiments that are conducted. In this chapter variables that are being tested, detailed experimental procedure, preparation of the samples and all test cases are explicitly outlined.

Chapter 4 presents the empirical results of the experiments and analysis of these results in accordance with our hypotheses. In this section also the effects that are observed in all test cases are presented.

Chapter 5 reviews the main findings from experiments and proposes further implications of the results in correlation with a set of proposals to extend these findings for future research.

CHAPTER 2

LITERATURE REVIEW

In this chapter literature on convective heat transfer, which this thesis is grounded on, is overviewed. In section 2.1 relevant numerical modeling research and their experimental counterparts are reviewed in details. Consecutively, in section 2.2 literature on definition of roughness and textures are presented in accompaniment with a selected portion of research that focus on studying effects of these two concepts within the domain of convective heat transfer.

2.1. Convective Heat Transfer

In our era, in order to design buildings and to operate them readily available building energy simulation software and applications are used. Architects, engineers and others who get involved in the design process should benefit from these tools. These tools are being developed and advanced in parallel with the recent literature on building heat transfer. In general, these tools are grounded on basic theoretical principles of heat transfer in accompaniment with empirical findings of the literature. In this way, relevant energy flow processes of buildings can be captured, calculated and simulated on these applications.

When energy equilibriums within a building are concerned it can be stated that energy that is either lost or gained trough convection by a building is significant. To some extend, the effect of convection can triple the amount that other means contribute to energy loss or gain (Mirsadeghi et al., 2013). Therefore, it is a common practice to analyze convective energy fluxes while studying heat transfers that are related to a building, since it is a major factor. Accordingly, one of the substantial methods to calculate convective energy flux is to investigate convective heat transfer coefficient (CHTC). Therefore, calculations and simulations on building heat loss or gain can help to reduced and related to the research on convective heat transfer coefficients.

It is crucial to determine accurate heat transfer coefficients in order to come up with consistent and precise calculations of building heat transfer. Specifically, heat transfer coefficient for facade of a building is essential to characterize that buildings energy interaction with the surrounding exterior environment. Convective heat transfer coefficient and convective heat flux is related with the difference between the surface temperature of building facade and ambient temperature of the exterior environment under convection currents. Furthermore, when the concept convective heat flux, which

is a transient processes, is applied for building facades it will be definitive for describing the change in temperature of surface, while it converges to the temperature of the environment. Formally, convective heat flux can be defined with Equation 2.1 as it is excerpted from Incropera & de Witt (2011).

$$-hA_s(T - T_\infty) = \rho V c \frac{dT}{dt} \qquad (2.1)$$

Briefly, in Equation 2.1 h is the convective heat transfer coefficient, ρ is the density, V is the volume of the body, c is the specific heat, T is the surface temperature of the body, T_∞ is the ambient temperature, and $hA_s(T-T_\infty)$ is the convective heat flux. As it can also be observed from this formulization convective heat transfer coefficient is bound to numerous parameters, such as the geometry of the building, physical disposition of the surrounding of the building, position of the building, geometry of the facade of the building, wind speed and direction (Mirsadeghi et al., 2013). Therefore, it is a complex and difficult task to elicit and calculate the convective heat transfer coefficient.

In general, in order to calculate the convective heat transfer coefficient the research from the literature predominantly uses three distinctive methods. These methods can be listed as the analytic method, the numeric method and the experimental method. Within the literature analytic method is utilized for relevant specialized energy flow regimes of the building and for simplistic building geometries such as flat surfaces or cylindrical geometries. On the other hand, numeric methods like computational fluid dynamics (CFD) models are powerful for simulating building convective heat transfers. Particularly, experimental methods are used for measuring the relevant parameters and heat flows for certain environmental and building related conditions that can be used calculate convective heat transfer coefficients. In what follows, literature on two of the primary methodologies, namely numeric studies and experimental studies, on building heat transfer will be reviewed in details.

2.1.1. Numeric Studies

As it is mentioned earlier, numeric studies on heat transfer use specialized simulation software, which are grounded to numeric models of the processes that are involved in heat transfer, to calculate heat transfer coefficients. One of those numeric studies is the research conducted by Djunaedy, Hensen and Loomans (2005). In this study Djunaedy et al. (2005) focuses on a possible integration between readily available building energy simulation software that are currently in use and the computational fluid dynamics models. Djunaedy et al. (2005) point out that in order to obtain more accurate results in building heat transfer calculations over building energy simulation software these applications have to be coupled with findings from computational fluid dynamics models. In this way, it is argued that significant innovations can be introduced in building energy simulation software that are used for calculation of

building heat transfer coefficients.

As Djunaedy et al. (2005) pinpoint distinctive building energy simulation applications are characteristically implemented to carry out calculations for distinct parameters of building heat transfer, so they cannot provide holistic computations. The basis of Djunaedy et al. (2005) research is to integrate computational fluid dynamics models with these software for carrying out heat transfer calculations so that both holistic heat transfer computations for buildings and narrower scope computations for specific parameters can be carried out more accurately. In order to accomplish this Djunaedy et al. (2005) realize a case study. In this case study a test cell, which is a small-scaled building, in Bedfordshire, UK is analyzed with the proposed novel methodology. As a result of this case study, it is found that their novel methodology can predict the convective heat transfer coefficient for the test building more precisely from other methods of the literature, which supports the need for integration of computational fluid dynamics models with building energy simulation software.

In another research on simulations of heat transfer in atmospheric boundary layers Blocken, Stathopoulos and Carmeliet (2007) draw attention to ever-increasing utilization of computational fluid dynamics modeling methodology within the field. It is stated that this method has started to be applied to distinctive processes in this area of research and thus with their research it has been presented that findings from other methods and procedures, specifically analytic methods, that are used for calculating heat transfer can be further supported and improved with empirical findings from computational fluid dynamics methods.

As a follow up study, Blocken, Stathopoulos, Carmeliet and Hensen (2011) mainly concentrate on application of computational fluid dynamics in simulating windy environments that are surrounding the building in relation with thermal performance of buildings. This research mainly focuses on pedestrian environments that surround a building, effects of varying wind conditions on rain that drops to a buildings facade, convective heat transfer coefficients of building facades and effects of air pollution around a building. However, among those concerns Blocken et al. (2011)'s research on convective heat transfer coefficients of building facades is the most relevant one to the research conducted in this thesis.

In this research, for all four areas of focus that are mentioned above it is stated that both wind tunnel modeling methods that are composed of semi-empirical formulas and computational fluid dynamics modeling methods have their own practical and methodological advantages. However, computational fluid dynamics methods are stated to be comparatively disadvantageous to be utilized in research, since it has certain amount of complexity in its application, it brings in computational cost and verification and validation of the results that are delivered by it is costly. Blocken et al. (2011) also underline the necessity of prior knowledge on statistical meteorological information, aerodynamics and human comfort criteria to carry out any computation on wind effects. Among those prior necessities outcomes of computational fluid dynamics models and wind tunnel modeling research provides majority of the

9

necessary prior information on aerodynamics.

In order to conduct computational fluid dynamics and wind tunnel modeling Blocken et al. (2011) propose a two-step approach. Accordingly, first a qualitative research must be conducted to identify the root cause of the essential problems. Then, as a follow up accurate measurements must be carried out to concentrate on specific and specialized issues in order to revise the problems in question as a whole. Moreover, it is also stated that despite the rareness of onsite measurements within the field, application of computational fluid dynamics is increasingly gaining acceptance for studying wind effects. Furthermore, Blocken et al. (2011) underline the significance of calculation and determination of convective heat transfer coefficients for building facade surfaces although it is a complex and demanding process, since these coefficients are bound to a wide range of parameters such as wind speed, wind direction, surface roughness, surface texture, surface geometry, building geometry, surrounding topology and intensity of wind turbulence. In parallel, within the literature computational fluid dynamics studies on analysis of convective heat transfer coefficient of building facade surfaces are small in number, since it requires extremely high computational costs to be embedded in building energy simulation software.

Another crucial point that is put forth by Blocken et al. (2011) is that the validation research that is conducted for windward facades of a cubic building, which is the surface that is directly exposed to wind, by using computational fluid dynamics models that increases the accuracy of the results by 10 %. However, it is also pointed out that in order to construct computation fluid dynamics models for buildings with geometries other than cubic, there is a necessity for devising an advanced wind flow modeling. That is, computational fluid dynamics models are potent for improving the accuracy of calculations and predictions on building facade surface under wind for any building geometry if prior required knowledge and tools are developed. In general, to calculate convective heat transfer coefficients for building facade surfaces empirical formulations are being used, however it is stated that these methods can only provide rough estimations rather than precise results.

Likewise, Defraeye, Blocken and Carmeliet (2011a) focus on calculating convective heat transfer coefficient for building facade surfaces by using computation fluid dynamics as an alternative to conventional correlation models. This research is also conducted for a cubic building, where correlations that are computed are in between convective heat transfer coefficient of this building and wind that it is exposed to. Specifically, it also aimed to lower the computational costs while calculating convective heat transfer coefficient. Defraeye et al. (2011a) underline the fact that wind tunnel experimentations would enable the researcher to focus on detailed analyses of the phenomenon when compared to full-scale on site measurements. However, findings on convective heat transfer coefficients from wind tunnel experiments cannot be always applicable to real life context, since real life environments generally diverge from experimental conditions. Defraeye et al. (2011a), try to overcome these limitations by modeling windward and leeward surfaces of a specific building configuration using computational fluid dynamics. With this model it

is found that simulating the conditions for just test cases with two or three distinct wind speeds would be enough for devising a reliable convective heat transfer coefficient of leeward and windward wall surfaces for cubic buildings.

In another research by Dafraeye, Blocken and Carmeliet (2011b) a new calculation scheme is proposed to determine the convective heat transfer coefficients of surfaces of bluff bodies that are coarse and simplistic. Methods and parameters of previous studies that are used to find the convective heat transfer coefficients yield a 40 % difference in their results, whereas the new calculation scheme that is proposed by Dafraeye et al. (2011b) reduce the divergence of the results to 10 %. These values that are used in extensive and sophisticated engineering calculations have been improved to be more accurate and to be fitting more to the real world processes. Results that are found in this research is an indication for the necessity of cautious and detailed calculations on heat transfer coefficients for them to be utilized in further building engineering (which is rather computationally costly) or in heat transfer of building surroundings research.

Furhermore, Defraeye, Blocken and Carmeliet (2012) investigate computational fluid dynamics models on simulating heat transfer coefficients of building facades. It is put forth that with a customized wall function accurate estimations of heat transfer coefficients can be obtained. Defraeye et al. (2012) point out that computerized computational fluid dynamics simulations can deliver more precise results when compared with other standard modeling methods of heat transfer.

Accordingly, Mirsadeghi, Costola, Blocken and Hensen (2013) highlight the importance of accurately calculating convective heat transfer coefficients of building facades or roofs in order to precisely find the amount of heat lost and gained through convection by using simulation software. It is stressed on the complexity of carrying out calculations for convective heat transfer coefficients, since these are dependent on numerous parameters related with the structure of the building. Mirsadeghi et al. (2013) conduct comparative research on models and their assumptions that are used to estimate these convective heat transfer coefficients over a case study, in order to define uncertainties that are involved in these models. Each model that are currently in use within the literature have their own specific set of assumptions, thus they can only be used for a specific range of calculations. Therefore, architects that are benefiting from computational capabilities of readily available simulation software need to choose the right model for analyses in parallel with their interests. Apparently, model specific uncertainties can result in a maximum of 30 % deviation in annual total energy requirement consumptions calculations for a building (Mirsadeghi et al., 2013).

Within the scope of this study a variety of simulation software are investigated by Mirsadeghi et al. (2013), which are ESP-r, EnergyPlus, IES, IDA, TAS, TRNSYS and SUNREL. Each of these software adopt their own methodology to calculate convective heat transfer coefficients. Specifically, Mirsadeghi et al. (2013) point out that most of these tools are still unable to deliver accurate estimations for convective heat transfer coefficients of building facades, because of model driven uncertainties.

For instance, it is found that estimates that are gathered from all of these models for a simplistic cubic building can deviate from each other for 30 %. It is stated that these uncertainties can be minimized with utilization of high quality data that is explanatory about real world processes, which can be used for validating the results. However, it is underlined that most of the research within the literature is focused on bringing up novel models for carrying out numeric heat transfer calculations, rather than delivering reliable experimental data. Accordingly, Mirsadeghi et al. (2013) pinpoint the need for further well-defined and well-structured experimental data. In general, preceding research of the literature on simulation software does not publish the raw data that is adopted by these applications to compute heat transfer coefficients; therefore their accuracy and acceptability of the results that are delivered by them cannot be comparatively studied. Correspondingly, Mirsadeghi et al. (2013) question the reliability of the results on convective heat transfer coefficients that are calculated with these software.

Mirsadeghi et al. (2013) also criticize these models since they disregard the effect of surface texture on convective heat transfer coefficients. Empirically, because of this deficiency it is found that the heat transfer coefficients that are calculated with these models can deviate 10 % on average from their real values. For instance, particularly DOE-2 models deviates from real values for rough surfaces for up to 17 %. Thus, these findings underline the importance of further research on effects of surface roughness on convective heat transfer coefficients. Another crucial deficiency of all models as it is presented by Mirsadeghi et al. (2013) is that they assume an average convective heat transfer coefficient value for all types of surfaces. Overall, Mirsadeghi et al. (2013) propose to carry out further investigation on four variables, which are effects of buildings height, shadowing, natural and forced convection on convective heat transfer coefficients, in order to improve the accuracy of all models that are examined with a precise estimation model, while eliminating abovementioned causes of uncertainties in heat transfer calculations.

In this regard, Tavil (2004) also aims to advance simulation models with several extensions in order to calculate varying parameters that are not embedded within the simulation models. Moreover, to test whether human comfort criterion is also satisfied with these models, surface temperatures of the walls of the building that is being examined are also aimed to be calculated. Tavil (2004) use a version of DOE-2.1E simulation software that is upgraded by a company called EMPA (since only this version has the capability to calculate surface temperatures of walls) to implement and test the idea.

In this research, three different versions of two distinct wall types analyzed for Istanbul, Turkey. Herein, these samples are masonry walls made up of brick or concrete, whereas versions consist samples with no insulation, samples with only exterior insulation and samples with only interior insulation. While taking into consideration the legislations that are enforced by Turkish Government, calculations are carried on for a building with an area of 95 m^2 (9 m x 10.5 m). Internal surface temperature have been kept fixed at 21°C, while calculations are completed for

representative month of January and July (one being the maximum and the other being the minimum for heating and cooling energy requirements). These calculations are made with the aforementioned simulation software to investigate the thermal performance and thermal comfort of the building. For buildings with all samples heating and cooling loads are calculated and by using the local upgrade extension that is implemented to the simulation software by Tavil (2004) per hour interior and exterior surface temperatures for walls could also be calculated. Tavil (2004) specifically focus on the northern walls of the buildings in order to eliminate possible effects of radiation from sun on the calculations.

As a result, Tavil (2004) concludes that heating loads are more than cooling loads for all buildings that are examined. Particularly, heating loads of buildings with walls with no insulation is 28 % more than their cooling load per each year, whereas the difference between the heating loads and cooling loads of buildings with walls with insulation is less than this amount being approximately around 20 %. Furthermore, it is found that applying interior or exterior 5 cm of insulation on walls results in an energy saving of 42 % for concrete walls and an energy saving of 37 % for brick walls. Besides these results, the significance of the research conducted by Tavil (2004) is in its methodology. As it is also advised by other research groups of the field Tavil (2004) benefits from multiple parameters in its calculations by upgrading the simulation software to acquire a better characteristic of the real life phenomena, while increasing the accuracy of the results.

Simulation software and their underlying models are also used for studying internal heat transfer processes. Such as, Beausoleil-Morrison (2001) is a one of the significant works in literature that tries to combine findings from experimental research on convective heat transfer in a numerical model by using an ESP-r simulation program. Specifically, models that Beausoleil-Morrison (2001) focus on only includes heat transfer within internal areas of a building. In this research internal heat transfer methods of the literature are analyzed according to their efficiencies in order to come up with a novel methodology that can account for the internal surface convection over characteristic flow regimes. The model for internal surface convection that Beausoleil-Morrison (2001) puts forth can capture effects of mixed flow regimes on heat transfers while being distinctive from its precursors.

In fact, scope of heat transfer research cannot be limited with its application to standalone buildings. Within the literate numeric research on heat transfer within urbanized areas is also available. For example, Qu, Milliez, Musson-Genon, Carissimo (2012) analyze buildings thermal influence on each other in urban areas for low wind speeds while shadowing is also taken into consideration. The significance of this research is its utilization of an experimental data set in the validation of the outcome. The data set that is used for validation is the Mock Urban Setting Test (MUST). Detailed information on building facade temperature and wind is used to reveal the effect of convective flow on building facade. Results of Qu et al. (2012) indicate that thermal stratification on building facade has a significant effect on wind flow regimes. Furthermore, it has been found that building facade temperature and its vertical

alternation is notably sensitive to changes in physical parameters of the surface. For instance, a change in one of the simplistic physical characteristics building facade, its color, from black to white can result in a change in surface temperature for up to 2°C. Consequently, thermal flow on the building facade is found to be alternating for varying urban conditions. Qu et al. (2012) state that if a building is positioned in an urbanized area, then shadowing effects, multi-reflections and infrared emissions that are present in urban areas will cause a non-uniform and asymmetrical trend in cooling of building facade. Particularly, for leeward wall surfaces this effect causes a maximum of 2°C change in surface temperature and 0.3 m/s flow over the wall. Qu et al. (2012) clearly define that variation in exterior building facade causes noticeable and measurable differences in exterior surface temperature of the building.

Subsequently, Liu, Srebric and Yu (2013) present a numerical simulation on external convective heat transfer coefficients of building arrays. Within the scope of this work, windward, leeward, lateral and top building surfaces are investigated in order to estimate a heat transfer coefficient for all these surfaces. Particularly, regular arrays that are composed of cubic buildings are used to represent the urban environment and convective heat transfer coefficients for these cubic bodies are simulated over this representation. Furthermore, simulations are carried for varying urban plan densities (for values of 0.44, 0.25, 0.16, 0.11, 0.063 and 0.04 as a morphological parameter), which yielded distinctive representations of the urban environment.

One of the most significant outcomes of Liu et al. (2013) is the observation that increasing urban plan area densities results in an increase in convective heat transfer coefficient of leeward surfaces, whereas it results in a decrease in convective heat transfer coefficient of lateral surfaces. Increase in convective heat transfer coefficient of leeward surfaces is calculated to be 15 % maximum and decrease in the value of convective heat transfer coefficient of lateral surfaces is observed to be 16 % maximum. For this reason, Liu et al. (2013) conclude that in order to accurately estimate or calculate convective heat transfer coefficients for buildings within urban areas, urban plan area densities has to be taken into consideration within heat transfer analyses. Liu et al. (2013) also extend this modeling and simulation research for varying wind speeds. It is also found that varying urban area plan densities gives rise to distinctive wind flow regimes, all of which directly effects convective heat transfer coefficients for surfaces of individual buildings within the urban areas. Furthermore, results that are delivered by this numerical study are also validated with measurements from experimentation. Liu et al. (2013) report that heat transfer coefficients conform the data from experimental studies by 10 % on average.

Distinctively, Grimmond et al. (2011) is a global urban energy balance model comparison research. The findings of this international project are presented in Grimmond et al. (2011). Within the scope of this project 25 research teams from different countries work in collaboration with their own energy simulation models by using data set for 32 different urban land surface schemes, each of which consists of data for 16-month periods. Grimmond et al. (2011) is the first large-scale systematic global research that is conducted for assessing and evaluating models that are devised

for examining urban surfaces and relevant energy exchange processes.

The main aim of this research is to evaluate the average performances of distinct frequently used models in order to present how applicable they are to examine urban energy balance fluxes. Another aim of this research is to investigate performances of the models that are similar in characteristics and complexity, where results of this investigation can contribute for further developments of these models. The method that is used to complete this evaluation is to incrementally provide increasing amount of information to the research teams in four stages, where in each stage results that are gathered from each and every model is compared. For the first stage, only simplistic meteorological data and the coordinates of the sites that are going to be investigated by the research teams are delivered to them. Successively, in the second stage plan area fractions for the sites that will be investigated are delivered to the research teams. In the third stage, additional detailed information on plan area fractions and supplementary information on vegetation of the site are supplied to the research teams. Finally, for the last stage research teams gathered enriched information on characteristics of the buildings (such as the materials used in construction) that are on the sites under investigation.

As a result of the comparison, Grimmond et al. (2011) conclude that for accurate results researchers have to use more than one simulation models that are suitable for the problem in accompaniment with each other, rather than just using one of the models in simulations and analyses. This is because, holistic energy systems cannot be solely captured with a single model, since each simulation model has their unique characteristics on capturing a portion of the whole system. Considering the methodology that is adopted by Grimmond et al. (2011), these findings are significant and valuable for defining the accurate methodology for the research framework on heat transfer modeling.

Findings from modeling research can also be applied for practical real-life concerns such as cooling a building. For instance, in a research by Santamouris and Kolokotsa (2013) passive cooling techniques on buildings and building-like structures are examined. It is state that building sector occupies a significantly large portion within the global economy that can be quantified as a top of 3 trillion US dollars. Hence, energy that is used within the building sector is more than that of the energy used by other sectors that play a central role in global economy. Taken this economic fact into account Santamouris and Kolokotsa (2013) emphasize that passive cooling techniques can contribute greatly to energy savings of the building sector, therefore they examine various building passive cooling techniques to compare and contrast their effectiveness.

These passive cooling techniques that are investigated in this research are evaporative cooling, earth cooling and various types of ventilation. However, Santamouris and Kolokotsa (2013) do not include factors like type of the building material used in construction or building facade in their analysis. It is determined that utilization of passive cooling techniques in buildings can result in a maximum of 70 % energy

saving. Moreover, it is also concluded that implementation of passive cooling techniques in building also results in proper development of the surrounding of the building. Therefore, Santamouris and Kolokotsa (2013) propose that there is a need for further research on passive cooling techniques in order to enrich the methodology for their application and implementation.

Correspondingly, Allegrini, Dorer and Carmeliet (2012) analyze heat transfer between buildings that are positioned on street canyons in order to investigate cooling requirements of buildings in urban areas. Heat transfer coefficients for building facades are calculated and their effect on buildings cooling trends have been examined. Within this research, Allegrini et al. (2012) carried out analysis for individual single buildings and for buildings that lay on streets canyons with differing sizes. These results for standalone buildings and for street canyon buildings are then compared and contrasted with each other.

In order to test the effects seven different building geometries and building areas plans have been used. These geometries are obtained by altering dimensions of the standalone buildings or length and width of street canyons. For these distinct geometries correlations for heat transfer coefficients of windward and leeward walls of buildings are analyzed. The analysis is also extended for varying building geometries and differing street canyon aspect ratios by using computational fluid dynamics. Moreover, the correlations for heat transfer coefficients are also carried out for varying wind speeds, whereas the wind angle is kept fixed to be perpendicular to standalone buildings and to street canyons.

As a result of this analysis it has been found that building façade surface temperatures of buildings that are positioned on street canyons are more than that of individual standalone buildings for all conditions. Accordingly, Allegrini et al. (2012) report that this difference causes convective heat transfer coefficients of buildings that are in urban areas to be lower than standalone buildings that are positioned in rural areas. This is because buildings that are constructed within urban areas are exposed to radiation from surrounding buildings, which causes an increase in surface temperature on their facade. Moreover, it has been found that the difference between surface temperatures of building facade is observable to be the most at the first floor of the building. It has also been observed a decrease in the effect of surrounding buildings on increase in surface temperature of building facade for higher floors such as the second or the third. Overall, Allegrini et al. (2012) emphasize that utilizing real building geometries and wind conditions in calculating correlation is essential in order to accurately predict cooling needs and peak cooling load for buildings. Furthermore, it has been found that cooling needs of buildings that are positioned on street canyons are 1.8 times greater than cooling needs of standalone buildings.

2.1.2. Experimental Studies

In order to carry out validations over the findings of the numerical research on heat transfer, data sets from experimental studies are required. In parallel, Desta, Langmans

and Roels (2011) is a research that aims to compile such a dataset for heat, air and moisture (HAM) modeling, which will be representative of real life conditions. Experiments are conducted on a full-scale and lightweight building, which is the VLIET test building located at Leuven, Belgium. This building is constructed for the purpose of analyzing hygrothermal behaviors under prevailing climatic conditions. The test building is composed of several compartments and the data from this building is gathered from southwest and northeast facades of an isolated compartment. This compartment, which is a representative room, has the dimensions of 6.5 m x 1.8 m x 2.68 m. The insulation of this compartment consists of insulation of all its walls, its ceiling and its floor except its northeast facade against air flow and evaporation. Hence, the northeast wall of the compartment, which has no insulation, is the test wall for all measurements.

In the experiments that are conducted by Desta et al. (2011) between 7 October 2008 and 30 April 2010 55 thermocouples, 18 humidity sensors and 12 heat flux sensors are placed on the walls as its designed by their experimental procedure. These sensors are placed in the center of the walls of the compartment while they are 45 cm farther away from the ceiling and the floor. On the other hand, external weather conditions are measured and detected with a weather station. For the data to be further used in validations, material specifications for all the materials used in the test building are measured and they are also presented by Desta et al. (2011) along with the detailed technical specifications of the tools that are used in the experimental setup. The resulting dataset is valuable for HAM modelers, since it is effective for advancing existing HAM models and validating results that are obtained from them. However, the dataset by Desta et al. (2011) also exhibit some limitations. For instance, since the dataset is designed to validate diffusive convective transport processes, it cannot account for a complete description of the effect of radiation on the test wall. Those limitations of the dataset must be further taken into consideration if the dataset is intended to be used for validation.

Correspondingly, Palyvos (2008) reviews all formulations and values of convective heat transfer coefficient of building facades that is bound to wind speed and wind angle, from the literature on building heat transfer. This review aims to provide a collection of current knowledge on heat transfer through convection from building facade to architects, designers and others who carry out building energy calculations using simulation software. Since Palyvos (2008) is an extensive review, it serves as a comprehensive reference for researcher or practitioners of convective heat transfer. Palyvos (2008) also presents some baseline formulas for calculations of heat transfer on leeward and windward surface by combining the state-of-the-art knowledge. However, although these formulas can be applied for general-purpose calculations, those deliver coarse averages.

Another dataset compilation research, which is specialized locally for Turkey, is by Meteoroloji İşleri Genel Müdürlüğü. In order to make wind related data, which is defining for regional or local wind flows, available for public use Meteoroloji İşleri Genel Müdürlüğü published a 'Meteorology Atlas for Turkey' (Meteoroloji Genel

Müdürlüğü, 2002). This atlas is prepared in 2002 with a tool named Wind Atlas Analysis and Application Program (WAsP) by Dannish Meteorology Organization. This tool has also been used to compile European Wind Atlas. Basic information that is required to use WAsP for a region consists topography of the region, roughness measure of the region, obstacles that are present in the surrounding of the region, and hourly wind data for the region. In this research, wind data that are measured between 1989 and 1998 from 45 different meteorology stations, which are scattered around Turkey, have been used to prepare the atlas. These stations record wind data 10 m above from the ground, and obstacles that are close in proximity to the these stations are locally examined by using the 1/1000 and 1/5000 scaled development plans for the region from which the data is taken. Moreover, topography and roughness measures for all data acquisition regions have been excerpted from 1/25000 scaled maps that have been published by Harita Genel Komutanlığı. Specifically, roughness measures for these regions have been calculated by numerically analyzing the roughness bounds that are presented on these maps. All these data that is prepared have been statistically analyzed in the second stage of the research by using WAsP in order to compile the readily available wind atlas.

Within the published sources some of the significant pioneering experimental research focuses on effects of roughness on convective heat transfer and they belong to F.B. Rowley and his colleagues (W.A. Eckley, A.B. Algren and J.L. Blackshaw) as it is mentioned in Smith (2010). They investigate convective heat transfer coefficients of six distinct materials (such as plaster and glass) that are used on building facade, where each one differs from another by their roughness. In their research, change in surface temperatures of these materials is examined for cases when they are exposed to wind with varying speed. Furthermore, the research is also extended for an analysis of change in convective heat transfer coefficients, when the wind angle is altered. Likewise, as Smith (2010) highlights another founding significant research by R.J. Cole and N.S. Sturrock on observing the change in convective heat transfer coefficients of three-dimensional models of buildings in wind tunnel experiments, since there are only few studies that focus on the subject. In this research Cole & Sturrock conduct experiments with laminar flow wind tunnels. Although findings from these earlier experimental studies are rather limited, many contemporary researchers currently use findings of these researches in their calculations. For instance, some of the numeric findings that are reported in these researches are still being used in readily available simulation software (for instance DOE2 simulation software package benefit from the findings of Rowley and his colleagues in order to compute). Although, these studies formed a baseline for experimental researches of the field within the last five decades experimental methodologies and research interests diversified and became sophisticated. An overview of variety of wind tunnel implementations for buildings and structures that is presented by Isyumov (1998) highlights this diversity. However, in the rest of this section only a selected portion of the significant experimental research will be mentioned.

First one of these, Clear, Gartland and Winkelmann (2003) is a specialized experimental research for measuring convective heat transfer coefficients of exterior

surfaces of horizontal roofs in order to put forth empirical correlations. Clear et al. (2003) is a part of the Cool Roofs Project, in which loads of roofs with high reflection on overall air-conditioning loads of a building is investigated. As a result of this study, a distribution named day of the month distribution is elicited to be used in further research for estimating convective heat transfer coefficients for these types of roofs. Measurements are carried out for the flat horizontal asphalt cap sheet roofs of three single floored commercial buildings in North California, in order to create 17 monthly datasets. With these datasets two different analysis is completed, where first is a discrete analysis for data for each month, and the second is a holistic analyses that is carried on data for all months.

By using the surface heat transfer data that is gathered for these horizontal roofs correlation of exterior surface convective heat transfer coefficients have been devised as a function of wind speed, wind direction, roof dimensions, roof surface roughness and difference between surface temperature and ambient temperature. This correlation is intended to be used in building energy analysis software to calculate more precise per hour estimations for heat transfer correlations. Apparently, these calculations are specialized for roof heat loads that are sensitive to the convection of the exterior surface of the roofs. Moreover, within this research surface roughness of roofs is also taken into consideration to some extend throughout analysis with a model that is a combination of standard flat plate equations of natural and forced convection. Measurements and the successive modeling and correlation research yielded three distinctive equations for calculating convective heat transfer coefficients of roofs. Specifically, one of these equations is for calculating coefficients of any points on a convex shaped for any wind angle, second equation is for calculating average coefficients of whole surface of a rectangular roof for any wind angle, and the last equation is for calculating coefficients of average surface areas of a rectangular roof for average wind angles.

Like Clear et al. (2003), Hagishima and Tanimoto (2003) conducted another on-site measurement to calculate convective heat transfer coefficients of building facades. The aim of this study is to gather a collection of interpretable data on vertical walls and roof surfaces of buildings in order to qualitatively predict convective heat transfer coefficient for facades of buildings in urban settlings while also taking into account the shadowing effects in urban areas. These measurements also try to figure out the relationship between wind speed and convective heat transfer coefficients.

Particularly, within the literature there is no consensus on the ranges of wind speeds that can be used in qualitative measurement researches. Furthermore, within the experiments that are conducted with wind tunnels in general parameters like building positioning of standalone buildings, structure of the urban areas, wind directions are being tested. However, even in wind tunnel experiments real life processes that are taking place over the building facade surface cannot always be truly represented. Therefore, Hagishima and Tanimoto (2003) adopt an advanced methodology to overcome this representation problem. That is, within the experiments wind speeds are measurement from a point that is very close to the building facade, in order to assure

high correlation and universality in the obtained results. Data is simultaneously gathered from 16 distinct points that are on the building facades, hence multi-point measurement technique is applied. For the measurements that are carried on the roof surfaces wind speed data is gathered from a point that is 13 cm distant to the ground. By doing so, with their methodology Hagishima and Tanimoto (2003) made it possible to observe any edge effects that can possibly occur. From the data that is gathered it is concluded that there is a universal relationship between convective heat transfer coefficient and wind velocity, which is a positive correlation. Moreover, an increase in convective heat transfer coefficient is also found in areas that in close proximity to the data collection points.

Nottrott, Onomura, Inagaki, Kanda and Kleissl (2011) is another experimental research on 1/5 scale models of real-life urban areas. In this study measurements on convective heat transfer of leeward building walls are conducted. Nottrott et al. (2011) analyses the outputs of the experiments and measurements that they conduct and compare their findings with the results from other experimental researches that are available in the literature. Heat transfer mode of the leeward walls that are examined in this research is intermittent, thus it is problematic to extract parameters from these measurements to be used in a universal implementation. Moreover another significant conclusion that can be drawn from findings of Nottrott et al. (2011) is that if an engineering heat transfer correlation that is currently in use within the field does not account for intermittent heat transfer modes, then that correlation is not suitable to be used in research for urban environments. In addition, Nottrott et al. (2011) also state that height of the buildings must be decreased and the distance between buildings must be increased in urban areas in order to increase the convection of the leeward walls of the buildings to minimize the energy requirements of buildings for cooling. This finding is especially advised to be practiced for urban areas with hot climate, so that cost for cooling can be reduced.

One of the recent works on real-scale experimental research is Seferis, Strachan, Dimoudi and Androutsopoulos (2011), in which setups for AIRinSRUCT project are used to conduct experiments in an experimental test room. Seferis et al. (2011) carry out analysis with a model by using ESP-r simulation package and compare the model with the data that is gathered from experiments and measurements. Although the comparisons between the predictions of the model and the experimental data yielded a major correlation, specifically a significant dissimilarity between the model predictions and the data is observed for the calculations that are carried for summer nights. According to the sensitivity analyses that have been conducted by Seferis et al. (2011) this differentiation is found to stem from utilization of standardized conductance data for the exterior walls of the test room that is gathered from the literature within the calculations. That is, heat transfer coefficients of the buildings exterior walls that are measured throughout the experiments are calculated using readily available standardized conductance parameters. Hence, Seferis et al. (2011) emphasize importance of measuring all parameters that are dependent on convective heat transfer throughout experimentation instead of using predefined values from the literature in order to obtain more accurate results on heat transfer.

In addition, concerning on-site measurements it can be stated that there is little data available for low-rise single storey buildings within the literature. Liu and Harris (2007) is a distinctive experimental research in which measurements are made for this type of buildings. These full-scale measurements are completed with the aim of devising heat transfer coefficients for leeward and windward surfaces a vertical wall of low-rise single storey buildings on sheltered buildings that are located in rural areas, while the relationship between the parameters of wind speed and wind angle, and convective heat transfer coefficient is also analyzed. Liu and Harris (2007) research is distinctive from its precursors; since previous research conducted on this subject majorly focus on the effects of shadowing effects on heat transfer between buildings that are located in city centers. Therefore, previous studies conducted experiments on settings where there is more than one building with higher number of floors, therefore in those experiments on urban settings the wind speed that is introduced as a parameter in the experiments is measured from a comparatively higher point. However, experiment of Liu and Harris (2007) is designed to complete measurements on a single standalone building that lay in a rural area, where the shadowing effects are minor and solely caused by surrounding structures such as tress and vegetation. Research of the field that is antecedent to Liu and Harris (2007), were all conducted on wind tunnel experiments, therefore findings of Liu and Harris (2007) is intended to validate and update those previous findings on wind speed and convective heat transfer coefficients.

Throughout measurements data on wind direction is also recorded, hence convective heat transfer coefficients that are calculated with Liu and Harris (2007)'s are improved compared to that of the preceding literature. Accordingly, wind speed is measured from three distinctive places one of which being the height of this standalone building, second is a point that is close to the wall and the last is 10 m of height. Wind speed measurements yielded the result that wind speed interims are found to be 0 m/s – 1 m/s, 1 m/s – 2 m/s, and more than 2 m/s. These values for wind speeds are purely derived from natural environmental conditions. Moreover, Liu and Harris (2007) found that the trend that convective heat transfer coefficient exhibits for lower wind angles and higher wind speeds is the same of its trends for higher wind angles and lower wind speeds. Furthermore, it is presented that the peak values for convective heat transfer coefficient become observable between wind angles 50° and 60°, and also between wind angles 90° and 110°. This is because convective heat transfer coefficient is majorly dependent on wind angle between 50° and 60°, whereas it is dependent on wind speed between wind angles 90° and 110°. Particularly, it is also found that convective heat transfer coefficient is dependent more on wind speed for leeward test cases. Overall, Liu and Harris (2007) state that wind angle has a non-negligible effect on convective heat transfer coefficient.

There is also a different line of research within the literature of experimental studies, which differ from other by the experimental methodology they adopt. One of those studies, Barlow and Belcher (2002) conduct an experimental research with a wind tunnel with the aim of quantifying the fluxes in urban boundary layers to devise a

model. This experimental research adopts a special methodology called the naphthalene technique to investigate three different street configurations (with varying street canyon geometries) by using two distinct wind tunnels (one which larger and the other is rather smaller) to create wind with varying speeds.

Barlow and Belcher (2002)'s methodology is essentially significant since successful application of naphthalene technique that is adopted in the research can demonstrate that this methodology can be applicable to be used in research on urban meteorological problems. Besides, it is found that naphthalene technique is also practical and suitable to investigate heat transfer on urban surfaces. Briefly, naphthalene technique grounds on the idea that naphthalene evaporates when exposed to wind in room temperature. In order to apply this technique, in the first stage of the experiment experimental models of the buildings or street canyons are covered up with naphthalene and the whole model is weighted. Then these models, which are already covered in naphthalene, are placed in the wind tunnel for the experiment to be completed (in general wind tunnel experiments of this type lasts for 10 minutes to 30 minutes). When the experiment is completed model is taken out of the wind tunnel and it is weighted again. The difference in the initial weight of the model and its weight after the experiments gives an indication for the amount of wind effect on the model. Furthermore, by using this technique local effects of wind on specific portions of the model can also be measured, since naphthalene on portions that are effected more from the wind will evaporate more.

Particularly, Barlow and Belcher (2002) vary the building height and street width parameters to obtain three of the aforementioned experimental street configurations. Moreover, for all three configurations distinctive roughness elements against the wind flow is placed within the canyon models. From the data that is gathered from the experiments, Barlow and Belcher (2002) conclude that the most important factor that effects the wind flux within the street canyons as the proportion between the building height and street width. In addition, wind speed is also observed to be an influential parameter. Additionally, it is also found that the proportion between the roughness elements that are placed within the street models and the building heights is another crucial factor that effects wind flux in street canyons up to 19 %. Lastly, Barlow and Belcher (2002) state that canyon ventilation is less sensitive to the street geometry when compared with other parameters.

Similar to Barlow and Belcher (2002), in a recent extensive and comprehensive experimental research by Smith (2010) various street canyon models for urban areas have been tested in a wind tunnel and convective heat transfer coefficients for these models have been computed. The methodology that have been employed in this research is to cover the models with naphthalene before placing them in the test chamber of the wind tunnel, and to measure the differences in the thickness of the naphthalene covering that are on the models after they are exposed to wind, in addition to measurements on change in surface temperature, wind speed and wind angle. Previous commonly implemented experimental procedures for the naphthalene methods consisted of applying it to the models with thermal paste, spraying it to the

models, painting the melted naphthalene, or solely preparing models from frozen naphthalene using molds. These experimental methodologies have their own disadvantages, because measuring the change in naphthalene thickness, which are covered on the models, were practically problematic for all these methodologies. All previous experimental research of the field measured the change in the thickness of naphthalene, by measuring difference of weight of the model that is covered with naphthalene before and after the experiment. On contrary to these experimental procedures, experiments that are conducted within the scope of this research are innovative, since models are covered in naphthalene by bathing each one in molten naphthalene and variation in thickness of the naphthalene coverings are measured with a mobile thickness meter. By doing so, Smith (2010) assures better accuracy and precision of its findings and testifies the applicability of its novel experimental procedure in attaining successful results.

By taking gaps of the relevant literature into consideration, Smith (2010) aimed to detect the change in convective heat transfer coefficient for building models that are used, to examine how variation in wind direction effects convective heat transfer coefficients of models buildings facades, to merely calculate convective heat transfers from the building by completely isolating components that are related with radiative effects from formulas that are used in calculations, to revise convective heat transfer equations for building facades and to assure proper application of them in later calculations, to attain realistic atmospheric conditions within the wind tunnel by using accurate average wind speed profiles and turbulence levels.

Models that are prepared for the experiments and that are made of metal are representative for distinctive street canyon geometries. Particularly, street canyon geometries that are chosen to be tested within this research are those where canyons are relatively lengthy (with height to width ratio 0.5 like most of the contemporary real life streets have), and models are tested for placements in which wind is exposed perpendicular to the modeled street canyons. These models are scaled for in between 1/1000 and 1/1500. Before covering models with naphthalene they are placed in a hot water bath for some time to assure uniformity of naphthalene covering. When models are prepared with this covering technique they are tested in a 2 m wind tunnel against varying wind speeds and wind angles for 2 to 3 hours, while conditions of the models and the test environment are being monitored. Particularly, the wind tunnel that is used within this research is a close loop tunnel with 1.5 m width and 2 m height and it can produce wind with speeds up to 50 m/s. The most important reason behind using wind tunnels in such experiments is the independence of the shape of the velocity profiles that occur within the wind tunnel from the wind speed. That is, data is taken from samples placed in the wind tunnel throughout the experiments can be used for another wind speed after scaling up the data.

With the above-described methodology Smith (2010) records data for all surfaces of the representative buildings that are in the models including the roofs. It is found that building heights have significant effects on convective heat transfer coefficients. Besides, it is put forth that an increase in wind speed also results in an increase in

convective heat transfer coefficients. By using the findings from experiments Smith (2010) also carries out further corrections on the formulas that are used to calculate heat transfer coefficients, whereas average formulation for coefficients of windward, leeward and roof surfaces are also presented. The empirical results of the experiments are also compared and contrasted with other findings from the literature. As a result, it is concluded that for the highest and lowest wind speeds there exists apparent inconsistencies. Equations that are included in standards and guidelines to calculated heat transfer are applicable for laminar flow on flat plates in wind tunnels, though results of Smith (2010) indicate an obvious effect of atmospheric turbulence and surface roughness on convective heat transfer coefficients. Formally, increase of these two parameters also results in an increase of convective heat transfer coefficients, thus presenting the aforementioned inconsistencies. Therefore, it is concluded that formulas that are advised by standards and guidelines underestimate real life heat transfer coefficients.

Moreover, findings of Smith (2010) are also compared with findings from other research that are investigating effects of wind on real scaled models by using wind tunnels and naphthalene covering method. It is found that results of Smith (2010) are similar to that of findings from other research for low-rise buildings, however there is a discrepancy between the findings for high-rise buildings. That is, it is advised to utilize findings of Smith (2010) in later research that is on urban areas with low-rise buildings rather than ones that are composed of high-rise buildings. Distinctively, it can also be stated that findings of this research formulas that are obtained after analyses are accurately applicable for real world configurations, since it also takes into account varying building geometries. On the other hand, naphthalene technique that is employed by this research poses a problem, since naphthalene coverings makes it hard to measure the effects of surface roughness on convective heat transfer. Nevertheless, within the literature roughness of the building facades is assumed to be an essential factor that effects convective heat transfer on the surface.

Smith (2010) also presents a set of suggestions to improve latter research on the subject. It is stated that street canyon geometries that are going to be investigated needs to be elaborated and enriched with more configurations to obtain a broad view on the heat transfer phenomena. Furthermore, it is also advised to focus on optimum street canyon spacing's in order to maximize convective heat transfer on building facades and roofs. It is also emphasized the need for further research on inclined roofs and openings (such as doors and windows) that impose discontinuities on the models which are used in wind tunnel experiments. In addition, it is also proposed to apply naphthalene technique on comparatively complex geometries.

2.2. Texture & Roughness

Texture of an object is an implicit property of it, which is fundamental in how we perceive them. Therefore, it is essential to study its effects in perceptual classification and assessment of objects while it plays a crucial role in pattern recognition and emotional categorization of immediately perceived textures. Studies on texture come

in great variety from the domains of computerized image processing, industrial design and architecture.

These studies of the literature generally try to propose models for identifying and processing building blocks of textures regardless of their complexity (as they do within the scope of computer vision), or to exploit factors that induce the perceptual bias in assessing them (from an industrial designer point of view), or lastly the issues related with the aesthetical tendencies in utilizing a specific texture in whole body architectural design (which is one of the main design concerns of an architecture). Regarding the diversity of methods and motivations in studying texture as a physical phenomenon, it is hard to come up with a unified definition of what texture is. Notably, it has to be emphasized that the research on effects of surface texture and roughness on convective heat transfer of buildings is considerably few in number. Accordingly, this section will solely outline this limited literature on studying roughness and texture that is relevant to heat transfer instead of presenting how texture is studied in all these aforementioned domains.

As it is also pointed out in Chi, Ballinger, Olds and Zucchini (2005), a precise and correct description for surface texture can be devised as the deviances from the ideal form of a surface. Since surface texture is a non-quantifiable feature, it is also not possible to come up with a unique definitive surface texture value for each and every surface, whereas it is likely to define the character of a surface by measuring the parameters that characterize the surface texture. In this regard, the standards ANSI B46 (Surface Texture - Surface Roughness Waviness and Lay, 2002), ISO 4287 (Geometrical product specifications (GPS) - Surface texture: terms, definitions and surface texture parameters, 1987) are the basic resources on the surface texture parameters.

In fact, any research on how to accurately measure these characteristic parameters is valuable. Accordingly, Santos and Julio (2013) try to put forth a comparison of the well-known methods that are available for the quantification of surface roughness of building materials like concrete. These methods can be enlisted as concrete surface profiles (CSF), sand patch test, outflow meter, mechanical stylus, circular track meter, digital surface roughness meter, microscopy, ultrasonic method, slit-islands method, roughness gradient method, photogrammetric method, shadow profilometry, air leakage method, processing digital images (PDI), two dimensional laser roughness analyzer method (LRA), and three dimensional laser scanning method. Advantages and drawbacks are of all these methods are discussed by Santos and Julio (2013). It is underlined that the principal difference between these methods are their type of evaluation, the degree of damage given to the sample while testing and the presence of contact with the examined surface. Santos and Julio (2013) also present a comparison of these methods regarding their cost and portability.

Santos and Julio (2013) also compile a set of frequently used parameters within the field that are descriptive about roughness. These roughness parameters are summarized and the R_a - average roughness, R_q - root mean square roughness, and R_z -

mean roughness depth are pointed as the frequently used surface roughness parameters. Formal definitions of these measures are presented in equations 2.2, 2.3, 2.4.

$$R_a = \frac{1}{n}\sum_{i=1}^{1} R_{a_i} \qquad (2.2)$$

$$R_q = \sqrt{\frac{1}{n}\sum_{i=1}^{1} R_{a_i}} \qquad (2.3)$$

$$R_z = \frac{1}{n}\sum_{i=1}^{1} R_{z_i} \qquad (2.4)$$

From equation 2.2 it can be observed that average roughness is the arithmetic average of all roughness profiles (R_{a_i}), where a roughness profile is the smallest seemingly repetitive unit of deviation from flat surface. Likewise, equation 2.3 illustrates that root mean square roughness is the squared of average roughness. Moreover, from equation 2.4 it can be observed that mean roughness depth is the arithmetic average of each roughness depths (R_{z_i}). Among those measure, root mean square roughness is the most commonly used parameters within the literature.

Santos and Julio (2013) also state that characterization of the surface must cover both micro and macro-texture in order achieve a comprehensive definition of the surface. Accordingly, micro-texture is defined to be the roughness between 1 μm - 0.5 mm and macro-texture is defined to be the waviness between 0.5 mm – 50 mm. Santos and Julio (2013) recommend visual inspection to evaluate surface roughness if the classification of surface is defined as very smooth, smooth, rough and very rough. However, visual inspection may also lead to varying and incorrect assessment of surface roughness. It is also concluded that enhanced roughness measuring techniques can ideally be preferred over visual inspection since they will give no harm to the sample being tested and since they are more accurate.

These conceptualizations of roughness and texture have also been used by the researchers of the field in experimental and numeric studies. An example of the earliest studies, which use photogrammetric methods, is by Seker and Tavil (1996). Throughout this research exterior building roughness of several surfaces are examined. The solar absorbance values of the same samples are also measured, in order to determine the relation between the roughness and solar absorbance. Seker and Tavil (1996) state that the amount of solar energy absorbed by the surface increase with an increase in roughness. This observation leads to the point that surface roughness is a surface feature which effects the amount of energy gained by the building facade material showing that the selection of the roughness of finishing material to be used at the outer most exterior surface of a building considerably effects the energy gained by the building via incoming solar radiation. Distinctively, research by Wieringa, Davenport, Grimmond and Oke (2001) aim to put forth a novel revision for the classification of terrain roughness. In order to determine the roughness of the local site

in research on wind energy, it is required to obtain either a sufficient or reliable dataset on local wind profiles or data on local wind speeds that are measure from a point that is distant to roughness elements (such as buildings, trees or vegetation) on that site.

Lastly, Garcia, Hernandez and Ayuga (2006) is another intriguing research that investigates surface textures and materials of building facades in terms of its concord with buildings surrounding with a photo analytic method. The aim of this investigation was to provide a procedural process for building designers and architects that could be put in use to choose the appropriate material for building facades. Garcia et al. (2006) evaluated textures of the materials that are used in building facades with a computational analysis from their photographs for criterion of regularity, density, particle size and internal contrasts. The texture that is ought to be chosen by architects for a specific buildings facade is evaluated for its material, visual and topographical coherence with the environment. Properties of all materials that were examined within the scope of this work were numerically quantified so that a subjective evaluation was not adopted. In order to conduct photo analytic evaluation Adobe Photoshop toolkit was used. Current advancement in computer technology enables us to numerically evaluate these four aforementioned parameters; hence an average value for each criterion could be calculated for a selected area in a photograph. Garcia et al. (2006) signify that their novel photo analytic method can be further integrated with other domains of research on energy and heat transfer to attain an advance holistic methodology.

CHAPTER 3

METHODOLOGY

In this chapter description of the material used in these experiments and the method that is being employed to get the data is described in Section 3.1. Then, variables that are being tested in each experiment are defined and how those variables are being measured is outlined with test cases in Section 3.2. Finally, this chapter concludes as experimental hypotheses of these three sets of experiments are presented in Section 3.3.

3.1. Research Design

As it is mentioned earlier, three sets of experiments, which will be detailed hereby, are designed to observe cooling of the surface of the building materials with different types of surface textures under homogenous flow of wind. However, effects of two factors on thermal behavior that are aimed to be tested, namely the texture of the surface and type of the material, has to be observed in separate experiments in order to investigate their effects on building thermal behavior.

First set of experiments (which will be named as *Experiment Set A* in the rest of this thesis) is designed to examine effects of surface texture on thermal behavior against varying characteristic wind flows. In order to create a constraint-free testing environment samples that are used within this experiment set are designed to be prepared from the same material (gypsum). By doing so, it is assured that effects of surface texture on surface temperature decrease under predefined characteristic wind profiles are observed without any material dependence. Those predefined wind profiles constitute the set of wind test cases that are generated from the same source, namely the wind tunnel. That is, findings from this set of experiments will be defining only the trend in temperature decrease that are parallel to the nature of the surface textures while other parameters such as material type are kept fixed. Therefore, these set of experiments are designed in a way that side effects of change in material type are eliminated to concentrate on observing the changes created individually by surface texture.

Second set of experiments (will be referred as *Experiment Set B*) focuses on whether surface temperate decrease trends for surface textures that are used in Experiment Set A will also be observed when material type is altered. In order to test this, one of the most commonly used building materials cement plaster mix is used to create samples with the surface textures that are used in Experiment Set A. Cooling trends for each surface texture are aimed to be compared for two different materials by using the data from Experiment Sets A and B.

Third set of experiments (will be referred as *Experiment Set C*) distinctively tests and contrasts results of surface temperature decrease trends that are observed in Experiment Set A and B on several various building materials with their own

characteristic surface texture. Hence, results of Experiment Set C are aimed to provide us a ground for extending results and observations that are obtained for the effects of surface texture on surface temperature decrease from Experiment Sets A and B to other commonly used conventional building materials.

It is essential to note that for all experiments, in order to obtain a stable homogenous wind flow at several different wind speeds a wind tunnel is used (further details about the wind tunnel will be presented in Section 3.1.3). In the following section materials that are used for these experiments are explained.

3.1.1. Sample Description and Preparation

In this section samples of all three experiment sets are described in details alongside with their specifications for their preparation.

Sample Preparation for Experiment Set A

There are seven different samples that are used in Experiment Set A. These samples are prepared from gypsum powder by using wooden molds that are presented in Figure 3.1 to obtain plates of 200 mm x 200 mm with 30 mm thickness and they only differ in their surface texture. Particularly, width and height of samples are chosen to be 200 mm, since this is the appropriate dimension for a sample to be exposed to wind in the wind tunnel that is described in Section 3.1.3 without disturbing the homogeneity of the wind flow within the tunnel. In parallel, 30 mm is chosen to be the thickness of the samples in order to attain the samples to have a sufficient mass to be heated and cooled. For all other experiments these dimensions are kept fixed (expect for some of the samples of Experiment Set C as it is elaborated in sample preparation section for Experiment Set C).

Ingredients of the mixture from which all the samples are prepared from are solely water and gypsum powder. The proportion of the final mixture is 1 measure of water and 2 measures of gypsum powder. All samples are particularly built from this mixture with the aim of fixing the material type for each sample of this experiment while observing effects of varying surface texture on thermal behavior (for further specifications of the gypsum powder that is used refer to Appendix A).

Gypsum is chosen specifically throughout the sample preparation for Experiment Set A, since it is practical to give it the desired form in obtaining seven different surface textures. While preparing sample blocks first gypsum plaster is prepared in a separate bowl and it is poured into a wooden mold. The mold gives the block its desired shape and dimensions, whereas surface texture for each sample block is manually created on the surface that is exposed to air while plaster is still not dry.

Moreover, it is crucial to clarify the reason why this procedure is chosen for sample preparation. There are also other alternatives for preparing such samples as described above, such as cutting desired sizes of sample blocks from larger readily available gypsum blocks and then shaping the surface of the obtained sample block to the desired texture. Or, another method is to supply sample blocks from the market as they are sold. In this case, it is hard to compile a set of sample blocks with identical the dimensions for different textures. Such methods for sample preparation are either not practical or time consuming or they may not always be efficient to provide the desired sample set.

As it is mentioned above the main concern while designing Experiment Set A is to eliminate constraints that can be introduced by different material types that are having different physical properties. Hence, using above described molding technique provides a uniform physical property distribution among sample blocks. This means, any undesired effect of variation in dimensions or mass between the sample blocks are ruled out.

Sample Description for Experiment Set A

Below, all seven sample surface textures that are used in the experiments and presented in Figure 3.2 and 3.3 are listed with their full descriptions and their surface textures (for each sample the description is provided with *Name of the Sample – Sample #* tag couplings, i.e. Plain – A0):

- **Plain (A0):** very smooth surface.
- **Rough (A1):** surface with homogeneous texture with roughness less than 0.1 mm.
- **Wavy (A2):** surface with texture of randomly ragged with rag heights less than 10 mm.
- **Grooved Level 1 (A3):** surface with texture of horizontal groove lines in which each groove to groove distance is less than 5 mm with groove depth less than 1 mm and with groove width less than 1 mm.
- **Grooved Level 2 (A4):** surface with texture of horizontal groove lines in which each groove to groove distance is less than 10 mm with groove depth less than 3 mm and with groove width less than 5 mm.
- **Grooved Level 3 (A5):** surface with texture of horizontal groove lines in which each groove to groove distance is less than 10 mm with groove depth less than 5 mm and with groove width less than 10 mm.
- **Grooved Level 4 (A6):** surface with texture of horizontal groove lines in which each groove to groove distance is less than 20 mm with groove depth less than 10 mm and with groove width more than 20 mm.
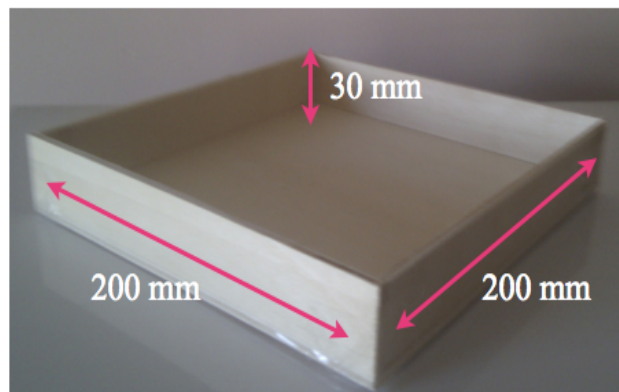
Figure 3.1. Molds that are used for sample preparation in Experiment Set A. Dimensions of the sample blocks are: width and height is 200 mm and thickness is 30 mm.
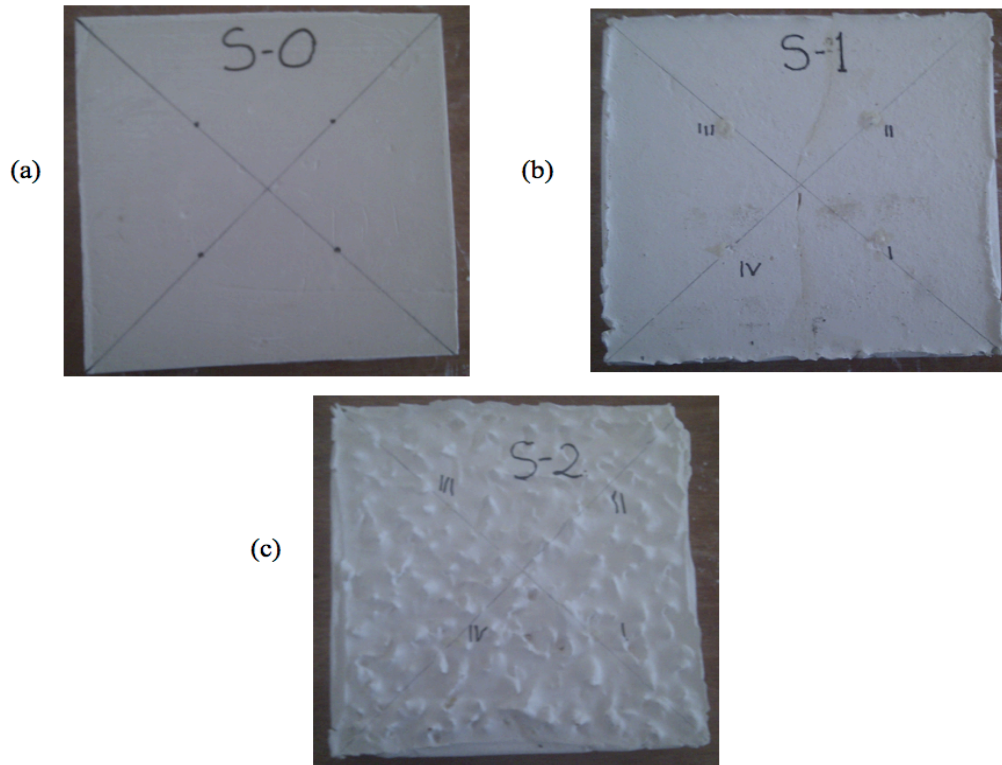
Figure 3.2 Samples blocks of Experiment Set A that are varying in roughness and waviness in the order of (a) Plain – A0 (b) Rough – A1 (c) Wavy – A2.
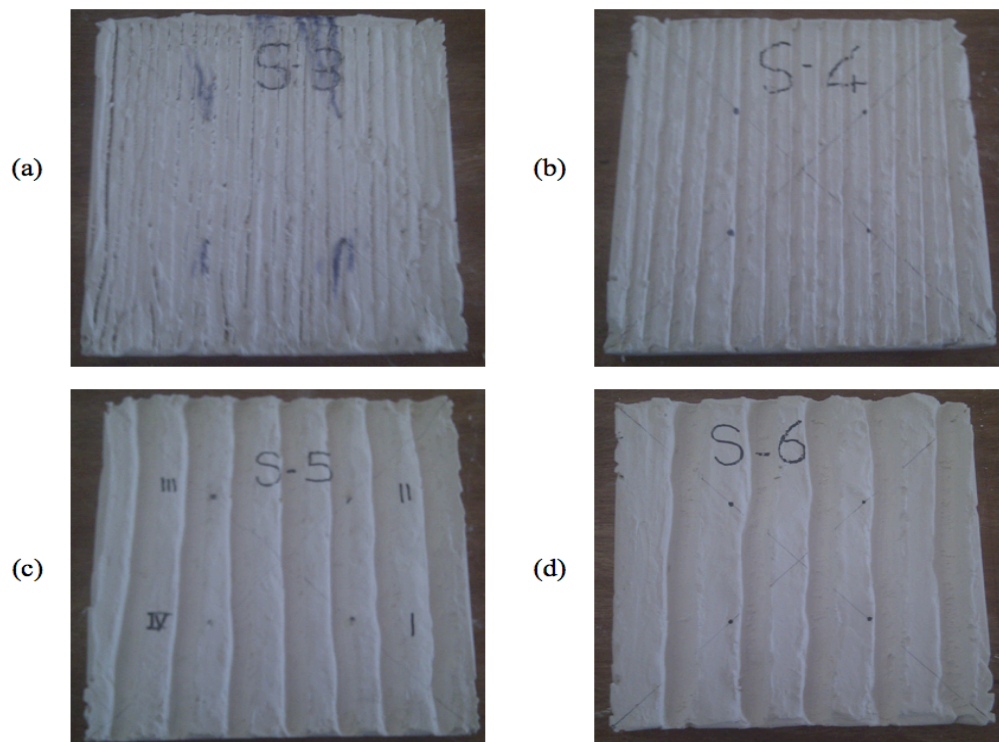
Figure 3.3. Samples blocks of Experiment Set A with grooves in the order of (a) Grooved Level 1 – A3 (b) Grooved Level 2 – A4 (c) Grooved Level 3 – A5 (d) Grooved Level 4– A6.
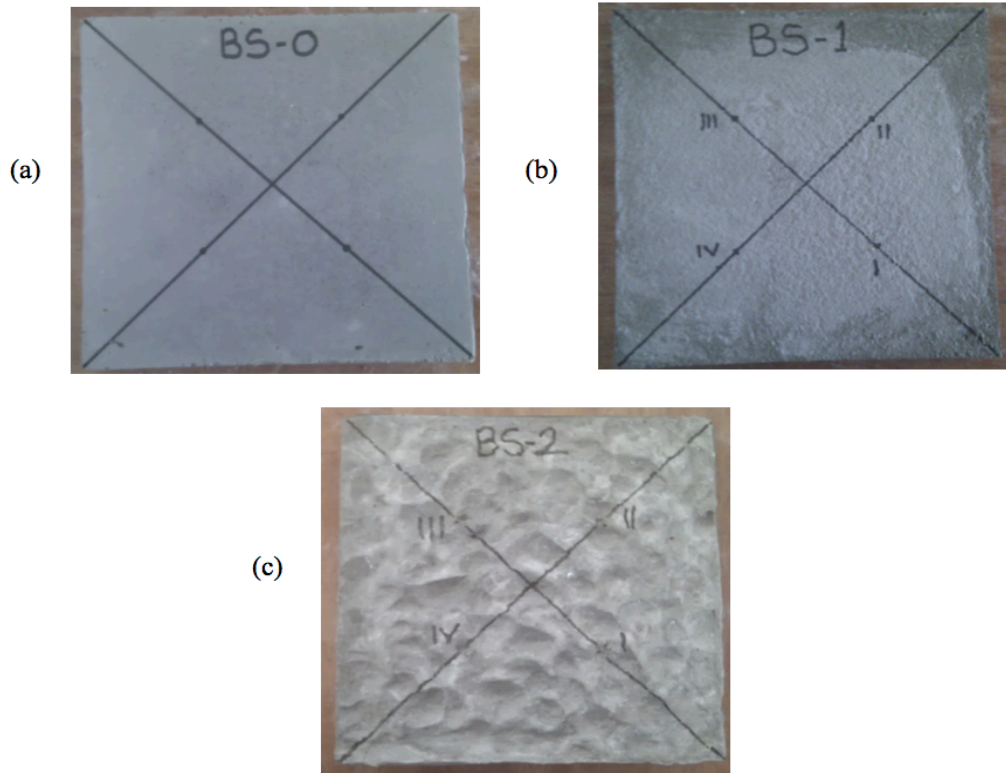
Figure 3.4. Samples blocks of Experiment Set B that are varying in roughness and waviness in the order of (a) Plain – B0 (b) Rough – B1 (c) Wavy – B2.
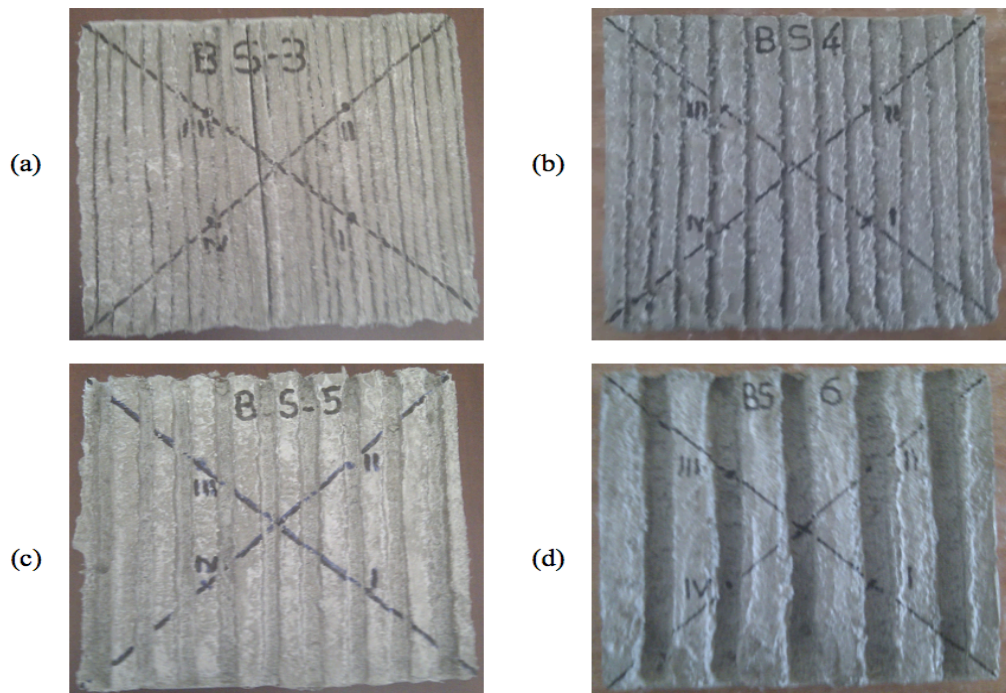
Figure 3.5. Samples blocks of Experiment Set B with grooves in the order of (a) Grooved Level 1 – B3 (b) Grooved Level 2 – B4 (c) Grooved Level 3 – B5 (d) Grooved Level 4– B6.

These specifications for the surface textures of samples are chosen to detect and observe the effects of three different textures as they are named as roughness and waviness, being grooved and being patterned. Samples A0 and A1 are plain and they only differ by their roughness. Texture alteration of A2 also extends in variation of waviness apart from roughness. So they form the first group in order to test the effects of textures having different roughness and waviness on the trend of decrease in surface temperature. Among those A0 represents a plain surface, A1 represents a regular surface roughness that occurs naturally on the material surface if no further intervention is applied to obtain a surface finishing and A2 represents a highly rough surface that is visually observable without even needing tactile feedback to classify it as rough. The scale for roughness and waviness in this sample set is limited to those three samples, since they represent roughness and waviness of the most commonly used typical building facade materials.

On the other hand, roughness and waviness of a texture is not classifiable in terms of the geometrical patterns that it imposes on the overall look of the texture. Therefore, another group of samples that A3, A4, A5 and A6 are designed to be used in this set of experiments to test one of the most basic patterns, which is a recurrent continuous grooved line. For these set of samples (A3-A6) the shape and dimension of the identifiable geometrical shape, which is the grooves in this case, that is present in the surface texture can be controlled. These dimensions that are altered in these set of samples are the groove depth, groove width and groove-to-groove distance. Groove depth is the distance from the bottom of the channel to the maximum height of the channel. Groove width is the distance between two maximas of the channel. Additionally, groove-to-groove distance is the distance between two adjacent channels. To clarify, this set of samples vary by these dimensions, while dimensions for A3 chosen to represent a rough surface with groove patterns and others A4, A5 and A6 cover up a group of several distinctly differentiating dimensions.

Sample Preparation for Experiment Set B

Samples that are used for Experiment Set B are prepared from cement plaster mix. Specifically, there are seven sample blocks with surface structures that are described for Experiment Set A in the previous section. The preparation method for cement plaster mix is the similar molding technique that is used for preparing gypsum samples of Experiment Set A and the resulting samples blocks have the same dimensions. Ingredients of the mixture to prepare cement plaster mix involve water and cement powder mix. These ingredients are mixed in the proportion of 1 measure of water and 3 measures of cement powder mix. All the samples are prepared from the same mixture (technical specifications of the cement powder mix is presented in Appendix A).

Sample Preparation for Experiment Set C

Samples that are used for Experiment Set C are selected among building materials that are currently existent in the market. Different than all the surfaces of samples of the Sets A and B, surface textures of samples for Experiment Set C are as that of the material of a building facade. These building materials are porcelain coated clay tile (for outdoor walls), travertine, marble, andesite and acrylic resin composite based material. Among those travertine, marble and andesite can be classified as samples of natural stone. All these materials have surface textures as they are manufactured so their textures are not further modified. All the samples are cut as 200 mm x 200 mm x 30 mm. Due to their manufacturing nature, samples of porcelain coated clay tile and

34

siding material have different thickness or size. Porcelain coated clay tile sample is 200 mm x 200 mm x 5 mm in size, whereas siding material has the dimensions 200 mm x 200 mm x 9 mm. It should be noted that only porcelain coated clay tile and siding material samples are manufactured products, whereas other samples are natural stones.
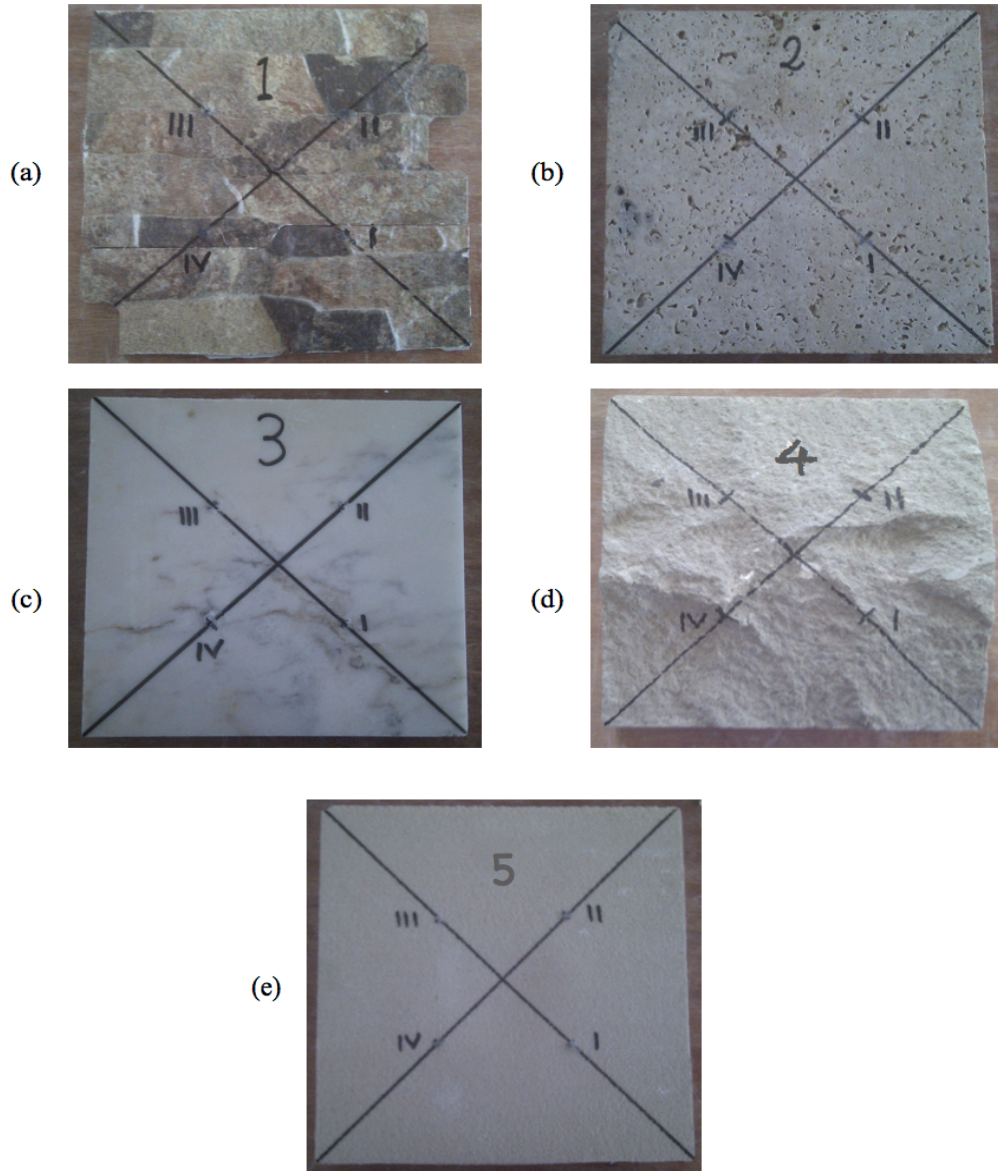
Figure 3.6. Samples blocks of Experiment Set C that are made up of materials in the order of (a) Porcelain Coated Clay Tile – C1 (b) Travertine – C2 (c) Marble – C3 (d) Andesite – C4 (e) Siding – C5.

Sample Description for Experiment Set C

Samples of Experiment Set C are named with *Material Type – Sample #* tag couplings, i.e. Porcelain Coated Clay Tile – C1 (C here stands for indicating that the sample is

that of Experiment Set C and technical specifications for the materials that is used in this experiment set is presented in Appendix A). Characteristic surface textures for these samples are elaborated below and presented in Figure 3.6:

- **Porcelain Coated Clay Tile (C1):** surface has a texture with natural stone patterns where pattern heights are between 0 mm – 2 mm.
- **Travertine (C2):** smooth surface with dents and holes that are randomly distributed.
- **Marble (C3):** very smooth polished surface.
- **Andesite (C4):** very rough wavy surface.
- **Siding (C5):** homogenous rough surface with roughness between 350 μm – 500 μm.

3.1.2. Integration of Surface Texture in Convective Heat Transfer Coefficient Calculations

Before elaborating integration of surface texture into the baseline formula that is used to calculate convective heat transfer coefficient (h), which is descriptive about the transient heat loss behavior of a sample and presented in Equation 3.1 must be reexamined. This formula could be re-written as in Equation 3.1'. In Equation 3.1', the volume to surface area ratio ($\frac{V}{A_s}$) is particularly separated from other factors that are involved in calculation of the heat transfer coefficient, since surface texture can be integrated in this formula by focusing on this ratio.

$$h = -\frac{\rho V c \frac{dT}{dt}}{A_s (T - T_\infty)} \tag{3.1}$$

$$h = -\frac{V}{A_s}\frac{\rho c \frac{dT}{dt}}{(T - T_\infty)} \tag{3.1'}$$

In order to integrate surface texture in this calculation, the definition of the surface area (A_s) must be revised. The tradition formula that is presented in Equations 3.1 and 3.1' assumes that the body has a uniform surface area; hence the surface area would be the multiplication of the total length of the sample (L) with its total width (w). However, as it is mentioned earlier samples that are used in the experiments have deviant surface areas. Specifically, samples that are used in Experiment Sets A and B are modified square tiles with different surface textures, where only one surface of the sample has a texture rather than being flat. Therefore, total volume of the sample cannot be calculated by simply using the conventional formula (length × breadth × height) since the top surface area is larger than the bottom of the tile sample. In details, in order to accurately calculate the volume of sample, the sample body can thought to be having two distinct pieces with their individual volumes, which add up to give the total volume of the sample. Therefore, to integrate surface texture within the calculation of convective heat transfer coefficient, a new parameter (RI) that is the ratio of the surface area of the uniform base of the rectangular prism ($A_{uniform}$) to the

surface area of the textured body ($A_{textured}$), as it is presented in Equation 3.2, can be introduced to in the formula as a multiplicand to the old surface area (A_s).

$$RI = \frac{A_{textured}}{A_{uniform}} \qquad (3.2)$$

To account for texture of all samples it has to have a roughness index (RI), which is the ratio between the areas of the textured surface and the footprint of the sample, as it is presented in Equation 3.2. If A_s is the surface area of the convective surface then it can be replaced with $A_{textured}$ in the formula and since the volume V is the sum of the textured and plain volumes then we can re-write the $\frac{V}{A_s}$ ratio as in Equation 3.3.

$$\frac{V}{A_s} = \frac{V_{uniform} + V_{textured}}{A_{textured}} \qquad (3.3)$$

If V is volume, A is area and H is the height then expanding the formula for volume in terms of area times height Equation 3.4 can be obtained.

$$\frac{V}{A_s} = \frac{(A_{uniform}\,H_{uniform}) + (A_{textured}H_{textured})}{A_{textured}}$$

$$\frac{V}{A_s} = \frac{(A_{uniform}\,H_{uniform})}{A_{textured}} + \frac{(A_{textured}H_{textured})}{A_{textured}}$$

$$\frac{V}{A_s} = \frac{A_{uniform}}{A_{textured}} H_{uniform} + \frac{A_{textured}}{A_{textured}} H_{textured}$$

$$\frac{V}{A_s} = \frac{1}{RI} H_{uniform} + H_{textured} \qquad (3.4)$$

This expression can then be integrated into the convective heat transfer coefficient as follows;

$$h = \left(\frac{1}{RI} H_{uniform} + H_{textured}\right) \frac{\rho\, c\, \frac{dT}{dt}}{(T - T_\infty)} \qquad (3.5)$$

In Table 3.1, corresponding surface area and height measurements for both uniform and textured bodies of the samples of Experiment Set A, B and C are presented in accompaniment with the calculated roughness indexes. These data are gathered with a 3-D scanning technique which will be further elaborated in Section 3.1.4. In addition, these data will be used in analysis of the results in Chapter 4.

Table 3.1. Surface area, height and roughness index values for both uniform and textured bodies of all samples of Experiment Sets A, B and C, where $A_{uniform}$ – surface area of the uniform body, $A_{textured}$ – surface area of the textured body, $H_{uniform}$ – height of the uniform body, $H_{textured}$ – height of the textured body and RI – roughness index.

Sample	$A_{uniform}$ (mm^2)	$A_{textured}$ (mm^2)	RI	$H_{uniform}$ (mm)	$H_{textured}$ (mm)
A0	31877.86	54,571.09	1.71	26.7	1.3
A1	32,400.00	49,856.83	1.54	24.1	1.0
A2	32,400.00	59,678.49	1.84	28.1	2.9
A3	32,400.00	61,483.14	1.90	24.3	2.4
A4	32,400.00	56,203.17	1.73	28.6	2.3
A5	32,400.00	71,386.52	2.20	18.3	6.4
A6	32,400.00	88,726.22	2.74	14.7	8.6
B0	26,795.21	58,082.43	2.17	30.1	1.8
B1	32,400.00	73,019.05	2.25	28.8	1.7
B2	32,400.00	119,026.25	3.67	26.5	3.5
B3	32,400.00	93,444.11	2.88	30.4	3.1
B4	32,400.00	93,574.03	2.89	30.2	3.9
B5	32,400.00	95,031.23	2.93	23.0	5.5
B6	32,400.00	106,485.58	3.29	19.6	8.3
C1	26,627.43	61,382.77	2.31	7.3	2.5
C2	32,400.00	58,375.10	1.80	10.3	2.1
C3	8,100.00	18,217.99	2.25	26.8	2.0
C4	32,400.00	75,715.99	2.34	35.4	12.9
C5	32,400.00	58,014.59	1.79	3.00	1.8

3.1.3. Experimental Setup

The experiments are realized in the wind tunnel at the RUZGEM Aerospace in Middle East Technical University. The structure and dimensions of the wind tunnel is as in Figure 3.7. A continuous-flow blower configuration is used. The wind tunnel consists of a radial, double intake blower (with a diameter of 0.6 m), an electric motor (18.5 kW, AC) drives the blower. The speed of the wind generated by the blower can be controlled by adjusting the frequency of the electric motor. A rectangular to square transitional diffuser (2.6 m) with a 7 degree diffusion angle, a 1.85 m long 1.1 x 1.1 m^2 square cross-section settling chamber, a contraction section (0.915) with an area ratio of 3.36. Test chamber where the samples are placed is a rectangular fiberglass prism with dimensions 1.40 m x 0.6 m x 0.6 m with a rotating sample holder with 0.4 m diameter.

The wind tunnel provides homogeneous flow of wind at desired speeds. Hence, wind speed can be adjusted at a required value between 0 to 15 m/s. Moreover, the angle between the surface of the sample and wing generated by the wind tunnel can be adjusted by using the rotating sample holder that is placed in the test chamber. In Figure 3.8 whole experimental setup is presented.
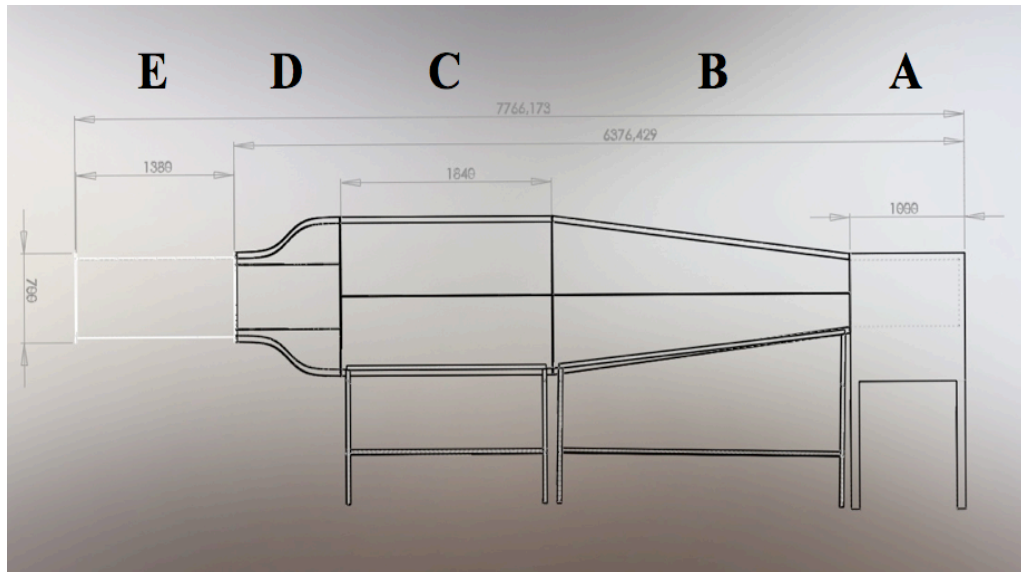
Figure 3.7. Dimensions of the wind tunnel parts. Figure excerpted from Ostovan (2011).

Figure 3.8. Test chamber that is attached to the wind tunnel with a rotating sample holder.

The experimental setup also contains a National Instruments NI cDAQ-9172 data acquisition system with four input channels for data recording. For controlling and design of the experiment process the software package LabVIEW 8.2 is used on PC with Windows XP operating system (for further specifications of the data acquisition system and experiment control software refer to Appendix B). LabVIEW is especially embedded in the experimental setup since it has user-friendly interfaces for designing

experimental block diagrams and instantaneous graphical data monitoring that are presented in Figure 3.9. The data acquisition system is connected to the PC and used in accompaniment with LabVIEW. This whole electronic interconnected system serves for design of the experiment process, data collection and processing. Additionally, to measure the surface temperature four chromel K-Type thermocouples are used. K-type thermocouples are readily available and consistently used for measuring temperatures between -200°C to 1350°C. These thermocouples are electrically, physically and technically matching with the processing modules of the data acquisition system.
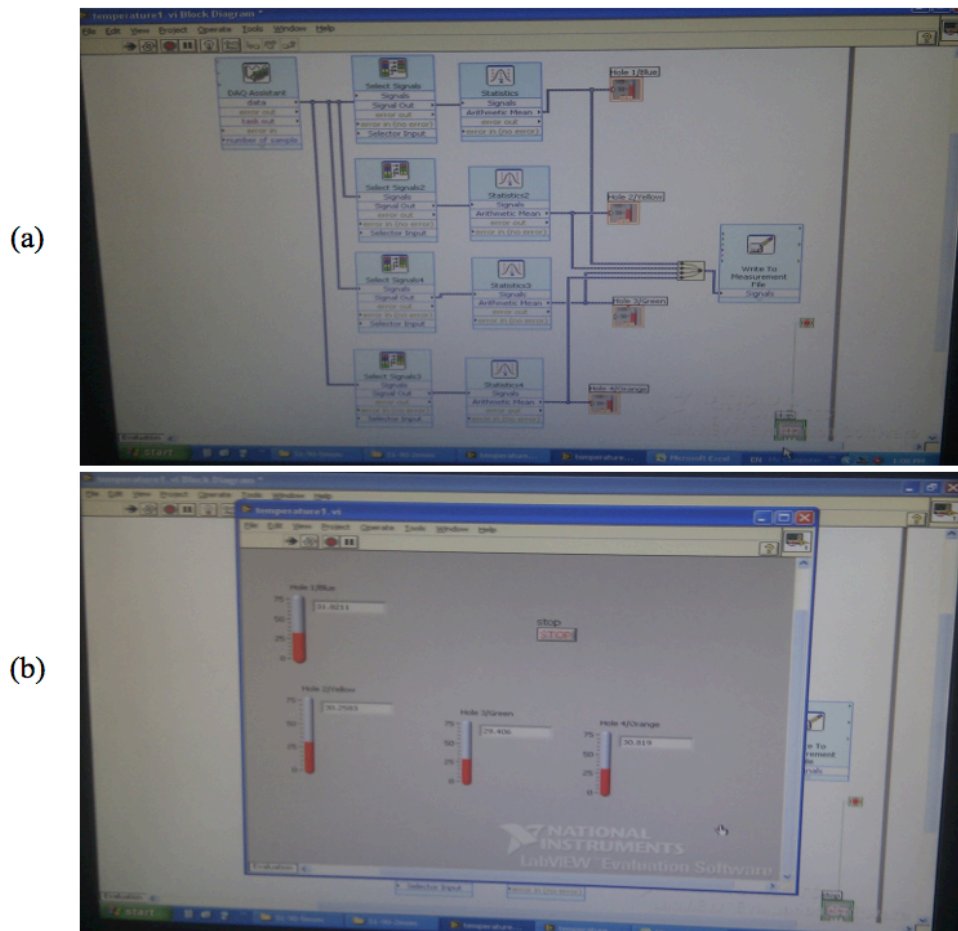
Figure 3.9. (a) Block diagram of the data acquisition, (b) Graphical data monitoring.

3.1.4. Data Collection Methodology

For each experiment following data collection procedure is applied by using the experimental setup and data acquisition system that is presented in Section 3.1.3:

1. The face surface of the sample is prepared by marking four predefined points for the thermocouple installation as it is presented in Figure 3.10-a.

2. The thermocouple junctions are fixed on these marked points at the surface of sample to be tested as it is presented in Figure 3.10-b. Metal holders are used to clip up the thermocouple cables on to the sample.

3. The data acquisition system is initiated and the inputs received by the thermocouples are monitored.

4. The sample is gradually heated up to 50°C - 55°C from the backside by using an electric heater. This temperature range is chosen to simulate the maximum surface temperature of an facade of a building in real life conditions can get by being directly exposed to sunlight throughout day time. This heating process lasts for approximately 10 minutes under the ambient temperature range between 25°C to 30°C.

5. During the heating the surface temperature of the sample is monitored from the related screen of LabVIEW data acquisition system till the surface temperature of the sample reaches around 50°C - 55°C.

6. The heater is turned off and the sample is left for a while for the heat inside it to be equally distributed within the sample body. During this stage, surface temperature is kept monitored so that the instants that the equilibrium reached between the temperature values measured via thermocouples are detected.

7. The sample is placed within the test chamber attached to the sample holder.

8. The humidity and the ambient temperature within the test chamber are noted manually. In order to record humidity and ambient temperature a thermometer and a hydrometer was attached within the test chamber. It is observed that these values did not alter significantly during the experiment.

9. The wind tunnel is started and homogenous continuous wind flow fixed at the desired wind speed starts.

10. Data collection and recording is initiated via the data acquisition system.

11. During the test, the surface temperature of the sample is being kept monitored from the related screen of LabVIEW data acquisition system (while also being recorded) till it reaches down to the ambient temperature. This monitoring also provides avoidance of any kind of technical troubleshooting (i.e. loosening of one of the thermocouples).

12. Data acquisition system is stopped via the related button from the screen of LabVIEW.

13. The sample is released from the sample holder and removed from the test chamber.

14. The recorded data is checked and then it is saved in the initially created files under a scheduled index.

15. If another sample is to be tested according to the test plan, then all four thermocouples attached on to the surface of the sample prior to the experiment are carefully detached and removed.

16. If the same sample is to be tested again with different parameters, then the sample is placed for heating and above steps starting from step 2 are applied.

It is noteworthy to mention that the placements of thermocouples on sample surfaces (through steps 1-2) are not random. They are placed to be in the center of sample surfaces while being equidistant to each other. Hence, to determine the position of each thermocouple first two diagonal lines are drawn on the sample from diagonal corners. Then, to ensure that each thermocouple is placed equally distant to the center of the sample, positions for thermocouple installations are marked to be 5 cm apart from the center of the sample, where two diagonals intersect. All the thermocouple wires, which are 5 m in length, are piled and tied up and they reach properly to the sample holder inside the test chamber of the wind tunnel. Moreover, the data acquisition system that is used within the experimental setup is programmed to record

the measurements that are received from the thermocouples approximately for each two seconds in order to have continuous data collection. For each experiment the mean of all the four recorded thermocouple readings are calculated and used as the average surface temperature. Although in normal circumstances the readings for four thermocouples do not vary drastically, it provides a solution to overcome the slight differences between the readings of different thermocouples.
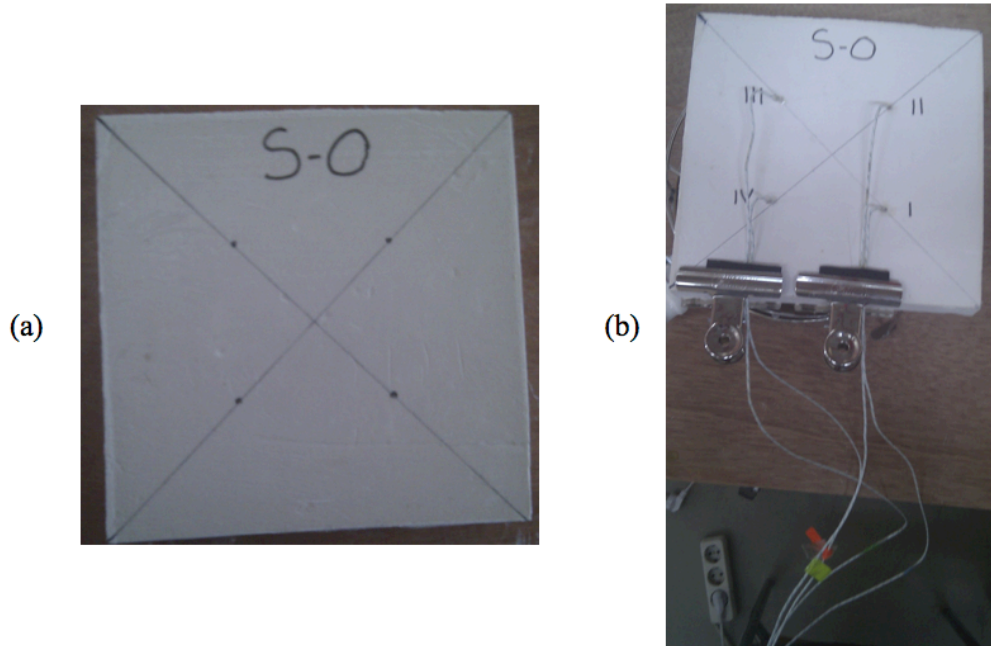
Figure 3.10. (a) Markings for thermocouple placement points on a sample, (b) Thermocouple installation on a sample.

To heat the samples before each experiment an electrical heater of 1000 W power is used. The heater that is used is in circular shape with the heating face having 11.5 cm diameter, whereas the overall outer diameter of the heater is 16 cm. Samples are heated as they are placed on a three-leg circular grate stand that has 19.5 cm diameter, 9 cm height, so that while samples are being heated an 2.5 cm distance between the heater and the sample is assured. Electrical heater is chosen to be circular in order to heat each sample from the center so that heat could be equally and uniformly distributed among the surface that is being heated. Samples are heated from the backside, which is the opposite side to the surface with the particular texture that is exposed to wind. Although in real life conditions building facade is heated through direct exposure to sun, it is chosen to heat the samples from backside in contrary to real life situation. This sample heating procedure is used to provide sufficient time for the sample mass to reach a thermal equilibrium after the heat is distributed all through. Since thermocouples are installed on the front side, by using the data acquisition system heating state of the sample can be monitored till it reaches thermal saturation before experimentation starts. The heating procedure that is outlined here is applied to each sample before each test.

In addition, the data which forms a basis for the roughness index values that are presented for samples of Experiment Sets A, B and C in Section 3.1.2 are collected by

using a 3-D laser scanner that is produced by Faro Technologies Inc. which is presented in Figure 3.11. Faro Focus 3-D laser scanner automatically performs a 3-D laser scanning of the desired target with optional data description (specification of the 3-D laser scanner that is used in data collection is presented in Appendix B). It scans the surface within a selected range as it takes a single data point for each 100 μm. The data that is collected by the 3-D laser scanner is transferred to a 3-D image processing software, which is AutoCAD Civil 3-D 2011, as dxf files. The data that is taken and processed by the image processing software contain more than 10 points for 1 mm^2 of a sample. However, in order to increase the efficiency in data processing the data sets having 5 data points per 1 mm^2 area is used.

(a)   (b)

Figure 3.11. (a) Faro Focus 3-D laser scanner. (b) 3-D laser scanner setup.

Figure 3.12. AutoCAD Civil 3-D 2011 screenshot of the 3-D image of a sample (right) and three sections of a sample (left).

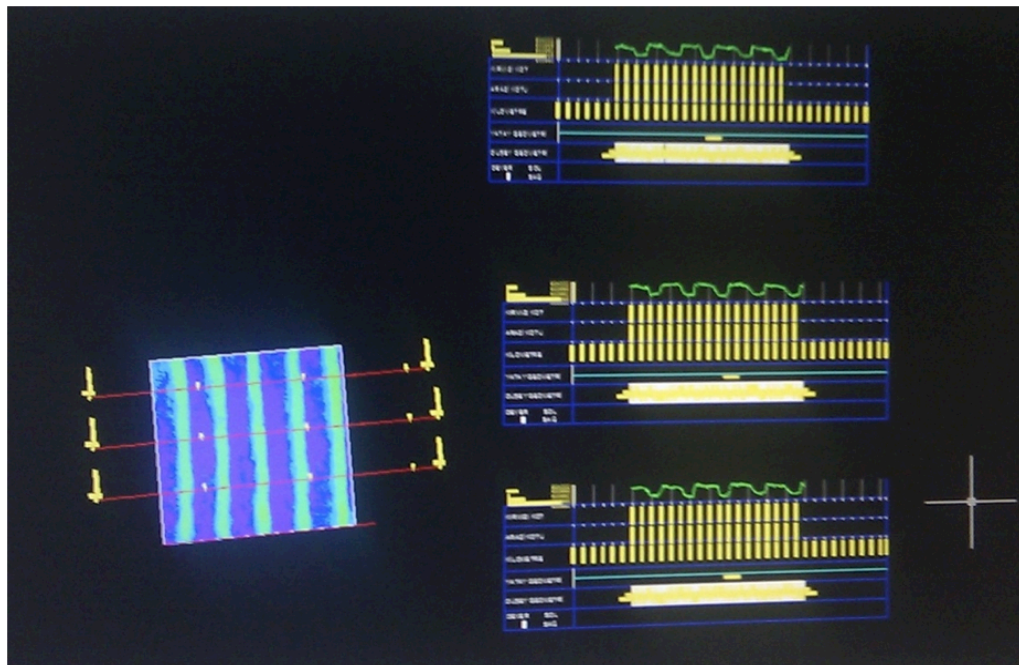With the features that are provided AutoCAD Civil 3-D, surface area and height of the textured and uniform parts of each sample are measured over the scan data that is produced by 3-D scanner as seen in Figure 3.12. To calculate the surface area raw data set that have been obtained from 3-D laser scanner have been imported to AutoCAD then the surface areas that need to be extracted area selected and marked. Three different vertical sections are taken and the average of the measured height of the textured and uniform parts for each section are calculated. In order to run AutoCAD Civil 3-D 2011, a high-end 64-bit PC with Intel(R) Core(TM) i5 2400 CPU, 3.10 GHz is used.

3.2. Data Description and Test Cases

The experiments that are outlined above are designed to capture the interplay between six variables that are assumed to be the fundamental ones in a surface convective heat transfer model. These variables are:

- **Independent Variables**

    o First independent variable that is included in the experiment is the *surface texture*. Surface texture is predefined for the samples used in the experiments as they are defined in Section 3.1.1, which is explicitly included in the experimental design. Therefore, surface texture is set and does not show variations depending on other variables. One of the main observation criteria of this study is the effect of surface textures on thermal behavior. Hereby, predefined surface textures are used which are distinctly physically differentiable from each other. According to the analysis of the outputs of the experiments a texture classification is planned to be proposed. Therefore, a numeric measurement of surface textures that can put forth the differences between the surface textures is not (or cannot) explicitly specified hereby.

    o Second independent variable is the *wind speed*. Wind speed is set to vary for predefined values of 2 m/s, 4 m/s and 6 m/s. These values for wind speed are kept the same all through the experiments. They are within the range of characteristic wind speed profiles that represent the most encountered wind speeds in Turkey (Meteoroloji Genel Müdürlüğü, 2012). Wind speed is adjusted to the abovementioned values by setting the frequency of the electric motor that is generating the blow of the wind.

    o Third independent variable is the *wind angle,* which can be defined as the angle between the wind direction and the face of the sample exposed to the wind. Wind angle is controlled for values 90°, 60°, 45°, 30° and 15°.

    o Last two independent variables are the *ambient temperature* and *humidity*. These two variables are always recorded for the experiments and they vary with the laboratory conditions, hence they are independent of any other parameters.

44

- **Dependent Variables**

  o The dependent variable that is going to be tested is the *surface temperature of the sample*. Surface temperature depends on the surface texture, wind speed, wind angle and ambient temperature and is monitored and recorded by using the experimental procedure that is elaborated in Section 3.1.4.

For Experiment Set A each sample is tested under varying wind speeds and wind angles. Each test approximately lasts for 1 hour including preparation of the samples and experimental setup. Test cases for this experiment set are:

- **Test Case A1 (Single Wind Angle – Variable Wind Speed)**
  For all samples A0 to A6 the wind angle is fixed to 90° and wind speed varies for 2 m/s, 4 m/s, 6 m/s. This test includes 21 test cases in total.

- **Test Case A2 (Single Wind Speed – Variable Wind Angle)**
  For all samples A0 to A6 the wind speed is fixed to 6 m/s and wind angle varies for 90°, 60°, 45°, 30° and 15° (test with 90° and 6 m/s are already covered by Test Case A1 therefore they will not be replicated here). This test includes 35 test cases in total.

Similarly, for Experiment Set B all samples that are made up of cement plaster mix are tested for varying wind speeds and wind angles. The duration of each test lasts approximately 1 hours. The test cases for Experiment Set B are:

- **Test Case B1 (Single Wind Angle – Variable Wind Speed for Cement Plaster Mix)**
  For all samples B0 to B6 the wind angle is fixed to 90° and wind speed varies for 2 m/s, 4 m/s, 6 m/s. This test includes 21 test cases in total.

- **Test Case B2 (Single Wind Speed – Variable Wind Angle for Cement Plaster Mix)**
  For all samples B0 to B6 the wind speed is fixed to 6 m/s and wind angle varies for 90°, 60°, 45°, 30° and 15° (test with 90° and 6 m/s are already covered by Test Case B1 therefore they will not be replicated here). This test includes 35 test cases in total.

Similarly, for Experiment Set C all samples of all materials are tested for varying wind speeds and wind angles. The duration of each test lasts approximately 1 hours. The test cases for Experiment Set B are:

- **Test Case C1 (Single Wind Angle – Variable Wind Speed for All Materials)**
  For all samples C1 to C5 of all materials the wind angle is fixed to 90° and wind speed varies for 2 m/s, 4 m/s, 6 m/s. This test includes 15 test cases in total.

- **Test Case C2 (Single Wind Speed – Variable Wind Angle for All Materials)**

     For all samples C1 to C5 of all materials the wind speed is fixed to 6 m/s and wind angle varies for 90°, 60°, 45°, 30° and 15° (test with 90° and 6 m/s are already covered by Test Case C1 therefore they will not be replicated here). This test includes 25 test cases in total.

In addition, for all samples of Experiment Sets A, B and C a baseline reference measurement for cooling of samples are conducted for the case where they are not exposed to wind. Duration of each test lasts approximately for 1.5 hours, while it varies depending on the material that is tested. These no wind test cases can be elaborated as follows:

- **Test Case No Wind**

     All samples of all experiment sets are prepared and heated according to the methodology that is outlined in Section 3.1.4, however this time no wind tunnel is utilized. Accordingly, surface temperatures, ambient temperature and humidity are all recorded with the corresponding data collection methodology until these samples reach ambient temperature while they are cooling on their own. This test includes 19 test cases in total.

Overall, in three experiment sets total of 152 experiments are performed. Including the pre-test and post-test preparations approximately 252 hours of experimental study is realized.

3.3. Hypotheses

The hypotheses for the variables defined above can be listed as follows:

- The total effect of increasing wind speed is more on heat loss for all samples (in Test Cases A1, B1 and C1) for a constant wind angle even if they have varying roughness indexes.
- The effect of surface texture on surface temperature decrease trends increases when roughness and waviness of the surface texture increases (i.e. A2 will have a more significant effect on surface temperature decrease trends compared to A1 and A1 will have a more significant effect when compared to plain A0). This effect must also be observable for cement plaster mix samples of Experiment Set B.
- The effect of surface texture on surface temperature decrease trends increases when dimensions of the grooves of the surface texture increases (i.e. A6 will have a more significant effect on surface temperature decrease trend compared to A5). This effect must also be observable for cement plaster mix samples of Experiment Set B.
- Surface textures of samples A3 to A6 (both included) and B3 to B6 (both included) have more significant effect on the surface temperature decrease trend compared to other surface textures.
- Surface temperature decrease trends will be similar for gypsum plaster samples of Experiment Set A and cement plaster mix samples of Experiment Set B that are having the same surface textures.
- Surface temperature decrease trends will be similar for samples of different materials having same surface textures (i.e. A0, B0 and C3 – Marble will have

similar cooling trends. Also, A1, B1 and C2 – Travertine will have similar surface temperature decrease trends.).

CHAPTER 4

RESULTS AND DATA ANALYSIS

In this chapter results that are obtained from the experiments are presented and evaluated. To start with, in Section 4.1 an overview of how results are analyzed is introduced. Respectively, in Sections 4.2 and 4.3 cooling behavior of samples from Experiment Sets A and B are evaluated for test cases of varying wind speed and wind angle depending on their surface temperature decrease trends. In Section 4.4 these results are compared and extended for the results that are obtained for samples of Experiment C, which are the conventional building materials. Successively, in Section 4.5, surface texture integrated average convective heat transfer coefficients and time constants for all samples of all test cases are calculated and analyzed with a novel formula that integrates surface texture in calculation of these two values. In addition in this last section correlation between surface texture integrated average convective heat transfer coefficients and wind speed is presented.

4.1. Surface Temperature Decrease Trends

Throughout this chapter, while analyzing the data that is gathered from the experiments, two distinct methods will be used to evaluate the findings. First method focuses on the surface temperature decrease trend, which is the characteristic curve that defines the cooling behavior of a sample. This trend is altered by two of the independent variables, namely the wind speed and the wind angle. Therefore, change in surface temperature decrease trends for each sample for varying wind speeds and wind angles will also be representative for analyzing and comparing cooling behaviors of samples with each other. Second method that will be used in this chapter to analyze the data is the examination of the surface texture integrated convective heat transfer coefficients and time constants. These values are essential for evaluating the surface temperature decrease trends, since they can deliver a comprehensive overview of the cooling behaviors of samples for predefined conditions, and they will be elaborated in Section 4.5.

For all experiments that are conducted with all samples from Experiment Sets A, B and C a surface temperature decrease trend curve is plotted (individual surface temperature decrease trend curves are presented in Appendix C). This curve presents the variation in surface temperature, which is measured in °C, versus time in minutes. Characteristically for all samples of all experiments this curve has a negative slope, meaning that the surface temperature decreases as time proceeds. Effect of either wind speed or wind angle, when they are altered, result in a change in the form of the curve. Thus, for each test case cooling behavior of a sample can be evaluated using the form of the curve (that is defined by its slope). In what follows, these characteristic curves are evaluated and contrasted with each other over differentiation of their characteristic surface temperature decrease trend curves. Specifically, it is focused on the rate of change in surface temperature for each sample till they reach the ambient temperature

(note that all environmental conditions including ambient temperature and humidity for each test case is presented in Appendix C). Therefore, if two data sets have similar surface temperature decrease trends than it is assumed that they behave the same when representational environmental conditions that are defined over wind speed and wind angle are kept the same.
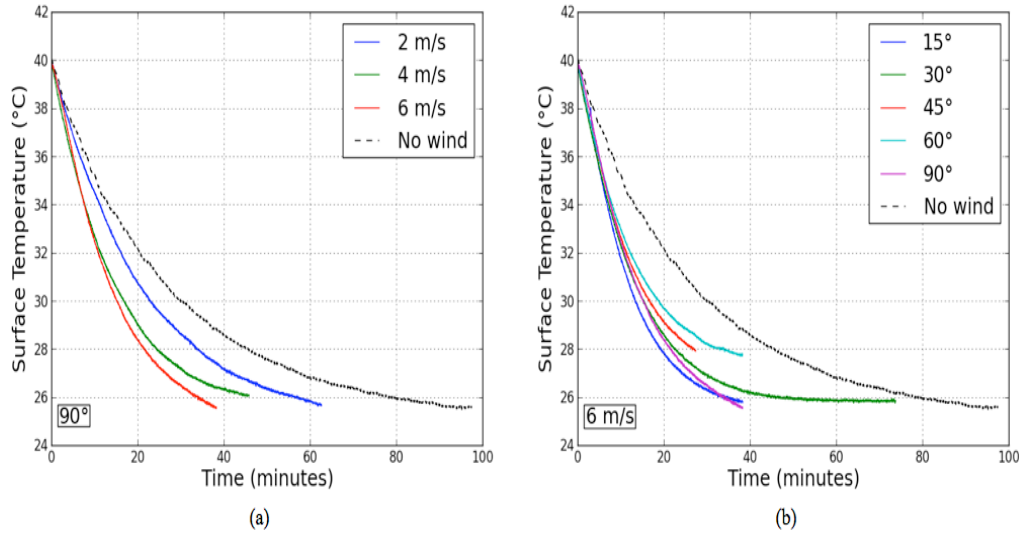

Figure 4.1. Plots of surface temperature (in °C) vs. time (in minutes) for sample A0 (a) for varying wind speeds of 2 m/s, 4 m/s and 6 m/s where wind angle is kept constant at 90° (b) for varying wind angles of 15°, 30°, 45°, 60°, 90° where wind angle is kept constant at 6 m/s. Note that no wind data for sample A0 is plotted with a dotted black line in both plots.

It is essential to note here that surface temperature decrease trend curves do not extend to the same values of surface temperatures. From surface temperature decrease trend figures that are presented in this chapter it can be observed that curves for some samples end earlier than others (they end for higher surface temperature values), whereas some others extend more. As it is explained in Chapter 3, the reason for this is that data collection is terminated for each sample when their surface temperature reaches the ambient temperature of the room at the time when the experiment is conducted. Furthermore, for convenience all surface temperature decrease trends are plotted from 40°C onwards till ambient temperature. The temperature range between 40°C and ambient temperature is representative for real-life conditions as it is explained in Chapter 3. In order to accomplish this in data analysis, the time step when a sample is in 40°C is normalized to be $t_0 = 0$ sec for all experiments.

To illustrate, Figure 4.1 presents surface temperature decrease trends for sample A0 for all test cases of different predefined wind speed and wind angle values. From Figure 4.1-a it can easily be observed that variation in wind speed alters the surface temperature decrease trend for sample A0. Specifically, when the wind speed increases sample A0 reaches thermal equilibrium at ambient temperature faster comparably to slower wind speeds. Thus, increase in wind speed has more substantial effect in cooling behavior of sample A0. Similarly, from Figure 4.1-b it can be observed that till 34°C (which is around 8 minutes) all cases in which only the wind angle varies surface temperature decrease trends overlap. The effect of wind angle on sample A0 then becomes observable as deviations between surface temperature decrease trend curves for distinct wind angles from 8 minutes and onwards.

50

The evaluation metric over surface temperature decrease trends that is presented in this section will be used in analyzing effects of wind speed and wind angle on surface temperature decrease in the following three sections.

4.2. Effect of Wind Speed on Surface Temperature Decrease

Surface temperature decrease trends for the first group of samples of Experiment Set A, which are A0, A1 and A2, is effected by variation in wind speed as it is presented in Figures 4.2, 4.3 and 4.4. From Figure 4.2 it can be observed that samples A0, A1 and A2 have distinctive surface temperature versus time curves when wind speed is 2 m/s and wind angle is kept constant at 90°. For this test case surface temperature of A2 decreases slower than A1, which is followed by A0. Notably, for wind speed of 2 m/s surface temperature decrease trends for sample with plain surface (A0) and rough surface (A1) show the same trend of surface temperature decrease with each other up till 32°C and their cooling trends differentiate for surface temperatures less than 32°C. For wind speeds 4 m/s and 6 m/s surface temperature decrease trends of A1 and A2 overlaps. Accordingly, for both wind speeds sample A0 behaves distinguishable than other two samples of this group while it presents a faster decrease of surface temperature.
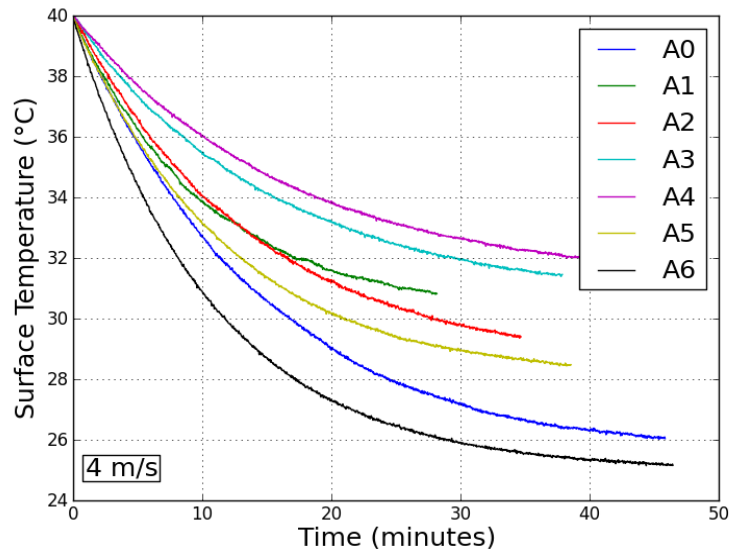

Figure 4.3. Plots of surface temperature (in °C) vs. time (in minutes) for samples of Experiment Set A for wind speed of 4 m/s and wind angle of 90°.

From Figures 4.2, 4.3 and 4.4, it can be detected that for all samples of Experiment Set A of both sample groups, increase in wind speed substantially effects surface temperature decrease trends as it increases the rate of decrease in surface temperature (It should be noted that surface temperature versus time curves in Figures 4.2 and 4.6 consists unexpected peaks due to electrical cut offs caused from human error). That is to say, higher the wind speed faster a sample reaches ambient temperature through cooling. To illustrate this effect surface temperature decrease trend of sample A2 from Figures 4.2, 4.3 and 4.4 can be compared with each other. Sample A2 reaches down to

51

the same temperature faster when wind speed increases. For instance, for sample A2 to reach down 30°C it takes 48.87 minutes for wind speed of 2 m/s, 27.63 minutes for wind speed of 4 m/s and 21 minutes for wind speed of 6 m/s. For sample A2, difference in time for cooling from 40°C to 30°C due to increasing wind speed between 2 m/s and 6 m/s is 42.97 %. Although the magnitude of this effect of increasing wind speed on surface temperature decrease trends varies for different samples of Experiment Set A, it is observable and applicable for them all.
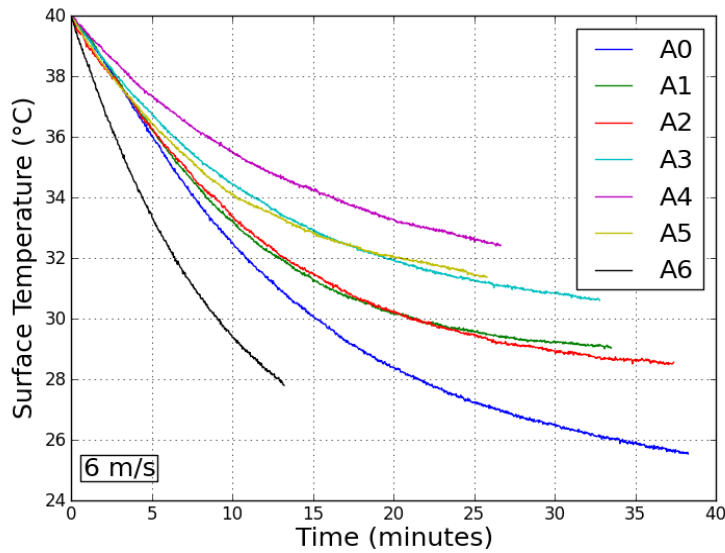

Figure 4.4. Plots of surface temperature (in °C) vs. time (in minutes) for samples of Experiment Set A for wind speed of 6 m/s and wind angle of 90°

Figure 4.5. Plots of surface temperature (in °C) vs. time (in minutes) for samples of Experiment Set B for wind speed of 2 m/s and wind angle of 90°.

For the first group of samples of Experiment Set B, which are B0, B1 and B2, surface temperature decrease trends for varying wind speeds are presented in Figures 4.5, 4.6 and 4.7. It can be stated that for all wind speeds 2 m/s, 4 m/s and 6 m/s surface temperature decrease trend curves for all three samples exhibit the same behavior. For lower wind speed of 2 m/s cement plaster mix sample with plain surface (B0) diverges from surface temperature decrease trends of samples B1 and B2.

For the second set of samples of Experiment Set B, for all wind speeds samples B4, B5 and B6 forms a group with their similar surface temperature decrease trends. However, specifically behavior of B3 is different from this group. In details, for wind speed 2 m/s sample B4 exhibits the fastest cooling behavior, whereas for increasing wind speeds of 4 m/s and 6 m/s it presents a slower rate of cooling behavior when compared to the grouping of other three samples.

In parallel with results for samples of Experiment Set A, rate of decrease in surface temperature increases for all samples of Experiments Set B with increasing wind speeds. From Figures 4.5, 4.6 and 4.7 it can be concluded that the degree of the effect varies among different samples, however it is observable in all test cases for all samples of Experiment Sets A and B. Therefore, it can be stated that increase in wind speeds substantially effects rate of decrease in surface temperature without depending on the material of the samples, as it can be expected.
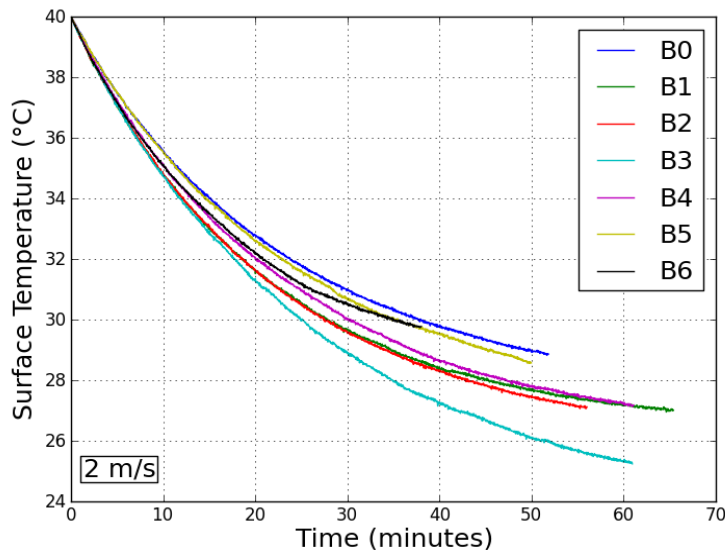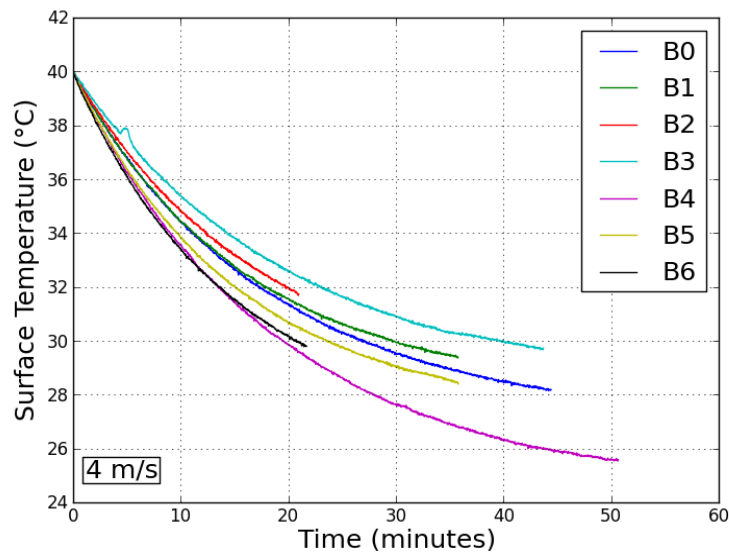

Figure 4.6. Plots of surface temperature (in °C) vs. time (in minutes) for samples of Experiment Set B for wind speed of 4 m/s and wind angle of 90°.

Surface temperature decrease trends of samples of first group of Experiment Set A and Experiment Set B can be correlated. That is, samples A1 and A2 in Experiment Set A and samples B1 and B2 in Experiment Set B form within set groupings, while A0 and B0 behave differently from these groupings for varying wind speeds. Moreover, for the second group of samples of both experiment sets, there is also clustering of samples according to their surface temperature decrease trends. In Experiment Set A samples A3, A4 and A5 form a grouping and A6 presents different surface temperature decrease trends depending on variation in wind speed, whereas grouping in samples of Experiment Set B is between B4, B5 and B6 while leaving B3 out.
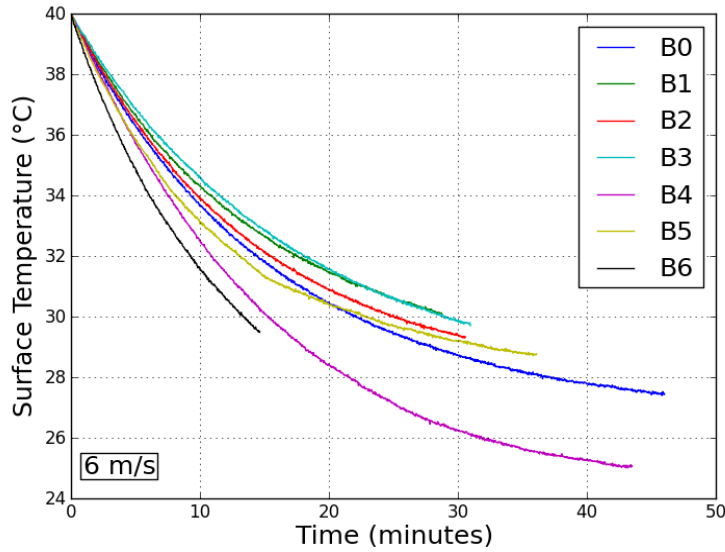
53

Figure 4.7. Plots of surface temperature (in °C) vs. time (in minutes) for samples of Experiment Set B for wind speed of 6 m/s and wind angle of 90°.

4.3. Effect of Wind Angle on Surface Temperature Decrease

For the first group of samples of Experiment Set A, surface temperature decrease trends of samples A1 and A2 are the same for wind angles of 15°, 30°, 45° and 60°. For all these wind angles surface temperature of sample A2 decreases faster than of sample A1 and the difference between rates of decrease in surface temperatures of these two samples remains the same for all wind angles. Apart from samples A1 and A2, surface temperature decrease trend A0 deviates from them for increasing wind angles between 15° and 60°. For sample A0, when the wind angle increases rate of decrease in surface temperature decreases.

For instance, from Figures 4.8 - 4.11 it can be observed that sample A0 reaches down to 30°C in 13.42 minutes for wind angle of 15°, in 15.33 minutes for wind angle of 30°, in 16.76 minutes for wind angle of 45°, and in 18.81 minutes for wind angle of 60°. On contrary, decrease in surface temperature does not vary substantially for samples of A1 and A2 when wind angle is increased. For all three samples surface temperature decrease trends are different that of they have in wind angles between 15° and 60°, for perpendicular wind angle 90°. For wind angle of 90°, surface temperature decrease trends of samples A1 and A2 overlap and differentiate from sample A0 as it is presented in the previous section.

In Figures 4.8 - 4.11 it can be seen that surface temperature decrease trends for samples A3, A4 and A6 form a grouping, while they exhibit same cooling behavior for wind angles between 15° and 60°. Within this set of samples, between wind angles 15° and 60° sample A5 behaves considerably different from this grouping as it presents a faster cooling trend than all other three samples. In addition, from these figures it can be deduced that rate of decrease in surface temperature for all these samples A3, A4, A5 and A6 does not get substantially effected from increasing wind speed. Therefore, these samples can be correlated with samples A1 and A2 over this observation. Likewise to the first sample group of Experiment Set A, these samples

54

also behave differently for wind angle of 90°. When wind angle is 90° samples A3, A4 and A5 exhibit a grouping, as it is mentioned in the previous section, and surface temperature decrease trend of the sample A6 is different from their surface temperature decrease trends.

Figure 4.8. Plots of surface temperature (in °C) vs. time (in minutes) for samples of Experiment Set A for wind angle of 15° and wind speed of m/s.

Figure 4.9. Plots of surface temperature (in °C) vs. time (in minutes) for samples of Experiment Set A for wind angle of 30° and wind speed of 6 m/s.

Figure 4.10. Plots of surface temperature (in °C) vs. time (in minutes) for samples of Experiment Set A for wind angle of 45° and wind speed of 6 m/s.

Figure 4.11. Plots of surface temperature (in °C) vs. time (in minutes) for samples of Experiment Set A for wind angle of 60° and wind speed of 6 m/s.
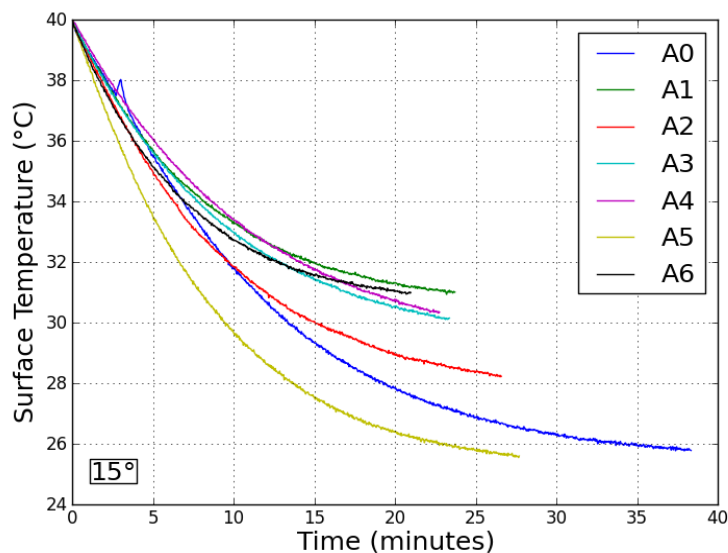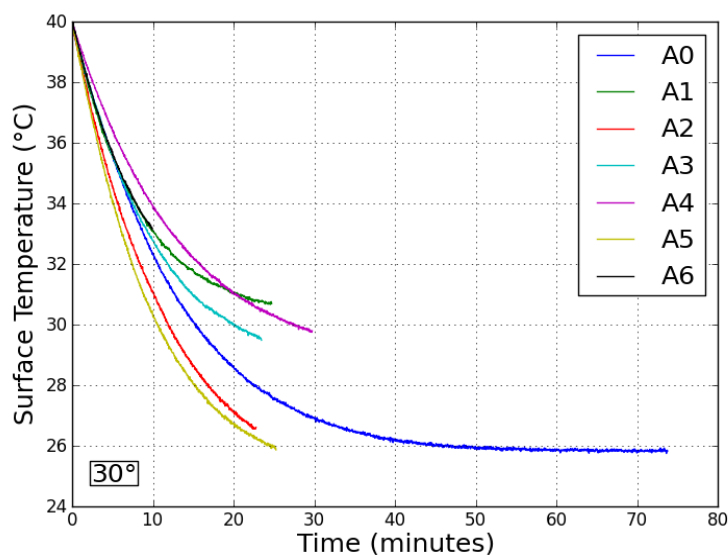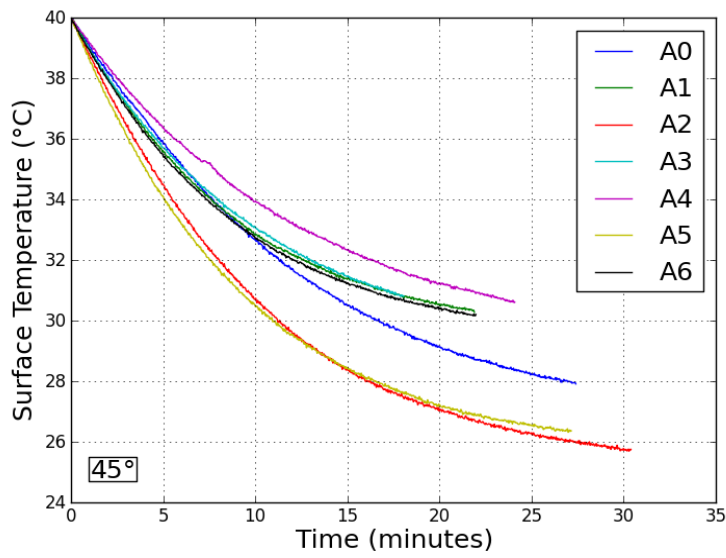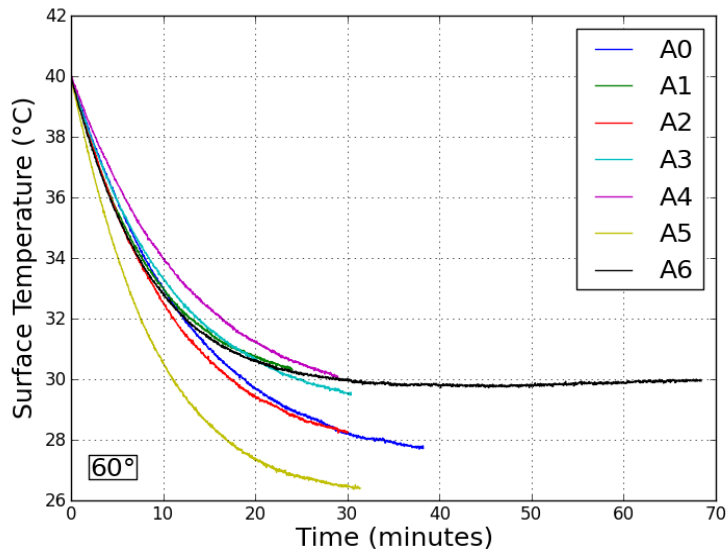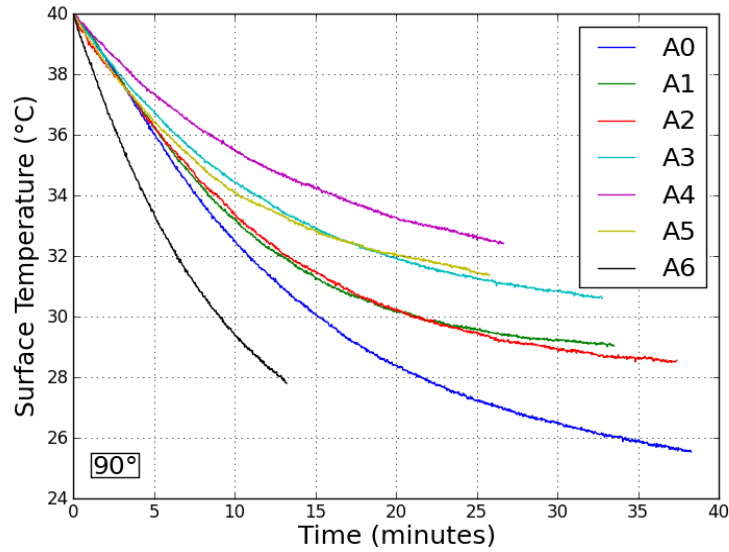
Figure 4.12. Plots of surface temperature (in °C) vs. time (in minutes) for samples of Experiment Set A for wind angle of 90° and wind speed of 6 m/s.

Regarding Figures 4.13 - 4.16 first group of samples of Experiment Set B, which are B0, B1 and B2, between wind angles 15° and 60° samples B1 and B2 has similar surface temperature decrease trends. However, starting from wind angle of 60° and for higher wind angle values as 90° the overlap in surface temperature decrease trends of samples B1 and B2 tend to disappear. In addition, for all wind angles sample B0 has a dissimilar surface temperature decrease trend than that of samples B1 and B2. Similar to results gathered for Experiment Set A, surface temperature decrease trends for this group of samples are different for wind angle 90° when compared with their surface temperature decrease trends at lower wind angles. When wind angle is 90°, sample with plain surface (B0) has the highest rate of decrease in surface temperature, which is respectively followed by sample with wavy surface (B2) and sample with rough surface (B1).

Surface temperature decrease trends of other samples of Experiment Set B for varying wind angles is presented in Figures 4.13 - 4.17. From Figures 4.13, 4.14 and 4.15 it can be observed that two groupings among samples B3, B4, B5 and B6 emerged for wind angles 15°, 30° and 45°. In these three figures it is clear that surface temperature decrease trends of samples B3 and B4 exhibit parallel behavior, hence they form a grouping. Furthermore, surface temperature decrease trends of samples B5 and B6 nearly overlap for wind angles of 15°, 30° and 45° and they form the second grouping.

Between these two groupings the one that is composed of samples B5 and B6 have higher rate of decrease in surface temperature when compare to the grouping that is formed by B3 and B4. When wind angle is 60° these two groupings disappear and surface temperature versus time curves of B3 and B4, and B5 and B6 diverge from each other. In this test case, sample B5 has the highest rate of decrease in surface structure, which is followed by B6, B4 and B3 respectively. Like surface temperature decrease trends of all other samples for perpendicular angle, samples B3, B4, B5 and B6 also behave differently for wind angle of 90°. For wind angle of 90° order of rate of decrease in surface temperature for sample B6, B4, B3 remains relatively the same

57

of the case of 60° wind angle, however rate of decrease in surface temperature decreases for B5.

Figure 4.13. Plots of surface temperature (in °C) vs. time (in minutes) for samples of Experiment Set B for wind angle of 15° and wind speed of 6 m/s.

Figure 4.14. Plots of surface temperature (in °C) vs. time (in minutes) for samples of Experiment Set B for wind angle of 30° and wind speed of 6 m/s.

When the effect of change in wind angle while wind speed is constant is compared for samples of Experiment Set A and Experiment Set B, it can be stated that samples with plain surfaces (A0 and B0) differ in surface temperature decrease trends from samples with rough and wavy surfaces (A1, A2 and B1, B2). Moreover, for the second group of samples it can be stated that samples with higher groove dimensions (A6 and B6)

always exhibit different cooling behaviors when compared to other grooved samples that have smaller groove dimension. However, particularly for Experiment Set A sample with groove level 3 (A5) also behaves distinctive from samples with smaller grove dimensions (A3 and A4). In general, it will not be an extreme statement to point out that change in wind angle has an effect on surface temperature decrease trends of samples with groove dimension higher than 5 mm. This is because samples with groove dimensions higher than 5 mm has comparatively higher RI values. To illustrate, samples A6 has a RI value of 2.74 and A5 has a RI value of 2.20, whereas A3 and A4 have RI values of 1.90 and 1.73 respectively. Similarly, sample B6 has a RI value of 3.29, whereas B3, B4 and B5 have RI values of 2.88, 2.89 and 2.93 respectively.
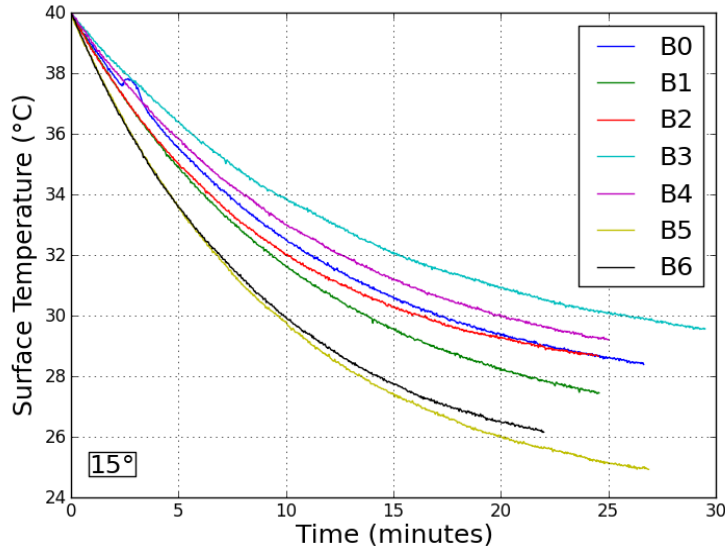

Figure 4.15. Plots of surface temperature (in °C) vs. time (in minutes) for samples of Experiment Set B for wind angle of 45° and wind speed of 6 m/s.
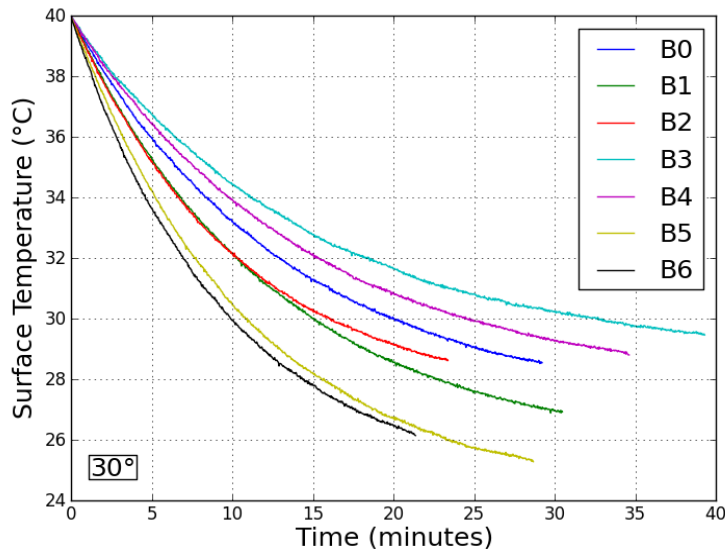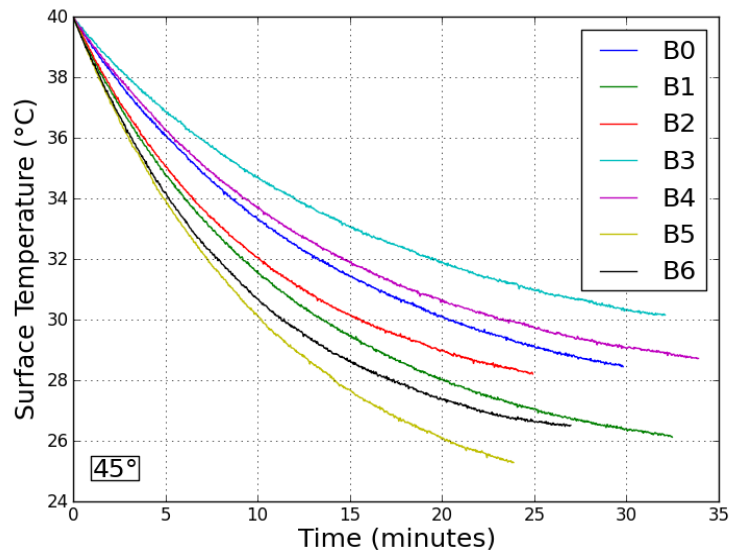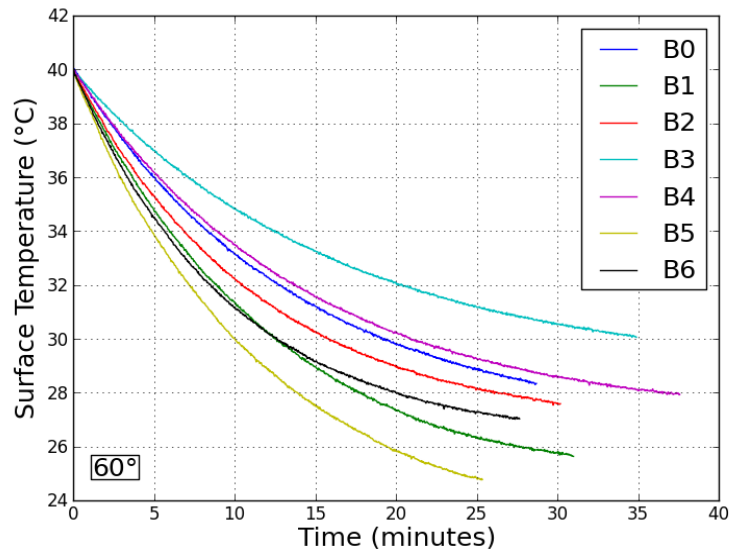

Figure 4.16. Plots of surface temperature (in °C) vs. time (in minutes) for samples of Experiment Set B for wind angle of 60° and wind speed of 6 m/s.
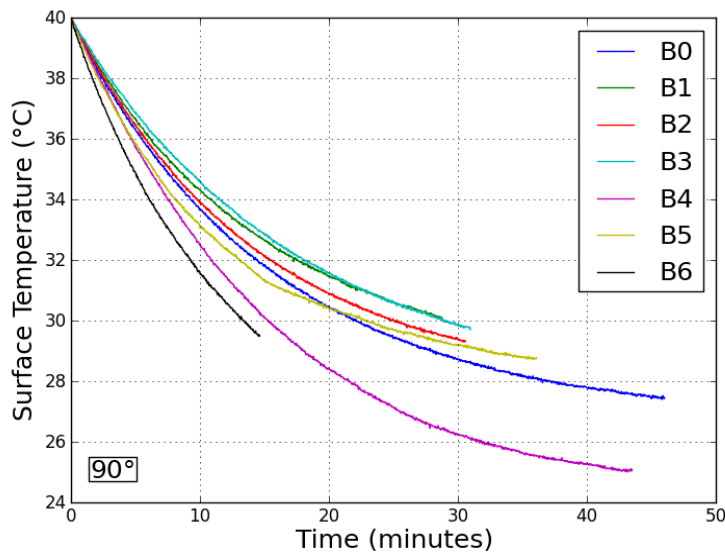
59

Figure 4.17. Plots of surface temperature (in °C) vs. time (in minutes) for samples of
Experiment Set B for wind angle of 90° and wind speed of 6 m/s.

4.4. Surface Temperature Decrease Trends for Conventional Building Materials

The effect of varying wind speed on surface temperature decrease trends of conventional building materials is presented in Figures 4.18, 4.19 and 4.20. It can be observed that samples that are made of marble (C3) and andesite (C4) form a grouping on their own for all wind speeds that are 2 m/s, 4 m/s and 6 m/s. Furthermore, samples that are made of porcelain coated clay tile (C1), travertine (C2) and acrylic resin based composite siding material (C5) form a second grouping again for all wind speeds, since they have similar surface temperature decrease trends.

Within the first grouping sample C3 has a higher rate of decrease of surface temperature compared to sample C4, meaning that surface temperature versus time curve of marble sample has a higher degree of negative slope. Moreover, sample made of andesite (C4) has a rougher and wavier surface when compared to the surface texture of sample made of marble (C3). One of the factors that result in this difference of rate of decrease in surface temperature is the difference between surface textures of these two samples. As it is also found for samples of Experiment Set A and B, sample with rougher and wavier surface looses heat slower when compared with plain surfaces. This observation can also be extended to conventional building materials. Thus, it can be stated that marble exhibits a rapid cooling behavior when compared to andesite, since it has a plain surface.

Likewise, samples of porcelain coated clay tile (C1), travertine (C2) and siding material (C5) form a second grouping, in which rate of decrease in surface structure for all these samples are higher in overall when compared to samples of the first grouping (C3 and C4). Within this grouping, siding material (C5) has the greatest rate of decrease in surface temperature, which is followed by travertine (C2) and porcelain coated clay tile (C1) respectively. The difference in surface temperature decrease

60

trends between porcelain coated clay tile (C1) and travertine (C2) can also be explained with previous findings on effect of wind speed for different roughness and waviness measures. Sample that is made of porcelain coated clay tile has rougher and wavier surface texture when compared to the sample that is made of travertine. Therefore, it is expectable and observable that travertine to have a faster rate of decrease in surface temperature. In comparison with sample that is made of travertine (C2), sample made of siding material (C5) has a similar surface temperature decrease trend, but higher rate of decrease in surface temperature. This distinction between surface temperature decrease trends of these two samples can be an indication that difference in physical properties of the samples (such as height, weight and thickness) effect rate of decrease in surface temperature, since sample C5 is physically different from sample C2.

Figure 4.18. Plot of surface temperature (in °C) vs. time (in minutes) for sample C1, C2, C3, C4 and C5 for wind speed of 2 m/s and wind angle of 90°.
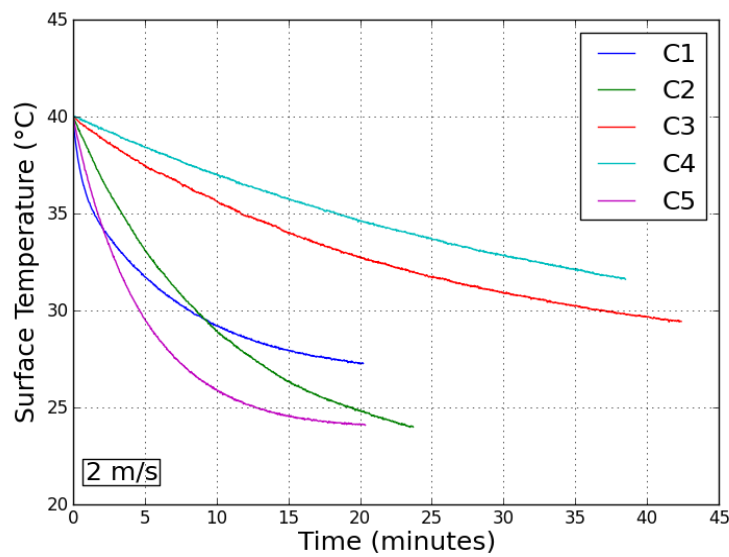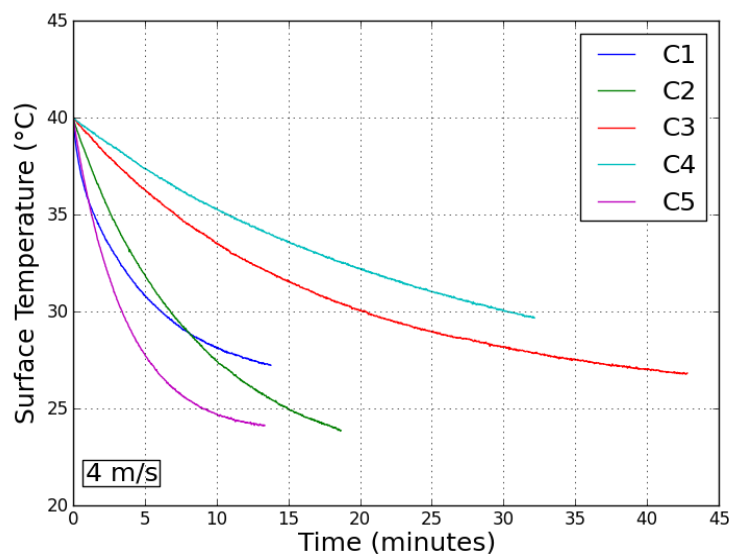

Figure 4.19. Plot of surface temperature (in °C) vs. time (in minutes) for sample C1, C2, C3, C4 and C5 for wind speed of 6 m/s and wind angle of 90°.
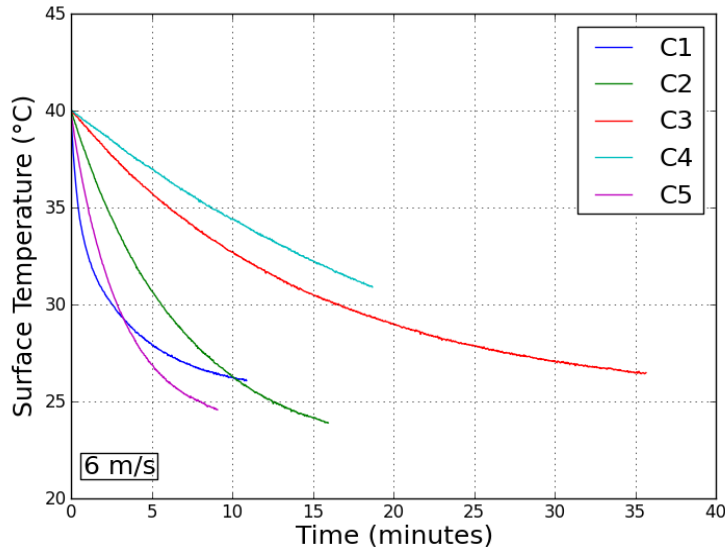
61

Figure 4.20. Plot of surface temperature (in °C) vs. time (in minutes) for sample C1, C2, C3, C4 and C5 for wind speed of 6 m/s and wind angle of 90°.

From Figures 4.21 – 4.25 effects of varying wind angle on surface temperature decrease trends of conventional building materials can be observed. Data that is presented in Figures 4.21 – 4.25 suggests that there are also two groupings like the one that is observed on Figures 4.18 – 4.20. Therefore, variation in wind angle while keeping wind speed constant does not disturb the characteristic surface temperature decrease trends for each sample. Similar to the results on experiments with varying wind speed on samples of conventional building materials, samples that made of andesite (C4) and marble (C3) behave distinctive from other samples for varying wind angles. On the other hand, porcelain coated clay tile (C1), travertine (C2) and siding material (C5) groups together for all wind angles between 15° and 90°.

For all samples of conventional building materials surface temperature decrease trends are effected by increasing wind speed. That is, increase in wind speed decreases the rate of decrease in surface temperature. For example, sample made of marble (C3) reaches down to 30°C in 36.78 minutes for wind speed of 2 m/s, in 20.13 minutes for wind speed of 4 m/s, and in 16.45 minutes for wind speed of 6 m/s. This trend is observable for all other samples for increasing wind speed.

In parallel, for increasing wind angle between 15° and 60° the rate of cooling decreases for all conventional building material samples. For instance, porcelain coated clay tile reaches down 28°C in 5.15 minutes for wind angle of 15°, 5.35 minutes for wind angle of 30°, 6.43 minutes for wind angle of 45°, and 7.23 minutes for wind angle of 60°. However, for perpendicular wind angle of 90° rate of decrease in surface temperature increases to the rates that are observed for wind angle of 15°. For example, it takes 4.98 minutes for the porcelain coated clay tile sample to cool down to 28°C when the wind angle is 90°. Therefore, it is observed that samples have the highest rate of decrease in surface temperature for the angles that are on the two extreme ends, which are 15° and 90°.

62

Figure 4.21. Plot of surface temperature (in °C) vs. time (in minutes) for sample C1, C2, C3, C4 and C5 for wind angle of 15° and wind speed of 6 m/s.

Figure 4.22. Plot of surface temperature (in °C) vs. time (in minutes) for sample C1, C2, C3, C4 and C5 for wind angle of 30° and wind speed of 6 m/s.

Figure 4.23. Plot of surface temperature (in °C) vs. time (in minutes) for sample C1, C2, C3, C4 and C5 for wind angle of 45° and wind speed of 6 m/s.

Figure 4.24. Plot of surface temperature (in °C) vs. time (in minutes) for sample C1, C2, C3, C4 and C5 for wind angle of 60° and wind speed of 6 m/s.
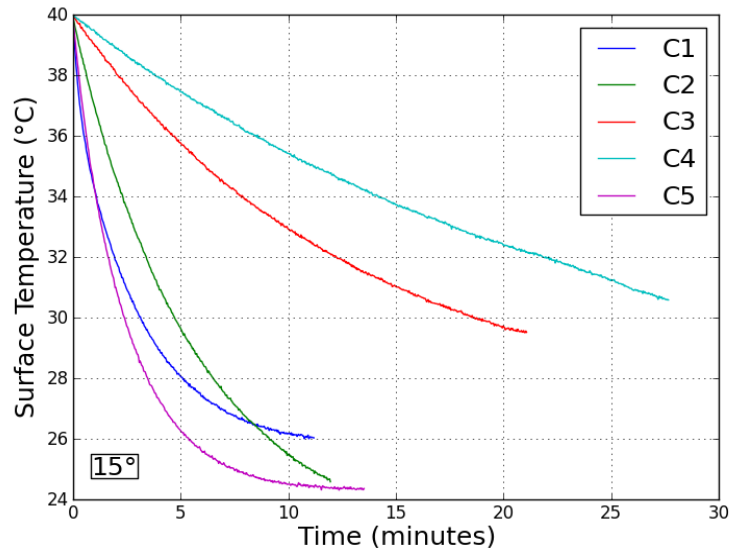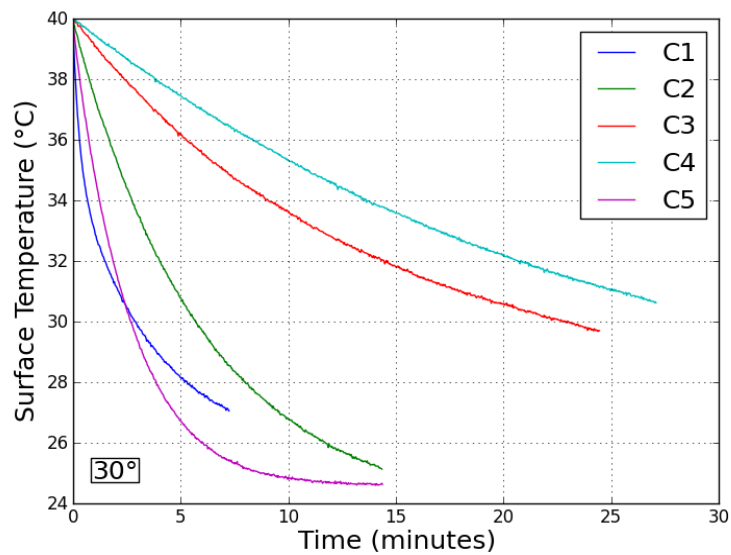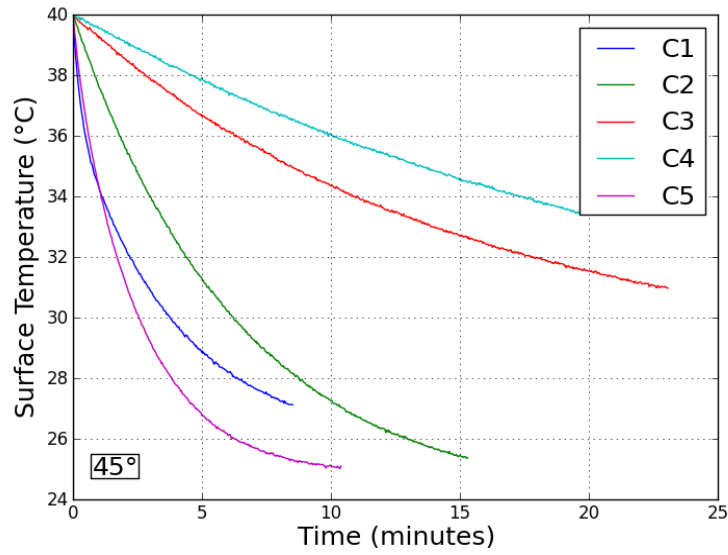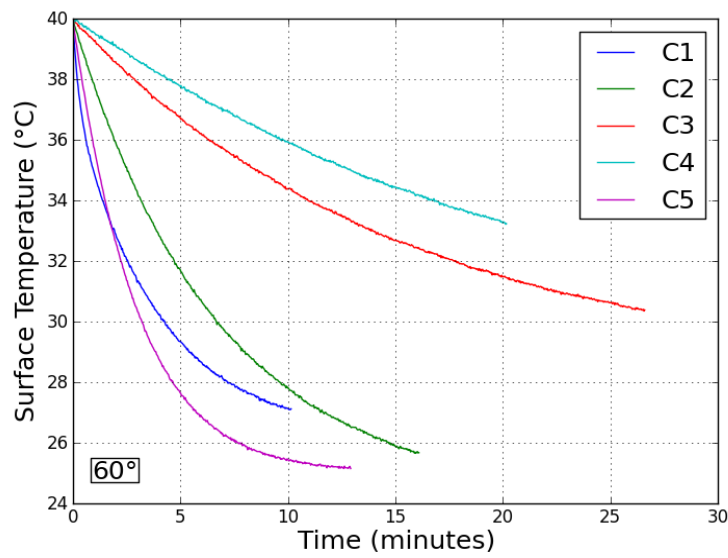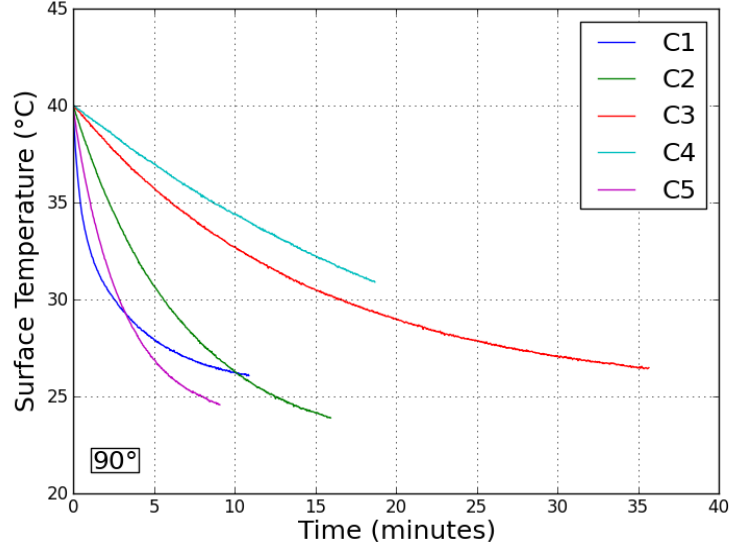
Figure 4.25. Plot of surface temperature (in °C) vs. time (in minutes) for sample C1, C2, C3, C4 and C5 for wind angle of 90° and wind speed of 6 m/s.

4.5. Surface Texture Integrated Average Convective Heat Transfer Coefficients (h-Values) and Time Constants (τ -Values)

In this section surface texture integrated average convective heat transfer coefficients for all samples that are used in all three sets of experiments are calculated and presented in correlation with the surface texture integrated time constants. Convective heat transfer coefficients (h-values) are dependent on density, volume and specific heat of the sample, surface area, ambient temperature and the rate of change in surface temperature of the sample till it reaches ambient temperature, as it is presented in Equation 2.1. Particularly, since it is a transient state there is an h-value for a sample for each recorded temperature while the sample looses heat till it reaches ambient temperature, thus average convective heat transfer coefficients for each sample will be indicative about the heat flux from the sample body surface to environment by convection. In details, in this section the surface texture integrated convective heat transfer function, which is presented in Equation 4.2, is used to calculate the h-values (components of Equation 4.2 is elaborated in Section 3.1.2). In parallel, surface texture integrated average convective heat transfer coefficient for a sample between its two specific surface temperatures, arithmetic mean of convective heat transfer coefficients for the surface temperatures that lies between those two boundary temperatures can be calculated as it is presented in Equation 4.3.

$$h = (\frac{1}{RI} H_{uniform} + H_{textured}) \frac{\rho \, c \frac{dT}{dt}}{(T - T_\infty)} \qquad (4.2)$$

$$h_{i_{avg}} = \frac{1}{n} \sum_{k=0}^{n} h_{i_{t=k}} \qquad (4.3)$$

In Equation 4.3, surface texture integrated average convective heat transfer coefficient of sample i ($h_{i_{avg}}$) is presented to be the arithmetic mean of surface texture integrated

65

convective heat transfer coefficients (h_i) at each time step k ($h_{i_{t=k}}$), where the data is recorded. In correlation, time constant values for each sample is indicative for how rapid that sample looses heat. Equation 4.4 presents how surface texture integrated time constants are calculated, while it is dependent on the density of the sample (ρ), specific heat of the sample (c), roughness index of the sample (RI), height of the part of the sample that has a uniform surface ($H_{uniform}$), height of the part of the sample that has a textured surface ($H_{textured}$) and surface texture integrated convective heat transfer coefficient (h). Surface texture integrated time constants are also calculated for the same surface temperature interval by using the average convective heat transfer coefficients that are obtained from Equation 4.3.

$$\tau = (\frac{1}{RI} H_{uniform} + H_{textured}) \frac{\rho c}{h} \qquad (4.4)$$

Specifically, in this section average convective heat transfer coefficients for each sample is calculated for surface texture integrated h-values in between 40°C and 35°C, so that it will be representative about the heat loss trend for this interval. Hence, at $k = 0$ surface temperature is at 40°C because of the time-step normalization that is carried out on data as it is explained in Section 4.1. Accordingly, n will be the time duration in which the mean surface temperature of a sample reaches 35°C. Surface texture integrated average convective heat transfer coefficients and time constants for all samples of all test cases with varying wind speed and varying wind angle is presented in Figure C.39 – C.50 in Appendix C in accompaniment with the values of surface texture integrated average convective heat transfer coefficients and time constants.

From Figures C.39 and C.41, it can be observed that surface texture integrated average convective heat transfer coefficients of samples with textures (which is the second group of samples that are A3, A4, A5, A6 and B3, B4, B5, B6) are increasing with increasing wind speeds. That is, for these set of samples heat loss flux increases for higher wind speeds. Likewise, this behavior is also observable for the first group of samples of Experiment Set B (which are B0, B1, B2) that have variation in roughness and waviness. This trend can also be deduced from Figures C.40 and C.42 since surface texture integrated time constants for these samples decrease when wind speed increases.

However, this trend is partially observable for the first group of samples of Experiment Set A (which are A0, A1 and A2). In details, for these samples an increase in wind speed from 2 m/s to 4 m/s a substantial increase in surface texture integrated average convective heat transfer coefficients is observable. Though, for higher wind speed 6 m/s average convective heat transfer coefficients of these samples do not vary notably or decrease for some amount. This is because, material used for samples of Experiment Set A, which is gypsum, have a comparably low density and specific heat. Therefore, effect of wind speed on surface texture integrated average convective heat transfer coefficients for samples A0, A1 and A2 starts to diminish around a threshold wind speed that is 4 m/s. Moreover, for a specific wind speed when average convective heat transfer coefficient of a sample of Experiment Set A with a given surface texture is compared with the average convective heat transfer coefficient of a sample of Experiment Set B that has the same surface, it is always observed that samples of Experiment Set B has a greater average convective heat transfer coefficient than that of samples of Experiment Set A. This is a material effect, since density and

specific heat of cement plaster mix is greater than gypsum.

For the samples of Experiment Set C that are composed of conventional building material, it can be stated that surface texture integrated average convective heat transfer coefficients for all samples increase with increasing wind speed as it can be observed from Figure C.43. Travetine (C2), marble (C3) and andesite (C4) have similar surface texture integrated average convective heat transfer coefficients since they are all natural stones, thus sharing similar physical properties. Distinctively, surface texture integrated average convective heat transfer coefficient of porcelain coated clay tile (C1) sample drastically increases with an increase in wind speed to 6 m/s, since its dispositions is notably different from other samples (such as difference of its thickness). In addition, another observation that can be made from this figure is that surface texture integrated average convective heat transfer coefficients of all samples are within the same range for no wind test case and lower wind speed of 2 m/s, yet distinction in their behavior becomes observable for higher wind speeds.

In fact, for all samples of all experiment sets there is a clear wind effect on the average convective heat transfer coefficients. When the wind increases the surface texture integrated average convective heat transfer coefficients of all samples increase. From Figures C.39, C.41 and C.43 it can be observed that surface texture integrated average convective heat transfer coefficients of all samples increase within the range of 48 % - 433 %.

Table 4.1. Results of correlation test between surface texture integrated average convective heat transfer coefficients and wind speeds (including Pearson r, r^2 and p values).

	r	r^2	p
A0	0.97	0.95	0.013
A1	0.83	0.68	0.086
A2	0.79	0.62	0.107
A3	0.94	0.89	0.029
A4	0.97	0.94	0.016
A5	0.94	0.88	0.031
A6	0.96	0.93	0.018
B0	0.92	0.85	0.039
B1	0.99	0.99	0.003
B2	0.99	0.98	0.005
B3	0.98	0.96	0.010
B4	1.00	1.00	0.001
B5	0.98	0.96	0.009
B6	0.95	0.91	0.023
C1	0.90	0.81	0.050
C2	0.99	0.98	0.005
C3	0.96	0.92	0.020
C4	1.00	0.99	0.002
C5	0.99	0.98	0.004
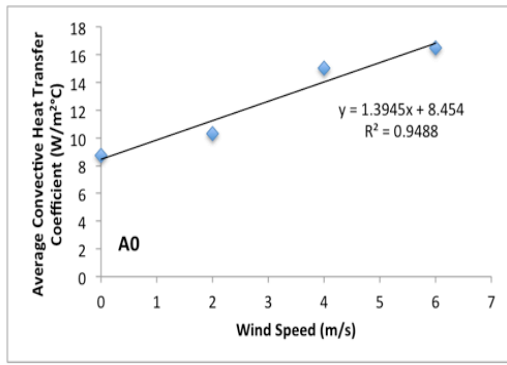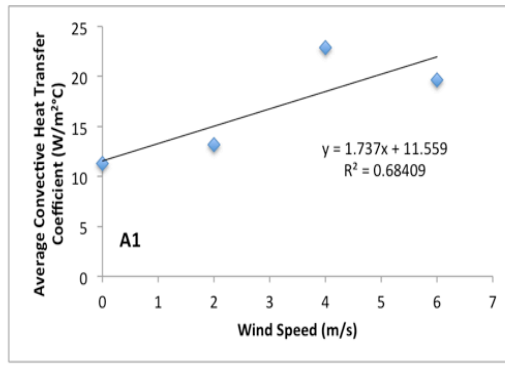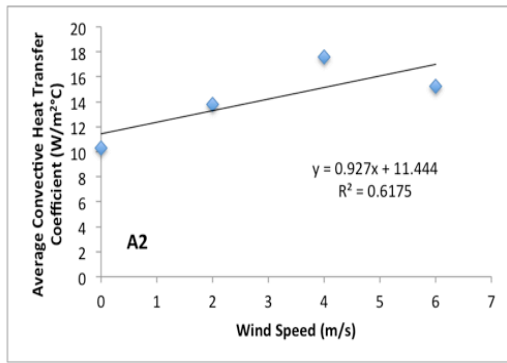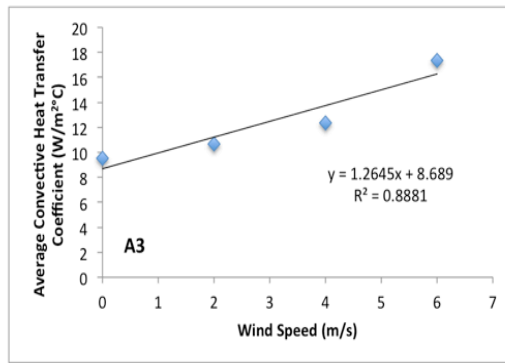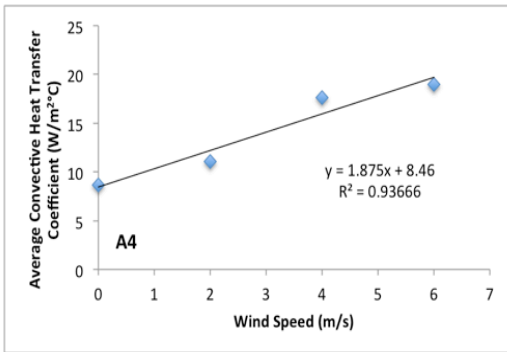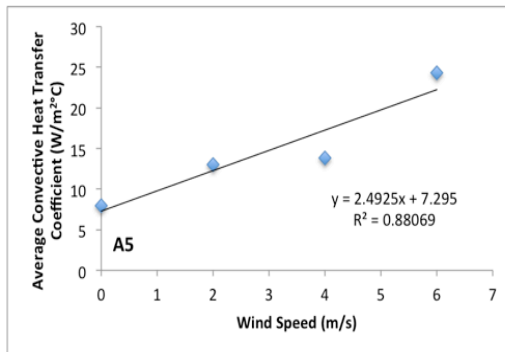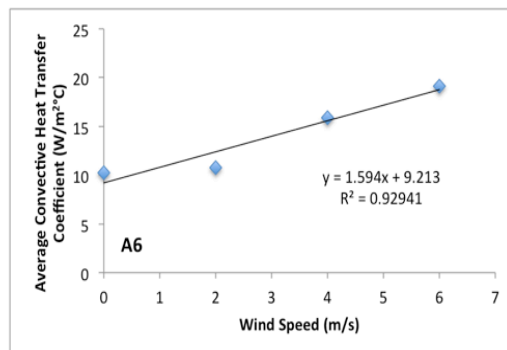
Figure 4.26. Plot of surface texture integrated average convective heat transfer coefficients (in W/m^2°C) vs. wind speed (in m/s) for samples of Experiment Set A with best fitting lines and r^2 values.
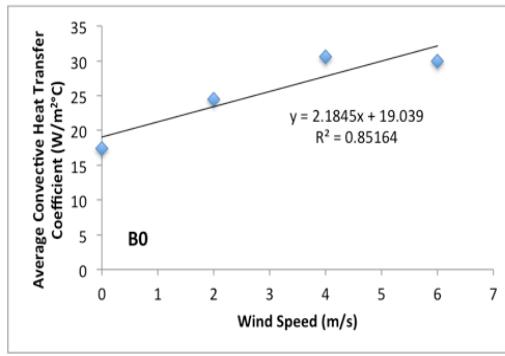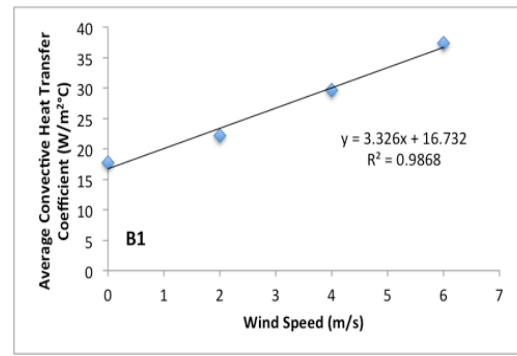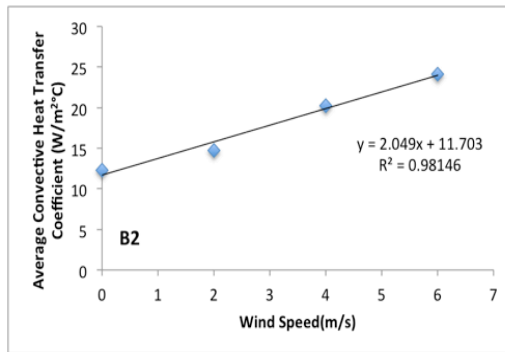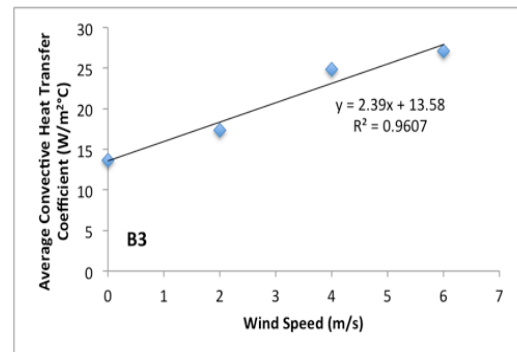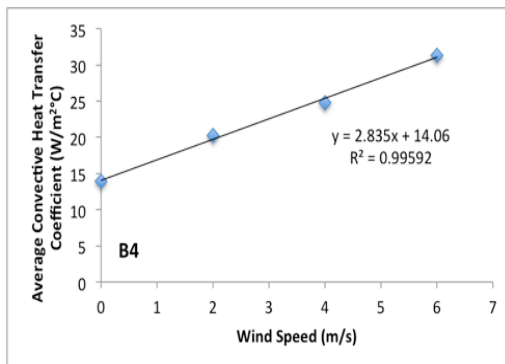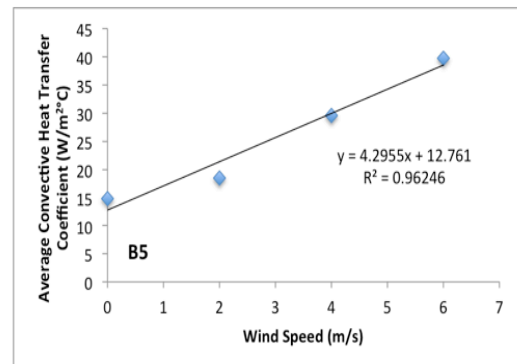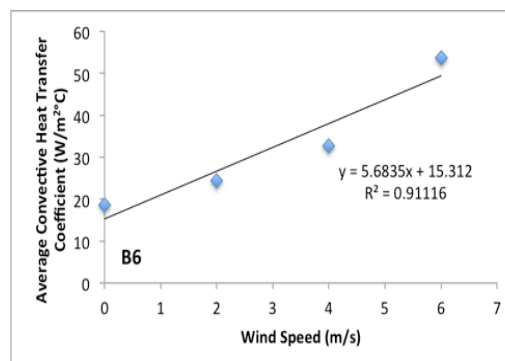
Figure 4.27. Plot of surface texture integrated average convective heat transfer coefficients (in W/m^2°C) vs. wind speed (in m/s) for samples of Experiment Set B with best fitting lines and r^2 values.
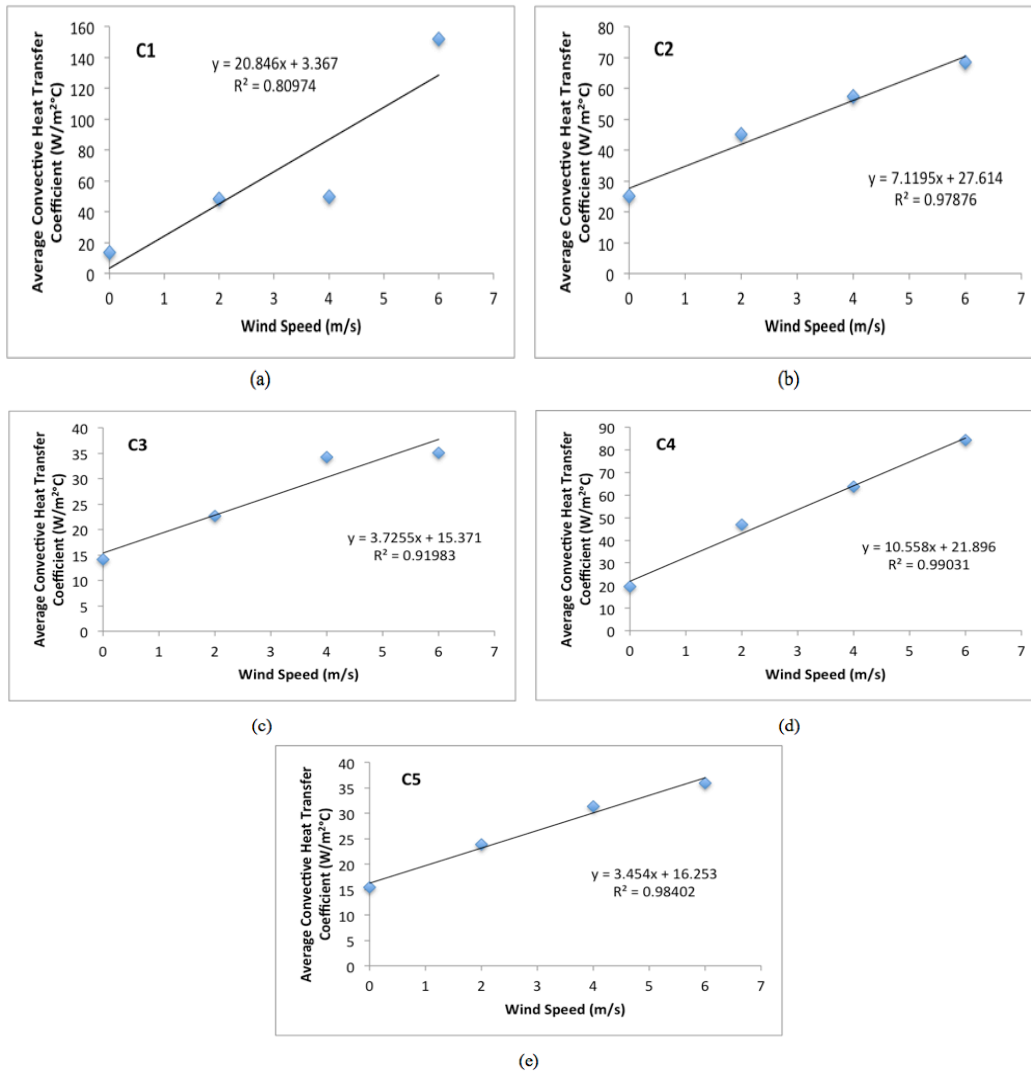
Figure 4.28. Plot of surface texture integrated average convective heat transfer coefficients (in W/m^2°C) vs. wind speed (in m/s) for samples of Experiment Set C with best fitting lines and r^2 values.

In order to examine this effect in depth, correlations between surface texture integrated average convective heat transfer coefficients and wind speeds are produced (Pearson r, r^2 and p values for these correlations are presented in Table 4.1 and individual plots for these correlations are presented in Figures 4.26, 4.27 and 4.28). It has been found that for all samples of all experiment sets there was a significant positive correlation between the surface texture integrated average convective heat transfer coefficients and wind speed, $r > .90$, $p < 0.05$ (it should be noted that only correlations for samples A1 and A2 are non-significant. This may be because of the limited number of data points that are no wind, 2 m/s, 4 m/s and 6 m/s. It is expected from the results that when a more comprehensive data set is collected for various other wind speeds correlations for these two samples would also be significant).

From Figures C.45, C.47 and C.49 it can be observed that the effect of wind angle on surface texture integrated average convective heat transfer coefficients are not as clear as the effect of wind speed. The most substantial behavior that can be deduced for Experiment Set B is that sample with roughness (B1) has the highest average

70

convective heat transfer coefficient within the group of samples that vary in texture (B0, B1 and B2) for all wind angles. Likewise, this is also true for the first group of samples of Experiment Set A, where sample A1 has the highest average convective heat transfer coefficient for all wind angles.

In addition, when second group of samples with textures are considered, samples with highest groove dimensions (B6) also has the highest average convective heat transfer coefficient and the lowest time constant for lower all wind angles. However, this trend is only observable for sample A6 between wind angles 15° to 60°. It is noteworthy to mention again that data for these test cases are collected for wind speed of 6 m/s and as it is aforementioned Experiment Set A behaves distinctively after wind speed threshold of 4 m/s.

Particularly, for wind angles of 60° and 90°, there are no patterns that can be generalized for both experiment sets. Though, by referring to Figures C.45, C.47 and C.49 it can be stated that all samples behave distinctive for the edge angle of 90°. In particular, variation in surface texture of a sample also observed to effect their surface texture integrated average convective heat transfer coefficients and time constants when wind angle is altered.

CHAPTER 5

CONCLUSION

In this thesis the effect of variation in building facade surface texture, which is exposed to distinctive characteristic wind profiles, on heat loss of a building is examined in a series of wind tunnel experiments. The traditional equations that are used for calculating convective heat transfer coefficients does not take into account the effects that are imposed by the surface texture. Therefore, in order to integrate surface texture into convective heat transfer coefficient calculations a new mathematical model has been presented in this thesis as it explained in Chapter 3. This model utilizes a parameter, namely the roughness index (RI), which mathematically defines the surface texture as a ratio of textured surface area to uniform base surface area of a sample. Integration of roughness index in traditional convective heat transfer coefficient equations, as it is presented in data analysis in Chapter 4, enables to normalize the coefficients that are gathered from traditional equations with respect to surface texture. Hence, in this way effects of surface texture of materials under windy conditions are taken into consideration with the calculation of convective heat transfer coefficients while providing more realistic h-values. In this thesis, this revised convective heat transfer coefficient is named as the 'surface texture integrated convective heat transfer coefficient'.

In what follows, empirical findings that are gathered from these sets of experiments are interpreted and concluded in correlation with hypotheses that are presented in Chapter 3 in order to put forth a set of proposals on convective heat transfer coefficient calculations that can be used in future studies by architects, engineers and designers, who are working on building energy fluxes. This chapter concludes with proposals for future research that can enhance or build upon the work that is presented in this thesis.

Overall, hypotheses respectively aimed to investigate the effect of increase in wind speed (for 2 m/s, 4 m/s and 6 m/s), variation of material that is used for preparing samples (gypsum, or cement plaster mix, or conventional building materials) and variation of the type of surface texture on heat loss of the samples. In terms of variation in surface texture two groups of samples that are prepared with gypsum and cement plaster mix are tested, where first involves samples that only vary in their roughness and waviness, and second involves samples that have a surface texture with a grooved line pattern in which all samples have distinctive groove dimensions (groove depth and width).

Accordingly first hypothesis, that states an increase in wind speed is expected to result in an increase in heat loss for all samples of all Experiment Sets A, B and C when the wind angle kept constant without depending on the roughness indexes of the samples, is observed to be consistent with the findings from the experiments. The statistically significant correlations between surface texture integrated average convective heat transfer coefficients and wind speed that are presented in Appendix C support this hypothesis.

Essentially, for all samples with all surface textures that are being tested, including the conventional building materials, an increase in wind speed from 2 m/s to 6 m/s considerably decreases the time that is required for the sample to reach the ambient temperature. This effect also shows up as an increase in surface texture integrated average convective heat transfer coefficients, and as a decrease in time constant values of all samples with increasing wind speed. However, it is crucial to note that this trend is not always applicable for an increase in wind speed from 2 m/s to 4 m/s or from 4 m/s to 6 m/s. For instance, surface texture integrated average convective heat transfer coefficients of some of the samples decrease to a lower value from its value when wind speed is increased from 4 m/s to 6 m/s (i.e. B0 has an surface texture integrated average convective heat transfer coefficient of 30.61 when wind speed is 4 m/s and it is slightly lower 29.92 when the wind speed is 6 m/s). This may be because 2 m/s increase (or change) in wind speed may not be enough for all samples to exhibit this trend. However, with a sufficient increase in wind speed all samples always behave consistent to this trend independent of their material, their surface texture or their roughness index.

In parallel to the effects of wind speed on heat loss trends of the samples, it might be expected to observe an increase in heat loss for all samples with an increase in wind angle from 15° to 90°. However, this prediction is partially coherent with the empirical results. Specifically, there is no linear increase in heat loss that can be correlated with an increase in wind angle. However, some meaningful patterns can be extracted from the behavior of the samples with respect to alternations of wind angle. In details, the grouping that is put forth in sample design is effective in interpreting patterns that occur in samples heat loss behavior. When empirical results are investigated it can be concluded that within the first group of samples, which have variation in roughness and waviness, of both Experiment Sets A and B, samples that have roughness (which are A1 and B1) has distinctive heat loss behaviors from plain and wavy samples (A0, A2 and B0, B2) only for angles within the range of 15° to 60° (both included). Within this range of angles samples with roughness have the highest surface texture integrated average convective heat transfer coefficients and lowest time constants. Moreover, also for the same range of wind angles within the second group of samples, which vary in groove dimensions, of both Experiment Sets A and B (specifically A3, A4, A5, A6 and B3, B4, B5, B6) only samples with highest groove dimensions A6 and B6 behave distinctively as they have the highest surface texture integrated average convective heat transfer coefficients.

These results are essentially a step forward to enlighten some of the gaps in the literature about effects of change in wind angle on heat loss behaviors. Specifically, it can be concluded that surface texture also plays a crucial role in determining heat loss behaviors over convective heat transfer coefficients and time constant values. That is to say, variation in texture from plain to rough, or from smaller groove dimensions to larger groove dimensions, result in an increase in heat loss.

Grouping effects are also supportive to conclude on second and the third hypotheses. Second hypothesis aimed to expect an increase in the effect that is observed for heat loss for the first group of samples of both Experiment Sets A and B, when texture alternates from being plain to rough or wavy. When the wind speed is kept constant and heat loss behaviors of three samples of the first group is examined for the samples of Experiment Set A it can be concluded that samples having surfaces with roughness and waviness have higher surface texture integrated average convective heat transfer coefficients and lower time constants for wind speeds 2 m/s and 4 m/s, when compared with sample that has plain surface (note that for the first group of samples of Experiment Set A that are prepared from gypsum this difference is not clearly observable when wind speed is 6 m/, yet reasons for this distinctive behavior will be elaborated in what follows when discussing material dependence). Similarly, this effect is also observable for first group of samples of Experiment Set B, but this time only for wind speed 6 m/s and only for sample with roughness B1 (likewise lack of this effect for wind speeds of 2 m/s and 4 m/s will be explained in relation with material dependence).

Therefore, from these empirical results it can be concluded that increase in roughness and waviness as a deviation from plain surface increases heat loss for specific ranges of wind speeds, where this range is dependent on the disposition of the sample. To be clear, effects that are expected by the second hypothesis are only observable for these specific ranges since a specific material effect gets involved in heat loss behavior of the samples.

In parallel, third hypothesis expects an increase in heat loss of the second group of samples of both Experiment Sets A and B with increasing groove dimensions and in regards with the empirical findings it can be concluded that this hypothesis holds. Particularly, for the second group of samples with grooved macro surface textures of both Experiment Sets A and B samples with two of the largest groove dimensions (which are A5, A6 and B5, B6) have the highest average convective heat transfer coefficients for highest wind speed of 6 m/s within the groups that they are a part of. Consequently, for wind speed of 4 m/s still A6 and B6 has the highest average convective heat transfer coefficients and lowest time constants within the second groups, while B5 also starts to behave distinctively like these two samples. Therefore, it can be stated that the effect that is described by the fourth hypothesis becomes observable for higher wind speeds.

Therefore, once again heat loss is crucially dependent on surface texture, since it increases when groove dimensions increase. Notably, it can be deduced that there is a

threshold wind speed for this effect to become observable, which indicates that physical properties of the sample also has an influence of the heat loss trend that it exhibits.

As a follow up, fourth hypothesis investigates whether variation in roughness and waviness has a greater impact on heat loss when compared with the effect that is caused by variation in surface texture through different groove dimensions. However, from all findings it can be concluded that there is not such hierarchy in the magnitude of the effect on heat loss. That is, having variation in roughness and waviness rather than grooved texture does not essentially have a greater impact on surface texture integrated convective heat transfer coefficients or on time constant values. Specifically, for both Experiment Set A and B within the first group of samples that have rough surface texture have greater average convective heat transfer coefficients and lower time constants from samples that have wavy surface texture for all wind speeds. Therefore, for the first group it can be concluded that having roughness on the surface increases heat loss more than having waviness on the surface. Similarly for the second group of samples only samples with the highest groove dimensions have comparatively higher average convective heat transfer coefficients from other samples of the group for all wind speeds.

In regards, fifth hypothesis expects these trends and effects to be observable in a material independent manner. To be clear, according to this hypothesis effects that are observed in the empirical results has to be generalizable for all samples that are having distinct materials but same surface textures. Therefore, it is watched for whether these are effects solely dependent on the variation in surface texture and nothing else.

However, it is hard to draw such a specific conclusion from the findings that are presented in Chapter 4. Particularly, as it is aforementioned surface texture integrated average convective heat transfer coefficients and time constants depend on specific material dependent variables, such as specific heat and density. Since each and every distinct material does not have the same physical disposition these variables vary for the material that is used to prepare the sample. As a result, heat capacities of samples that are prepared from different materials (such as gypsum and cement plaster mix in our case) alter even if they have the same surface texture and roughness index. Therefore, some of the effects that can be observed for a specific sample with a specific surface texture may not be observable for another sample if it is prepared from a distinct material within certain a range of wind speed and wind angle.

For instance, the discussion that is made for the second hypothesis on first group of samples of both Experiment Sets A and B may be illustrative for material effects. In that case, described effect becomes observable for samples of Experiment Set A at wind speeds 2 m/s and 4 m/s, whereas it is observable for samples of Experiment Set B only when the wind speed is 6 m/s. This is an indication that abovementioned material effects only allow samples that are prepared from gypsum and cement plaster mix to become observable only within specific ranges. It is essential to note that the heat loss trends that are being investigated are dependent on many distinct factors,

thus effects that are discussed here are results of an interplay of more than one straightforward variable.

Concerning the material effect that is described hereby, it is not possible to completely relate these findings with behaviors of conventional samples. However, as the last hypothesis expects heat loss trends of samples of conventional materials and samples of Experiment Sets A and B that are having similar surface textures can be compared and contrasted over their surface texture integrated average convective heat transfer coefficients and time constants. Among those sample of marble (C3) has a plain surface that is similar to that of A0 and B0. When time constants of marble are compared with those samples it can be stated that they behave similar to those samples and its surface texture integrated average convective heat transfer coefficient is within the same range of those for all wind speeds. Similarly, sample of travertine (C2) has a rough surface, which is similar to the surface texture of samples A1 and B1. Therefore, it can be concluded that samples that are having similar or the same surface textures have similar heat loss trends for a specific wind profile.

It is well known that simulation tools or calculation methods, which provide a medium for inspection of designs and for carrying out calculations, are at disposal of architects, researchers, technical designers and engineers that are working on building energy fluxes. Calculations that are used in these are based on the theory of building heat transfer, thus using accurate heat transfer coefficients in them is essential to obtain results that can precisely simulate real life phenomenon. As it is mentioned in Chapter 2, in order to enhance the accuracy of heat transfer calculations numeric or experimental studies are carried within the domain, yet none of those studies focus on the effect of varying surface texture on convective heat transfer coefficients. Findings that are presented in this thesis and the methodology that is adopted can serve as a baseline either for those who are using heat transfer calculations in numeric studies, or for enhancing precision of the calculations that are carried out on simulation tools.

Hereby some clear indications about the magnitude of effect of surface texture on convective heat transfer coefficients have been put forth. Specifically, convective heat transfer coefficient and time constant values that are presented in Appendix C can be used in calculations for the wind speeds, wind angles and materials that have been reported in this thesis. Notably, within the literature necessary data on wind maps are readily available and thus they can be used to find out the correct convective heat transfer coefficients for the surface that is under investigation from abovementioned reference tables of this thesis.

Moreover, these data could be useful for manufacturing prospect materials with the desired surface texture to be used in building facades or for choosing the right material with a suitable surface texture to be used for the facades of a specific building. Apparently, the choice that is made for using the suitable surface texture is beneficial for the designer and architect to apply passive cooling or heating depending on the location of the building. In addition, it is proposed that specific suitable customized surface textures (that are durable, easy to maintain, and in harmony with the

surroundings in terms of its color and other physical properties) can be manufactured for specific buildings and for specific locations with collaboration of industrial designers, architects, researchers and engineers.

The findings that are outlined herein are rather limited when whole span of wind profiles and materials that are actively used in building facades are taken into account. Therefore, following proposals for future research is presented here to enhance the results that are presented in this thesis:

- Experiments can be extended for a wider range of wind speeds and materials in order to provide more detailed data sets for convective heat transfer coefficients and time constant values, which are covering a broad span of situations.
- Distinct and reproducible surface texture groups should be created and investigated in order to detail the knowledge on its effects on convective heat transfer coefficients and time constant values for varying wind profiles. These surface textures may include patterns that are not tested within this thesis.
- Other than surface texture of building facades, effects of surface texture and material of other elements of a building (such as doors or windows) on heat loss must be investigated for varying wind profiles in an experimental study.
- Experimental setup of this thesis enforces to carry out an examination over windward surfaces, however further experimental research must also be conducted to examine leeward surfaces.
- A similar experimental study must also be completed in order to investigate effects that are caused by variation in surface texture of roofs and their heat loss behaviors, since roofs majorly effect the heating or cooling demands of a building.
- Full-scale experimental studies on real buildings must be realized at site for further validation of the effects that are presented.
- Further research must be conducted to devise a systematic method to find out the appropriate surface texture for a specific material in order for that material to have a desired convective heat transfer coefficient under predetermined wind profiles.

REFERENCES

Allegrini, J., Dorer, V., & Carmeliet, J. (2012). Analysis of convective heat transfer at building façades in street canyons and its influence on the predictions of space cooling demand in buildings. *Journal of Wind Engineering and Industrial Aerodynamics*, *104-106*, 464–473. doi:10.1016/j.jweia.2012.02.003

Barlow, J., & Belcher, S. (2002). A Wind Tunnel Model For Quantifying Fluxes In The Urban Boundary Layer. *Boundary-Layer Meteorology*, 131–150. Retrieved from http://link.springer.com/article/10.1023/A:1015555613672

Beausoleil-Morrison, I. (2001). Flow Responsive Modelling of Internal Surface Convection. *Seventh International IBPSA Conference*. Retrieved from http://www.inive.org/members_area/medias/pdf/Inive/IBPSA/UFSC507.pdf

Blocken, B., Stathopoulos, T., & Carmeliet, J. (2007). CFD simulation of the atmospheric boundary layer: wall function problems. *Atmospheric environment*, *41*(2), 238–252. doi:10.1016/j.atmosenv.2006.08.019

Blocken, B., Stathopoulos, T., Carmeliet, J., & Hensen, J. (2011). Application of CFD in building performance simulation for the outdoor environment : an overview. *Journal of Building Performance Simulation*, 4(2), 157–184. Retrieved from http://www.bwk.tue.nl/bps/hensen/publications/09_BS09_blocken.pdf

Cheng, Y., Niu, J., Gao, N. (2012) Thermal Comfort Models: A Review and Numerical Investigation. *Building and Environment*, 47(2012), 13-22.

Chi, T., Ballinger, T., Olds, R., & Zecchino, M. (2005). Surface Texture Analysis Using Dektak Stylus Profilers. *Veeco Instruments Application Notes*, 15.

Clear, R., Gartland, L., & Winkelmann, F. (2003). An empirical correlation for the outside convective air-film coefficient for horizontal roofs. *Energy and Buildings*, (January). Retrieved from http://www.sciencedirect.com/science/article/pii/S0378778802002402

Defraeye, T., Blocken, B., & Carmeliet, J. (2011a). An adjusted temperature wall function for turbulent forced convective heat transfer for bluff bodies in the atmospheric boundary layer. *Building and Environment*, *46*(11), 2130–2141. doi:10.1016/j.buildenv.2011.04.013

Defraeye, T., Blocken, B., & Carmeliet, J. (2011b). Convective heat transfer coefficients for exterior building surfaces: Existing correlations and CFD modelling. *Energy Conversion and Management*, *32*(0), 1–20. Retrieved from http://www.sciencedirect.com/science/article/pii/S019689041000333X

Defraeye, T., Blocken, B., & Carmeliet, J. (2012). CFD simulation of heat transfer at surfaces of bluff bodies in turbulent boundary layers: Evaluation of a forced-convective temperature wall function for mixed convection. *Journal of Wind Engineering and Industrial Aerodynamics*, *104-106*, 439–446. doi:10.1016/j.jweia.2012.02.001

Desta, T. Z., Langmans, J., & Roels, S. (2011). Experimental data set for validation of heat, air and moisture transport models of building envelopes. *Building and Environment*, *46*(5), 1038–1046. doi:10.1016/j.buildenv.2010.11.002

Duffie, J. A., & Beckman, W. A. (2006). *Solar engineering of thermal processes*. John Wiley & Sons.

Djunaedy, E., Hensen, J., & Loomans, M. (2005). External Coupling Between CFD and Energy Simulation: Implementation and Validation. *ASHRAE Transactions*, *111*, 612–624. Retrieved from http://www.bwk.tue.nl/bps/Hensen/publications/05_ashrae_cfd.pdf

García, L., Hernández, J., & Ayuga, F. (2006). Analysis of the materials and exterior texture of agro-industrial buildings: a photo-analytical approach to landscape integration. *Landscape and Urban Planning*, *74*(2), 110–124. doi:10.1016/j.landurbplan.2004.10.007

Grimmond, C. S. B., Blackett, M., Best, M. J., Baik, J.-J., Belcher, S. E., Beringer, J., Bohnenstengel, S. I., et al. (2011). Initial results from Phase 2 of the international urban energy balance model comparison. *International Journal of Climatology*, *31*(2), 244–272. doi:10.1002/joc.2227

Hagishima, A., & Tanimoto, J. (2003). Field measurements for estimating the convective heat transfer coefficient at building surfaces. *Building and Environment*, *38*(7), 873–881. doi:10.1016/S0360-1323(03)00033-7

Incropera, F. P., Lavine, A. S., & DeWitt, D. P. (2011). *Fundamentals of heat and mass transfer*. John Wiley & Sons Incorporated.

Isyumov, N. (Ed.). (1998). *Wind Tunnel Studies of Buildings and Structures* (No. 67). ASCE Publications.

Liu, J., Srebric, J., & Yu, N. (2013). Numerical simulation of convective heat transfer coefficients at the external surfaces of building arrays immersed in a turbulent boundary layer. *International Journal of Heat and Mass Transfer*, *61*, 209–225. doi:10.1016/j.ijheatmasstransfer.2013.02.005

Liu, Y., & Harris, D. J. (2007). Full-scale measurements of convective coefficient on external surface of a low-rise building in sheltered conditions. *Building and Environment*, *42*(7), 2718–2736. doi:10.1016/j.buildenv.2006.07.013

Lunde, P. J. (1980). *Solar thermal engineering: space heating and hot water systems*. John Wiley & Sons

Meteoroloji Genel Müdürlüğü (2002). *Türkiye Rüzgar Atlası*. Retrieved from http://www.mgm.gov.tr/arastirma/yenilenebilir-enerji.aspx?s=ruzgaratlasi

Mirsadeghi, M., & Cóstola, D. (2013). Review of external convective heat transfer coefficient models in building energy simulation programs: implementation and uncertainty. *Applied Thermal Engineering*, *56*(July), 134–151. Retrieved from http://www.sciencedirect.com/science/article/pii/S1359431113001543

Nottrott, a., Onomura, S., Inagaki, a., Kanda, M., & Kleissl, J. (2011). Convective heat transfer on leeward building walls in an urban environment: Measurements in an outdoor scale model. *International Journal of Heat and Mass Transfer*, *54*(15-16), 3128–3138. doi:10.1016/j.ijheatmasstransfer.2011.04.020

Ostovan, Y. (2011) *Experimental Investigation of Waveform Tip Injection on the Characteristics of the Tip Vortex*. Unpublished doctoral dissertation, Middle East Technical University, Ankara, Turkey.

Palyvos, J. a. (2008). A survey of wind convection coefficient correlations for building envelope energy systems' modeling. *Applied Thermal Engineering*, *28*(8-9), 801–808. doi:10.1016/j.applthermaleng.2007.12.005

Qu, Y., Milliez, M., Musson-Genon, L., & Carissimo, B. (2012). Numerical study of the thermal effects of buildings on low-speed airflow taking into account 3D atmospheric radiation in urban canopy. *Journal of Wind Engineering and Industrial Aerodynamics*, *104-106*, 474–483. doi:10.1016/j.jweia.2012.03.008

Santamouris, M., & Kolokotsa, D. (2013). Passive cooling dissipation techniques for buildings and other structures: The state of the art. *Energy and Buildings*, *57*, 74–94. doi:10.1016/j.enbuild.2012.11.002

Santos, P. M. D., & Júlio, E. N. B. S. (2013). A state-of-the-art review on roughness quantification methods for concrete surfaces. *Construction and Building Materials*, *38*, 912–923. doi:10.1016/j.conbuildmat.2012.09.045

Seferis, P., Strachan, P., Dimoudi, a., & Androutsopoulos, a. (2011). Investigation of the performance of a ventilated wall. *Energy and Buildings*, *43*(9), 2167–2178. doi:10.1016/j.enbuild.2011.04.023

Seker, D., & Tavil, A. (1996). Evaluation of Exterior Building Surface Roughness Degrees by Photogrammetric Methods. *Building and environment*, *31*(4), 393–398. Retrieved from http://www.sciencedirect.com/science/article/pii/0360132395000518

Smith, J.O. (2010). *Determination of the convective heat transfer coefficients from the surfaces of buildings within urban street canyons*. (PhD Dissertation). Department of Mechanical Engineering, University of Bath, UK.

Tavil, A. (2004). Thermal behavior of masonry walls in Istanbul. *Construction and Building Materials*, *18*(2), 111–118. doi:10.1016/j.conbuildmat.2003.08.014

Wieringa, J. (2001). New revision of Davenport roughness classification. *Proc., 3EACWE, Eindhoven, The Netherlands*, 285-292.

APPENDIX A

TECHNICAL SPECIFICATIONS OF THE SAMPLE MATERIALS

Table A.1. Technical specifications of the materials used for Experiment Sets A, B and C.

	Density (kg/m^3)	Specific Heat (J/kg°K)
Experiment Set A		
Gypsum Mix	975	787
Experiment Set B		
Cement Plaster Mix	2195	837
Experiment Set C		
Porcelain Coated Clay Tile (C1)	1900	800
Travertine (C2)	2640	1213
Marble (C3)	2720	795
Andesite (C4)	2663	840
Acrylic Resin Composite Siding Material (C5)	1190	1500

Source: technical specification sheet of Lafarge Dalsan SIVATEK Manual Plaster with Perlite for gypsum mix, from technical specification sheet of BASF EMACO S88 for cement plaster mix, from technical specification sheet of Ege Seramik Cronos Gold for porcelain coated clay tile, from technical specification sheet of Emek Mermer Sanayi Ticaret A.S for travertine, marble and andesite, and from technical specification sheet of Stropol Siding for acrylic resin composite siding material.

APPENDIX B

TECHNICAL SPECIFICATIONS OF THE EQUIPMENT AND SOFTWARE USED IN THE EXPERIMENTAL SETUP

Table B.1. Technical specifications of the data acquisition system. Excerpted from technical specification sheet of National Instruments NI cDAQ-9172.

Chassis	cDAQ-9172
Channels per Chassis	Up to 256 analog input, or 32 analog output, or 64 digital I/O
Analog Resolution	Up to 24 bits
Analog Sampling Rate	Up to 400 kS/s per module
Analog Throughput	3.2 MS/s throughput
Dimensions	25 cm x 9 cm x 9 cm
Power Supply	11 V – 30 V
Connection	High-speed USB connection to PC
I/O Module Slots	Up to 8 C series I/O modules
Environmental Certifications	0 to 55 °C operating temperature 30 g shock rating
Application and Technology	Mix analog, digital and sensor measurements in the same system
Operating System Compatibility	Windows, Windows 2000/XP, Windos Vista x64/x86
Driver Information	NI-DAQmx
Software Compatibility	LabVIEW

Table B.2. Technical specifications of the experimental control software. Excerpted from technical specification sheet of LabVIEW 8.2.

Application Areas	Automating measurements and processing signal data, instrument control, automating test and validation systems, designing embedded control and monitoring systems, academic teaching
Minimum System Requirements	Pentium III/Celeron 866 MHz or equivalent processor 256 MB RAM Windows 8/7/Vista/XP SP3/ Server 2003/ Server 2008 operating system 353 MB disk space

Table B.3. Technical specifications of the 3-D laser scanner. Excerpted from technical
specification sheet of Faro Focus 3-D laser scanner.

Size	24 cm x 20 cm x 10 cm
Weight	5.0 kg
Laser Power	20 mW
Laser Wavelength	905 nm
Range Focus 3D	60 cm – 12000 cm
Measurement Speed	122,000 / 244,000 / 488,000 / 976,000 points per second
Resolution	Up to 70 megapixel color
Dynamic Color Feature	Automatic adaptation of brightness
Vertical Field of View	305° / 360°
Step Size	0.009°
Max. Vertical Scan Speed	5,820 rpm or 97 Hz

Table B.4. Technical specifications of AutoCAD Civil 3-D 2011.

Application Areas

AutoCAD® Civil 3D® tools support Building Information Modeling (BIM) processes and help reduce the time it takes to design, analyze, and implement changes. Evaluate more what-if scenarios and optimize project performance. Streamline project workflows by automating time-consuming tasks.
Use an integrated process built on a coordinated, consistent, digital model for design, analysis, visualization, documentation, and construction.
Surface Modeling and Grading:
Civil 3D is a software package, which use tools for dynamic surface creation, can use point clouds to digitize as-built features and terrains models for grading. Surfaces from traditional survey data, such as points and break lines can be built. Utilize large data sets from aerial photogrammetry, laser scanning, and digital elevation models by taking advantage of the surface reduction tools. View the surface as contours or triangles, or create elevation and slope banding analysis. Use surfaces as a reference for creating intelligent objects that maintain dynamic relationships to the source data.

Minimum System Requirements

For 64-Bit AutoCAD Civil 3D 2011:
    Windows 7 Enterprise, Ultimate, Professional, or Home Premium (64-bit);
    Windows Vista Enterprise, Business, Ultimate (SP1 or SP2, 64-bit); or
    Windows XP Professional x64 Edition (SP2, 64-bit).
    AMD Athlon 64, AMD Opteron, Intel® Xeon with Intel® EM64T support,
    Intel® Pentium® 4 with Intel EM64T support.
    4 GB RAM minimum required, 8 GB RAM minimum recommended.
    7 GB disk space with 2 GB free after installation.
    1,280 x 1,024 true color video display adapter (true color) 128 MB or
    greater, Pixel Shader 3.0 or greater, Direct3D®-capable workstation-class
    graphics card. 1,600 x 1,200 or greater recommended. Multiple monitors
    are supported.
    Microsoft® Internet Explorer® 7.0 or later and DVD drive.

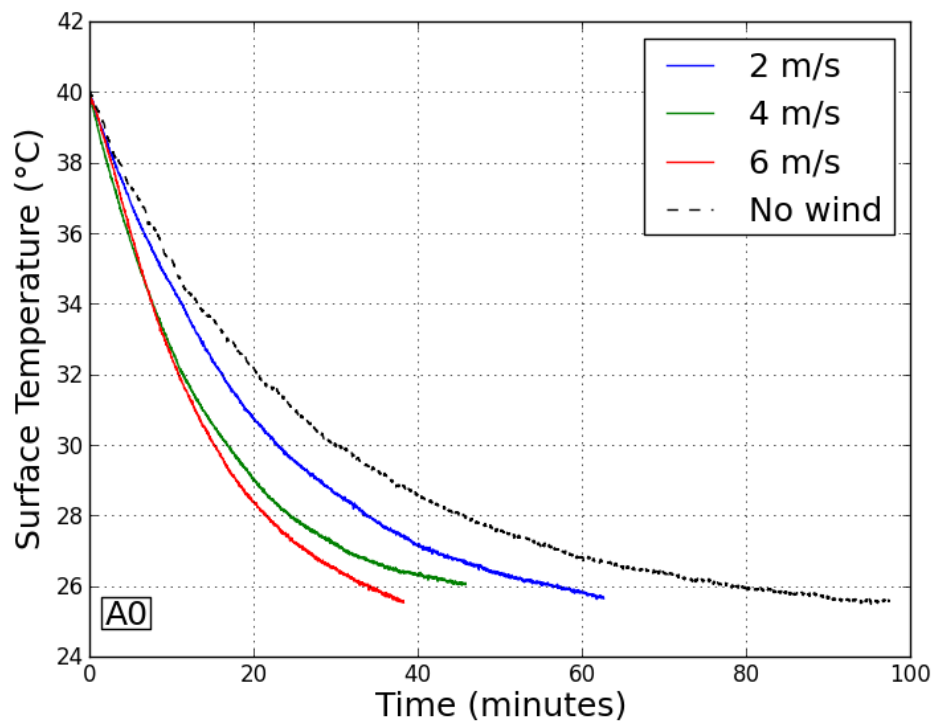# APPENDIX C

SUPPLEMENTARY FIGURES AND TABLES

Figure C.1. Plot of surface temperature (in °C) vs. time (in minutes) curves for sample A0 for varying wind speeds of 2 m/s, 4 m/s and 6 m/s where the wind angle is kept fixed at 90° and the no wind test case.
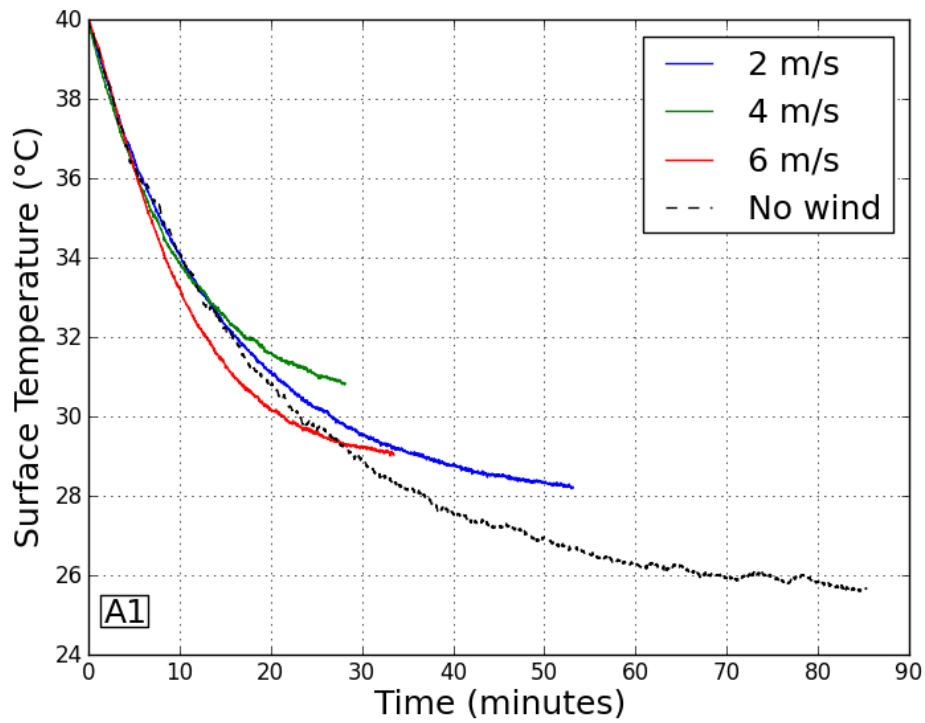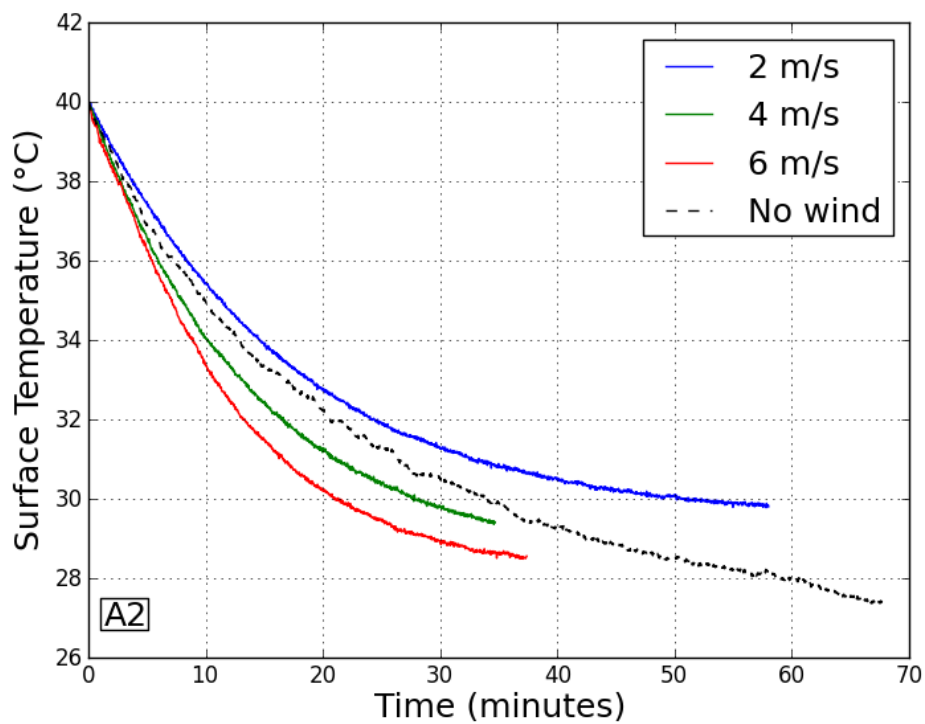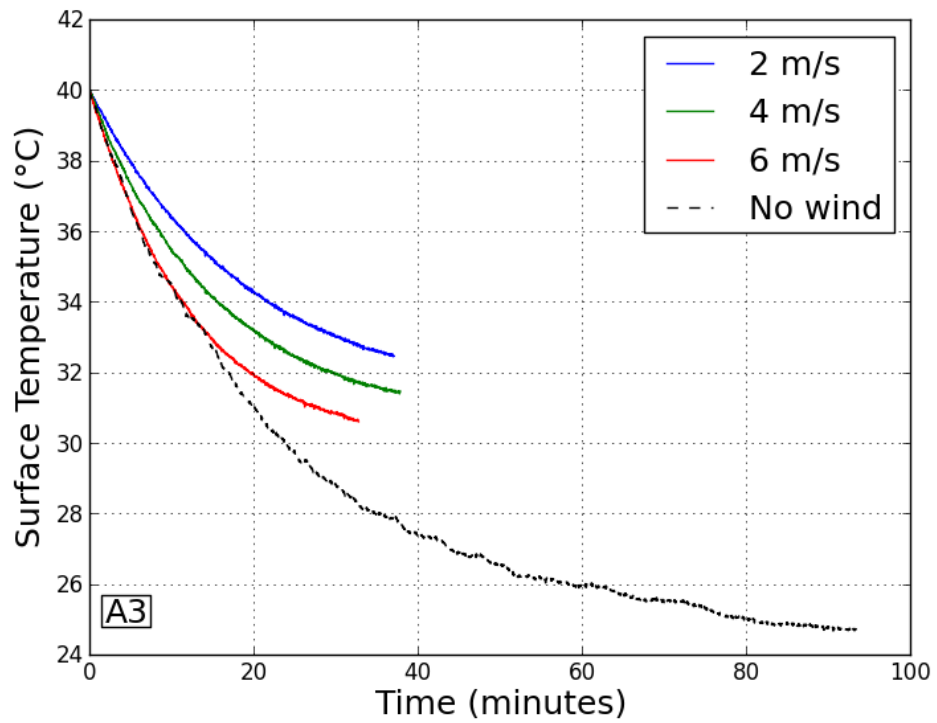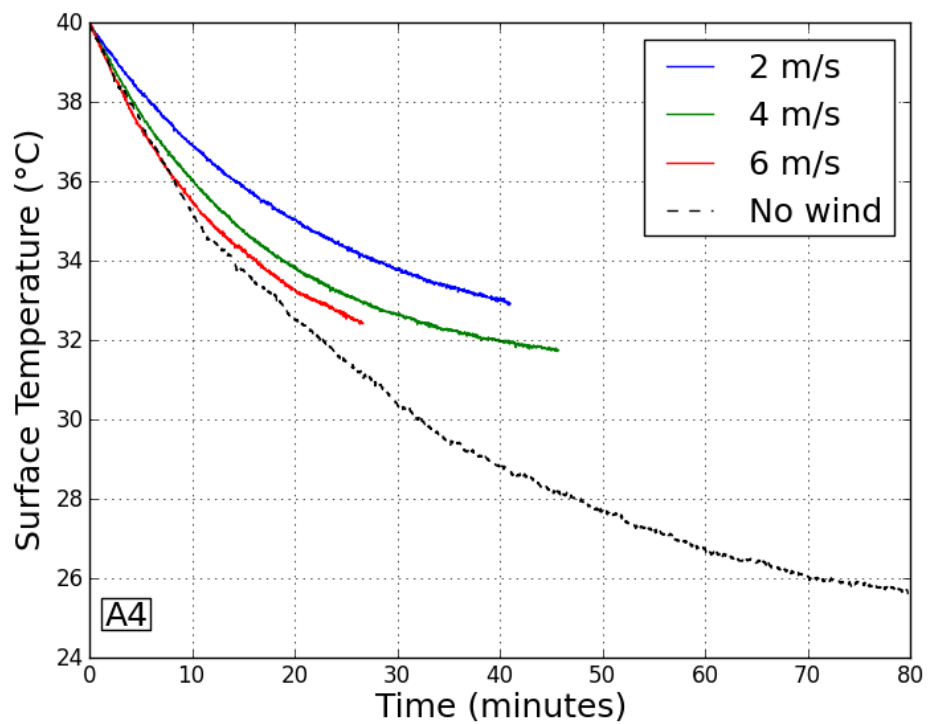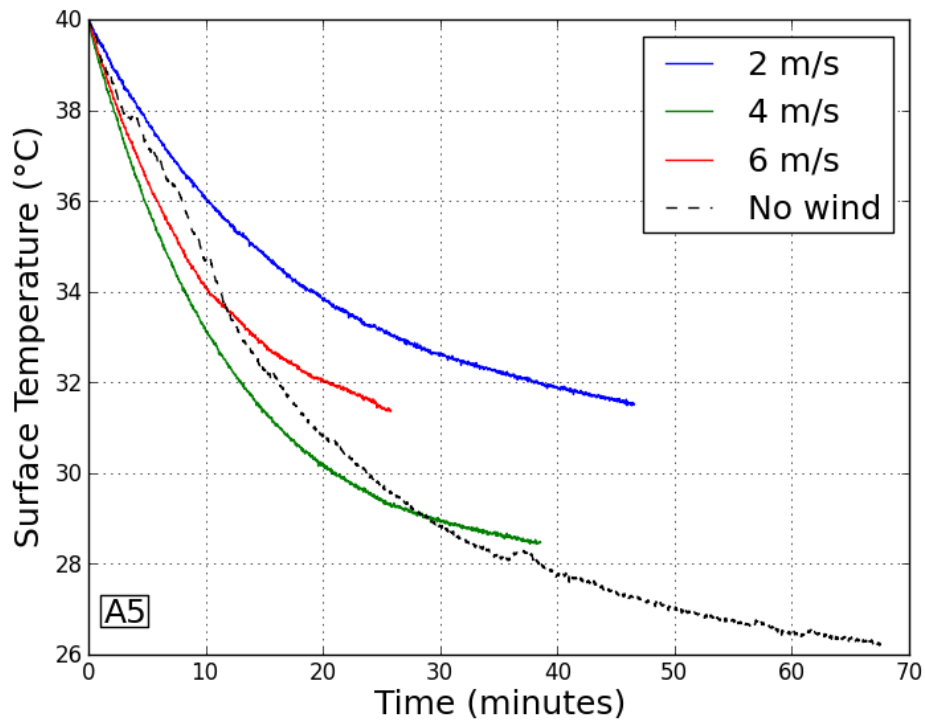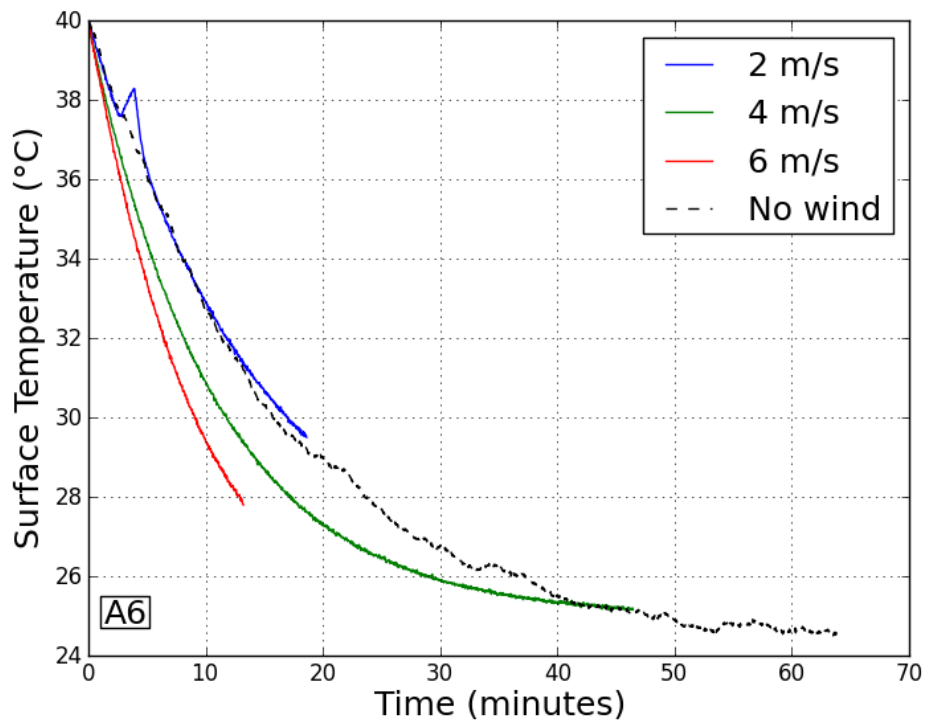
Figure C.2. Plot of surface temperature (in °C) vs. time (in minutes) curves for sample A1 for varying wind speeds of 2 m/s, 4 m/s and 6 m/s where the wind angle is kept fixed at 90° and the no wind test case.
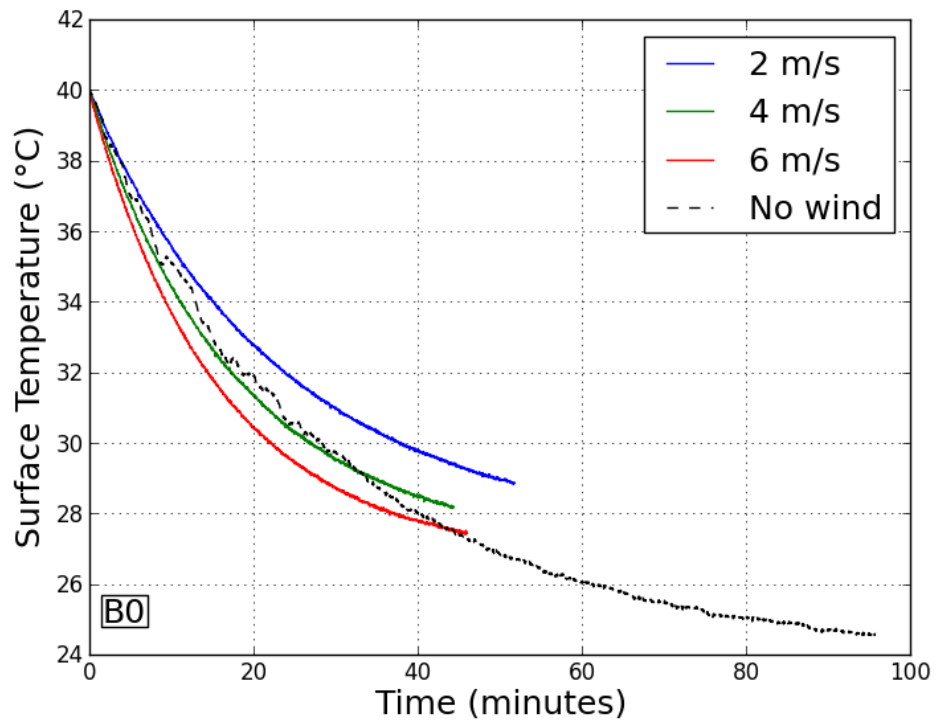

Figure C.3. Plot of surface temperature (in °C) vs. time (in minutes) curves for sample A2 for varying wind speeds of 2 m/s, 4 m/s and 6 m/s where the wind angle is kept fixed at 90° and the no wind test case.
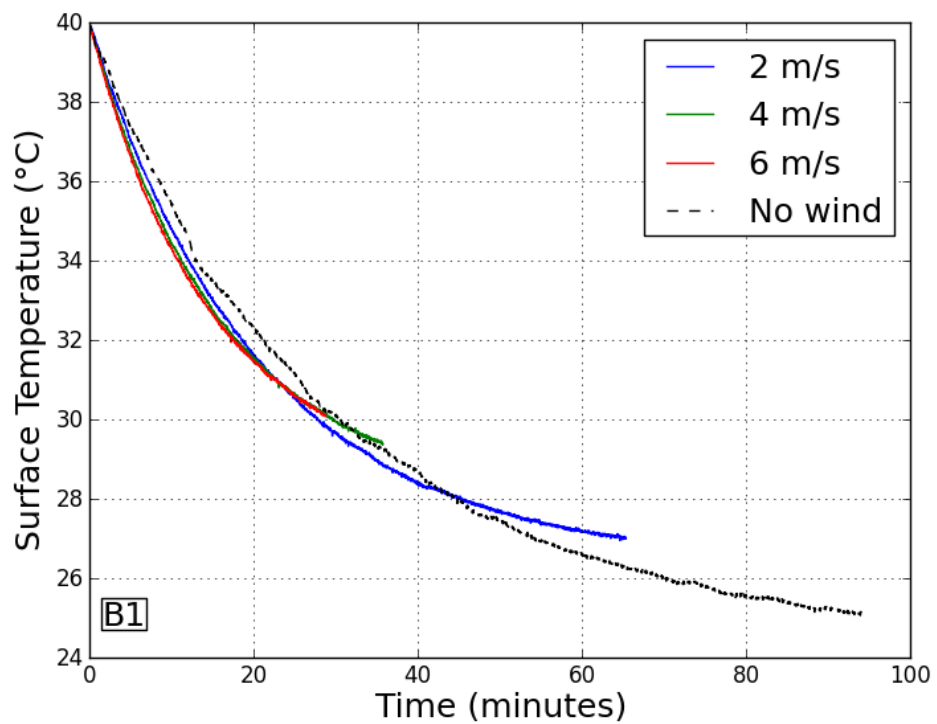
Figure C.4. Plot of surface temperature (in °C) vs. time (in minutes) curves for sample A3 for varying wind speeds of 2 m/s, 4 m/s and 6 m/s where the wind angle is kept fixed at 90° and the no wind test case.

Figure C.5. Plot of surface temperature (in °C) vs. time (in minutes) curves for sample A4 for varying wind speeds of 2 m/s, 4 m/s and 6 m/s where the wind angle is kept fixed at 90° and the no wind test case.
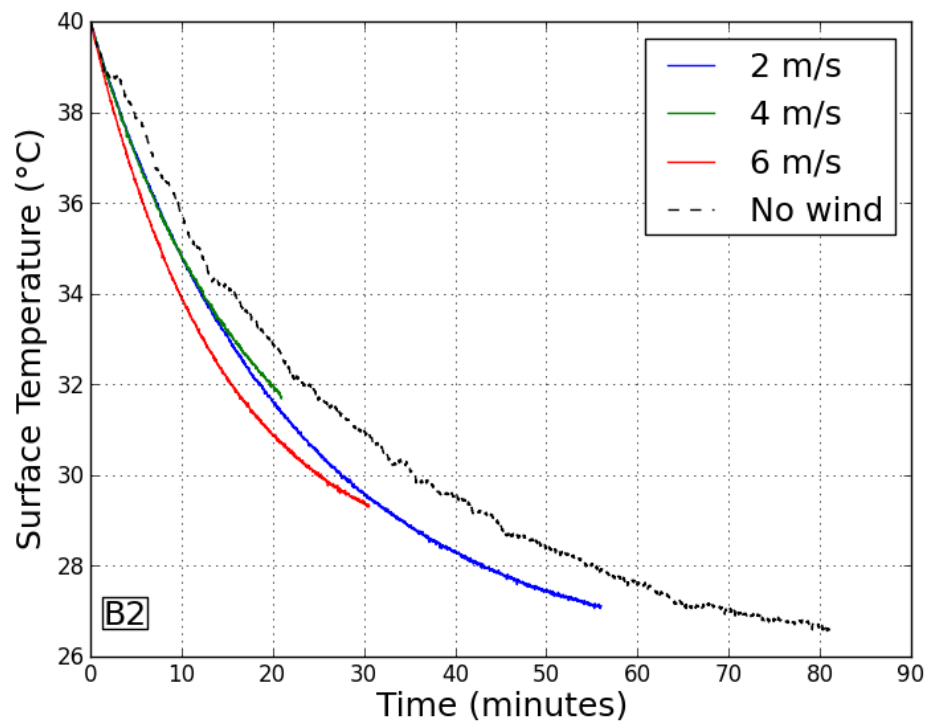
Figure C.6. Plot of surface temperature (in °C) vs. time (in minutes) curves for sample A5 for varying wind speeds of 2 m/s, 4 m/s and 6 m/s where the wind angle is kept fixed at 90° and the no wind test case.
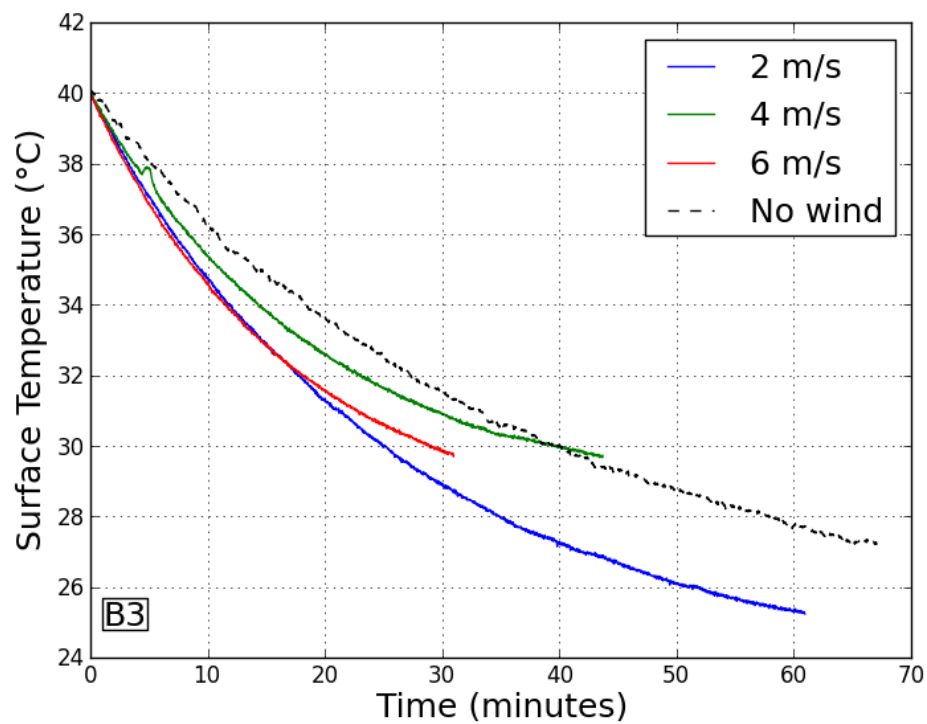

Figure C.7. Plot of surface temperature (in °C) vs. time (in minutes) curves for sample A6 for varying wind speeds of 2 m/s, 4 m/s and 6 m/s where the wind angle is kept fixed at 90° and the no wind test case.

Figure C.8. Plot of surface temperature (in °C) vs. time (in minutes) curves for sample B0 for varying wind speeds of 2 m/s, 4 m/s and 6 m/s where the wind angle is kept fixed at 90° and the no wind test case.
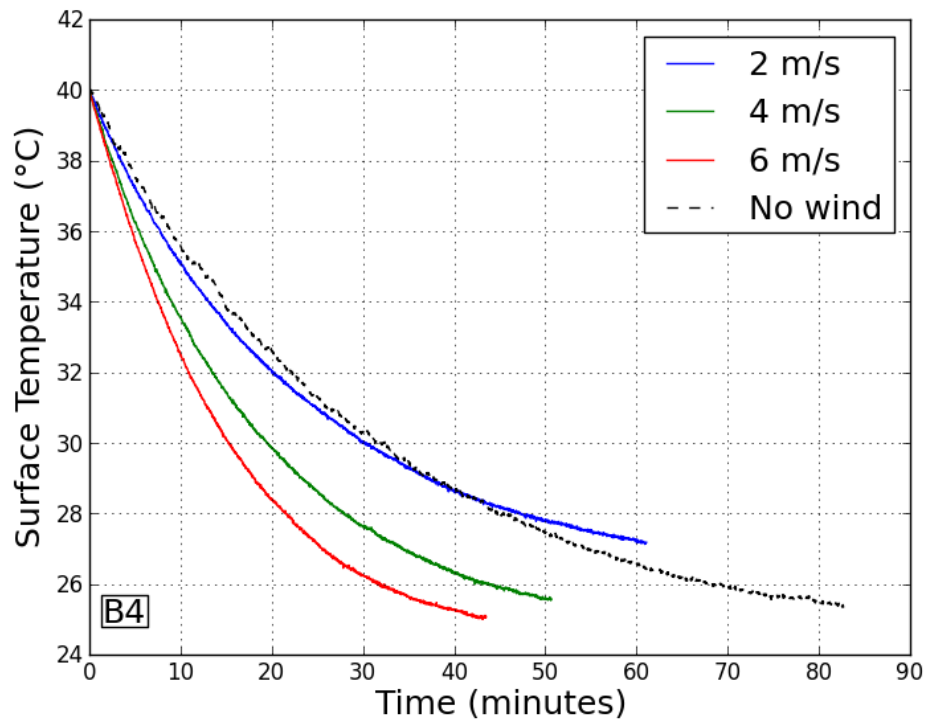

Figure C.9. Plot of surface temperature (in °C) vs. time (in minutes) curves for sample B1 for varying wind speeds of 2 m/s, 4 m/s and 6 m/s where the wind angle is kept fixed at 90° and the no wind test case.
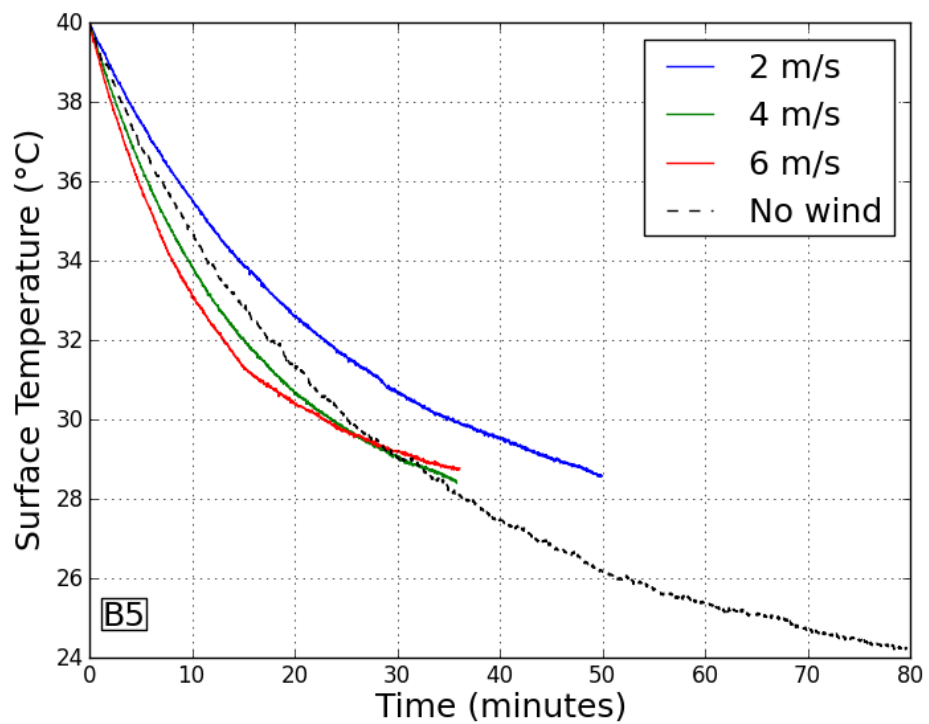
91

Figure C.10. Plot of surface temperature (in °C) vs. time (in minutes) curves for sample B2 for varying wind speeds of 2 m/s, 4 m/s and 6 m/s where the wind angle is kept fixed at 90° and the no wind test case.

Figure C.11. Plot of surface temperature (in °C) vs. time (in minutes) curves for sample B3 for varying wind speeds of 2 m/s, 4 m/s and 6 m/s where the wind angle is kept fixed at 90° and the no wind test case.
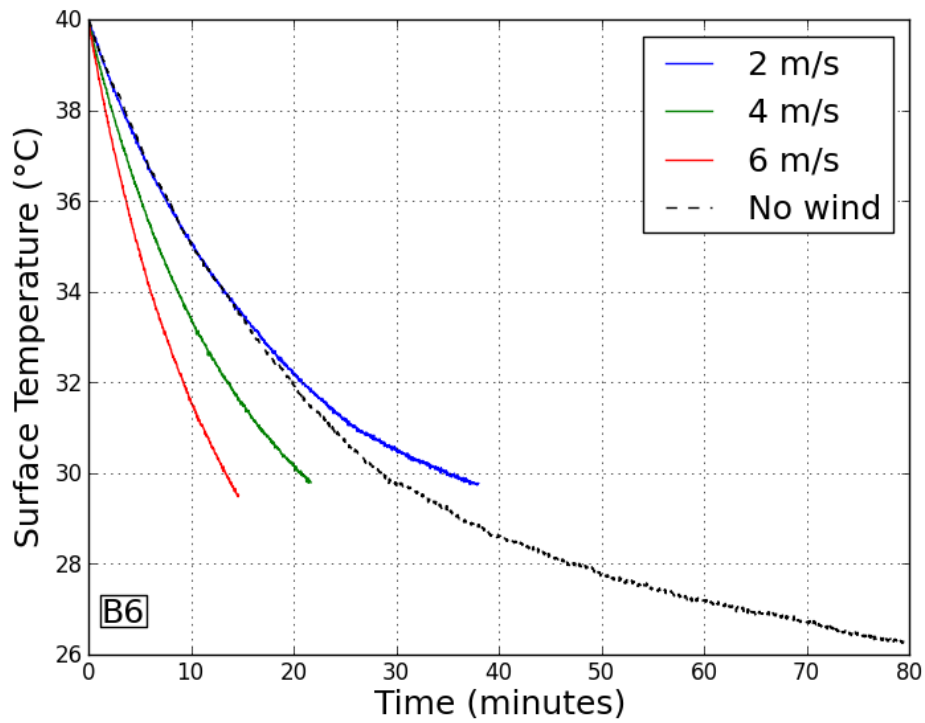
Figure C.12. Plot of surface temperature (in °C) vs. time (in minutes) curves for sample B4 for varying wind speeds of 2 m/s, 4 m/s and 6 m/s where the wind angle is kept fixed at 90° and the no wind test case.

Figure C.13. Plot of surface temperature (in °C) vs. time (in minutes) curves for sample B5 for varying wind speeds of 2 m/s, 4 m/s and 6 m/s where the wind angle is kept fixed at 90° and the no wind test case.
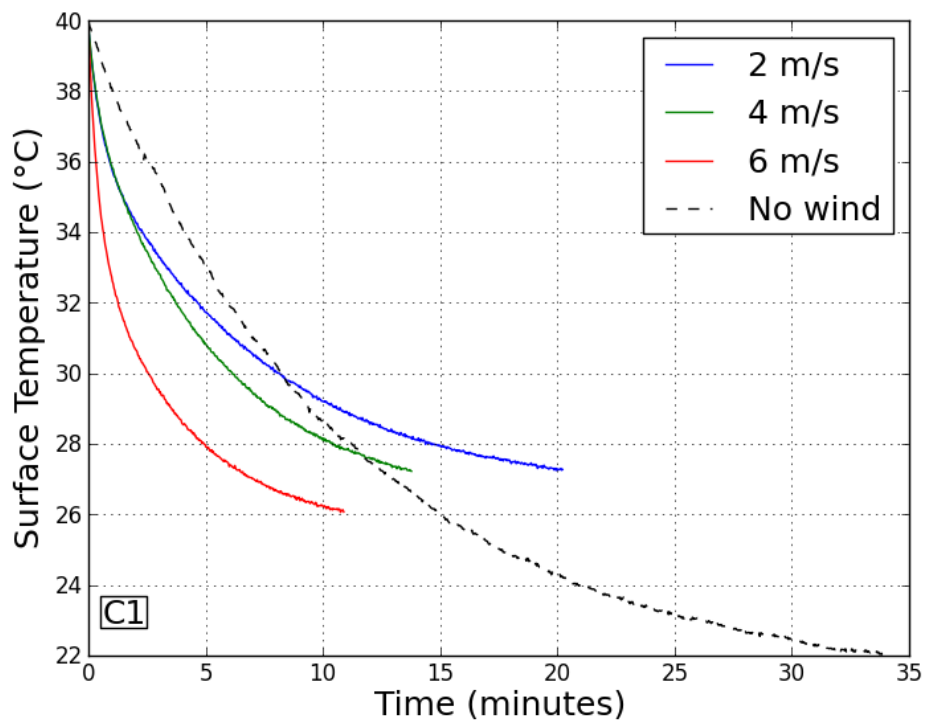
Figure C.14. Plot of surface temperature (in °C) vs. time (in minutes) curves for sample B6 for varying wind speeds of 2 m/s, 4 m/s and 6 m/s where the wind angle is kept fixed at 90° and the no wind test case.
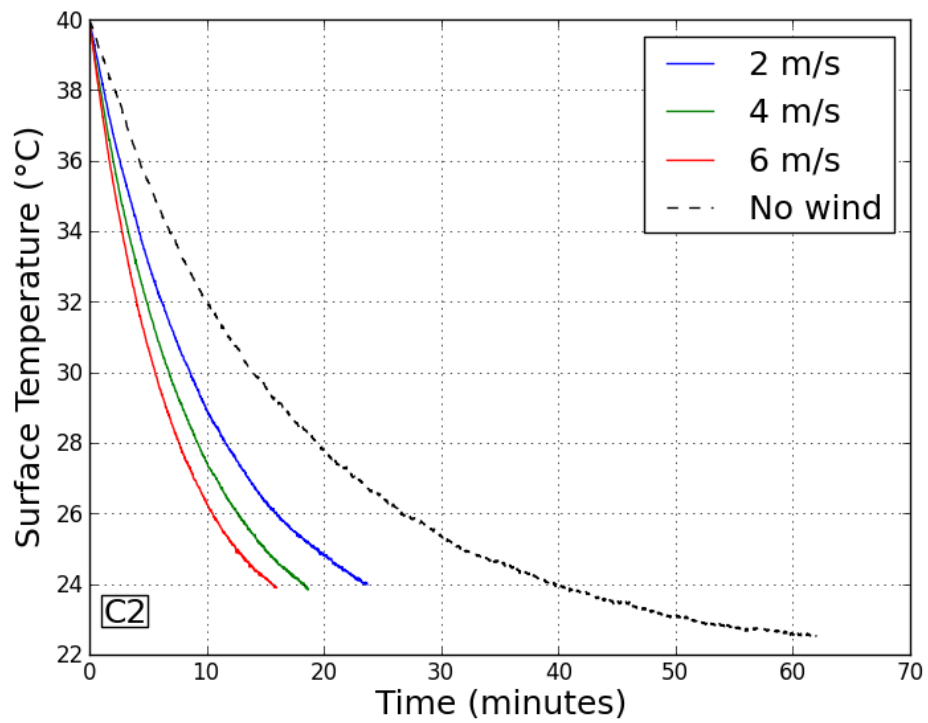

Figure C.15. Plot of surface temperature (in °C) vs. time (in minutes) curves for sample C1 for varying wind speeds of 2 m/s, 4 m/s and 6 m/s where the wind angle is kept fixed at 90° and the no wind test case.

94

Figure C.16. Plot of surface temperature (in °C) vs. time (in minutes) curves for sample C2 for varying wind speeds of 2 m/s, 4 m/s and 6 m/s where the wind angle is kept fixed at 90° and the no wind test case.
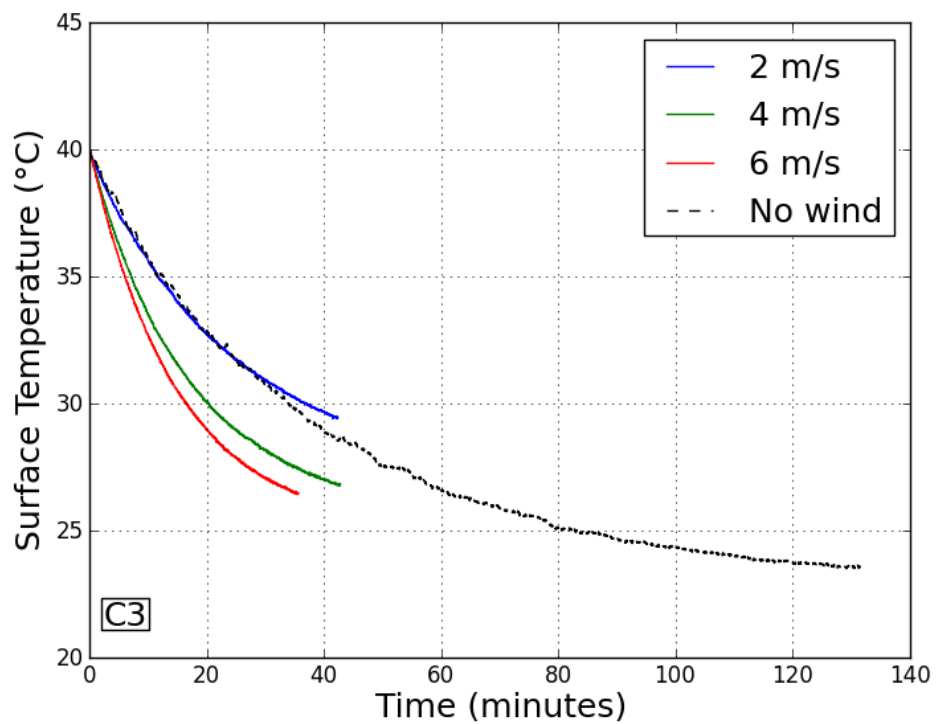

Figure C.17. Plot of surface temperature (in °C) vs. time (in minutes) curves for sample C3 for varying wind speeds of 2 m/s, 4 m/s and 6 m/s where the wind angle is kept fixed at 90° and the no wind test case.
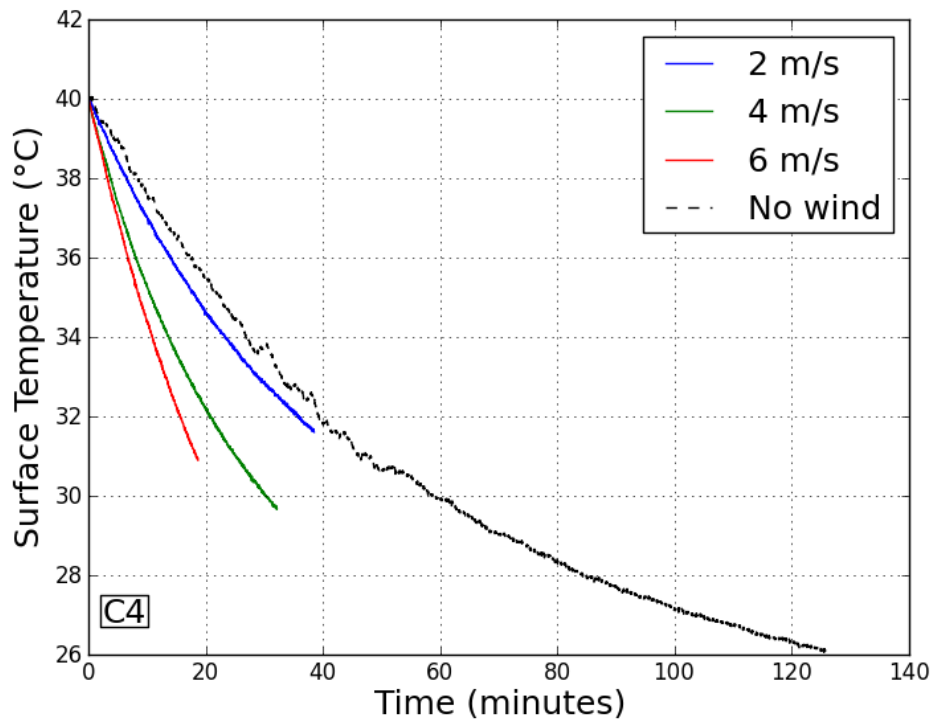
Figure C.18. Plot of surface temperature (in °C) vs. time (in minutes) curves for sample C4 for varying wind speeds of 2 m/s, 4 m/s and 6 m/s where the wind angle is kept fixed at 90° and the no wind test case.
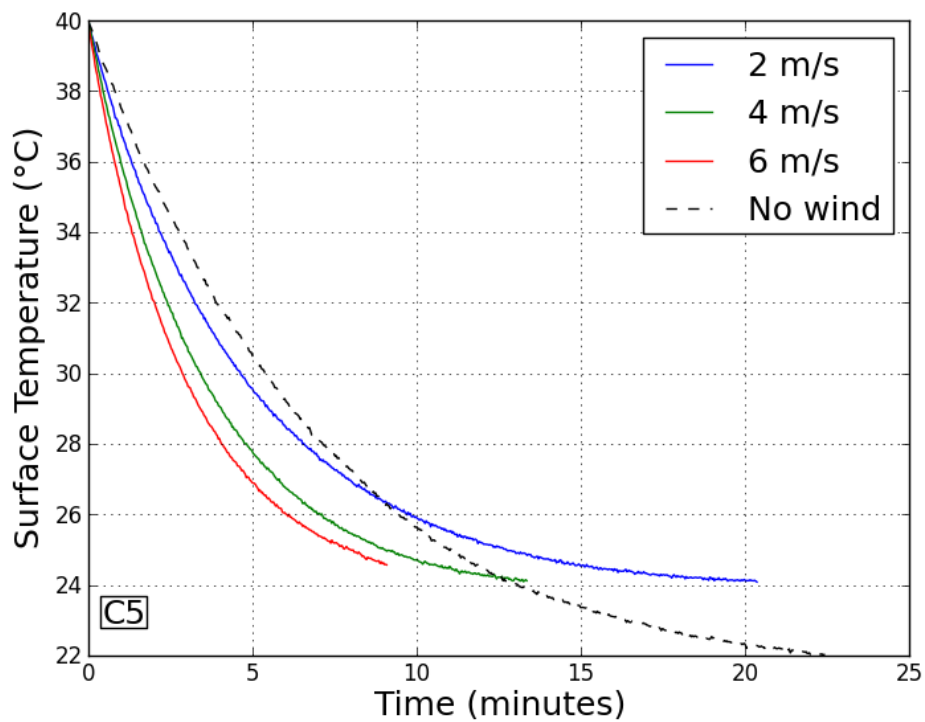

Figure C.19. Plot of surface temperature (in °C) vs. time (in minutes) curves for sample C5 for varying wind speeds of 2 m/s, 4 m/s and 6 m/s where the wind angle is kept fixed at 90° and the no wind test case.
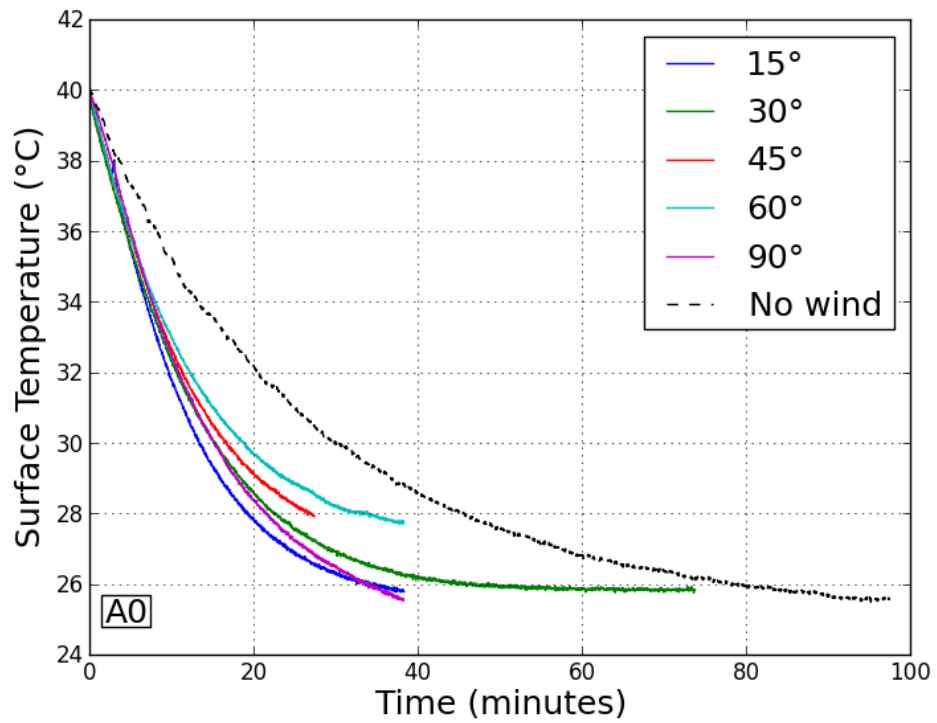
Figure C.20. Plot of surface temperature (in °C) vs. time (in minutes) curves for sample A0 for varying wind angles of 15°, 30°, 45°, 60°, 90° where the wind speed is kept fixed at 6 m/s and the no wind test case.

Figure C.21. Plot of surface temperature (in °C) vs. time (in minutes) curves for sample A1 for varying wind angles of 15°, 30°, 45°, 60°, 90° where the wind speed is kept fixed at 6 m/s and the no wind test case.

97

Figure C.22. Plot of surface temperature (in °C) vs. time (in minutes) curves for sample A2 for varying wind angles of 15°, 30°, 45°, 60°, 90° where the wind speed is kept fixed at 6 m/s and the no wind test case.
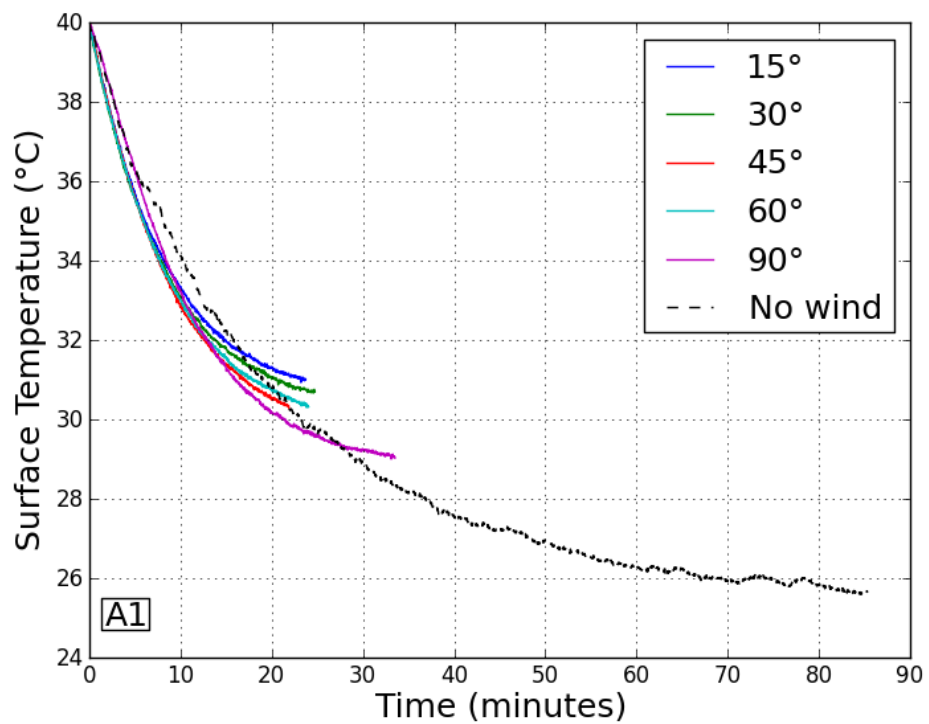

Figure C.23. Plot of surface temperature (in °C) vs. time (in minutes) curves for sample A3 for varying wind angles of 15°, 30°, 45°, 60°, 90° where the wind speed is kept fixed at 6 m/s and the no wind test case.
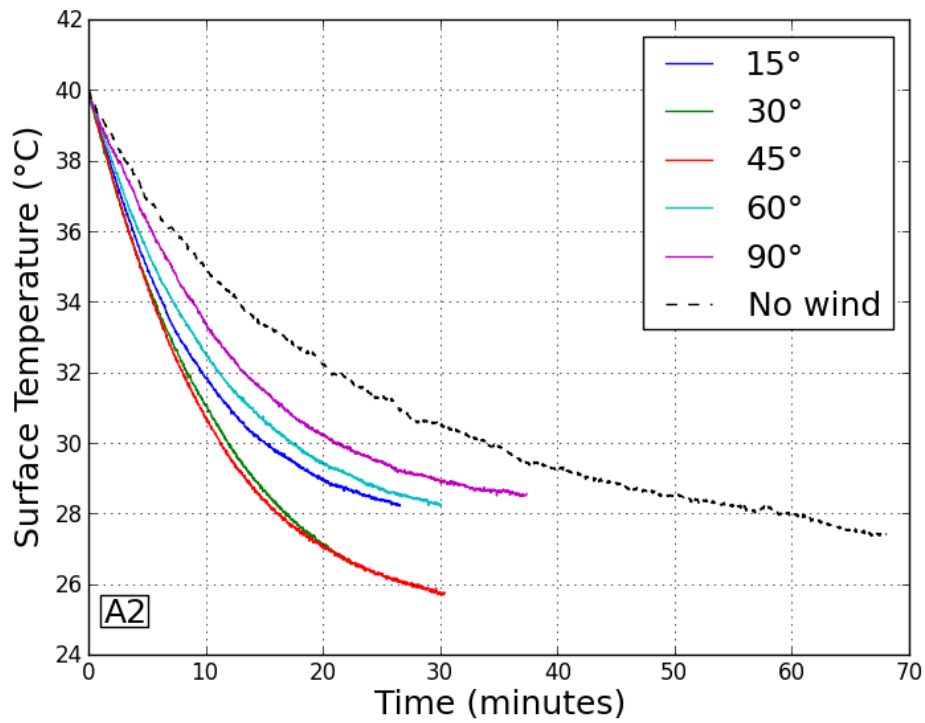
Figure C.24. Plot of surface temperature (in °C) vs. time (in minutes) curves for sample A4 for varying wind angles of 15°, 30°, 45°, 60°, 90° where the wind speed is kept fixed at 6 m/s and the no wind test case.

Figure C.25. Plot of surface temperature (in °C) vs. time (in minutes) curves for sample A5 for varying wind angles of 15°, 30°, 45°, 60°, 90° where the wind speed is kept fixed at 6 m/s and the no wind test case.
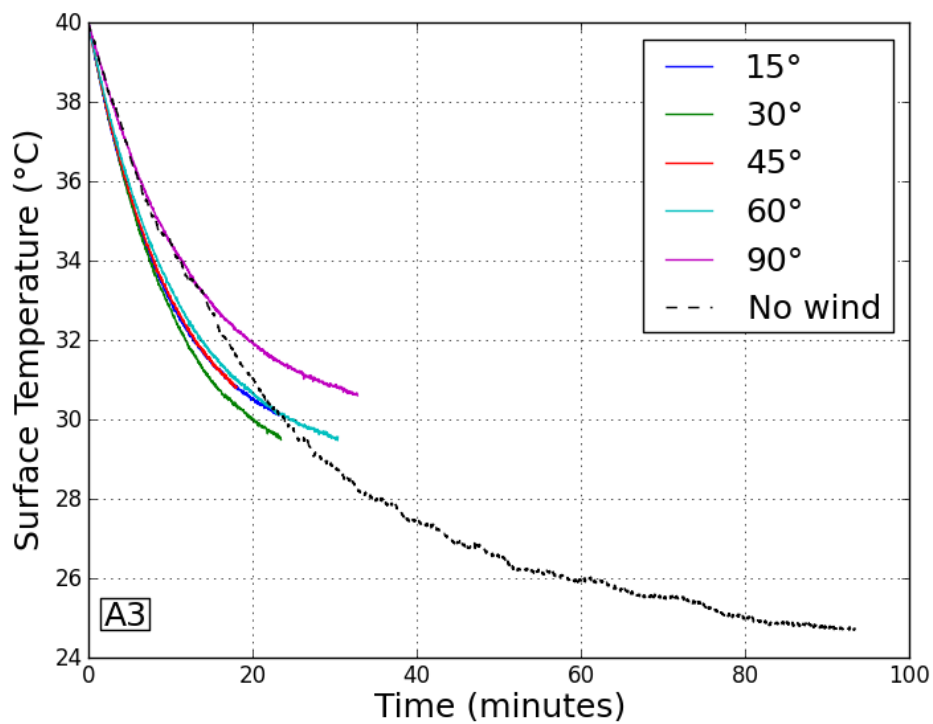
99

Figure C.26. Plot of surface temperature (in °C) vs. time (in minutes) curves for sample A6 for varying wind angles of 15°, 30°, 45°, 60°, 90° where the wind speed is kept fixed at 6 m/s and the no wind test case.
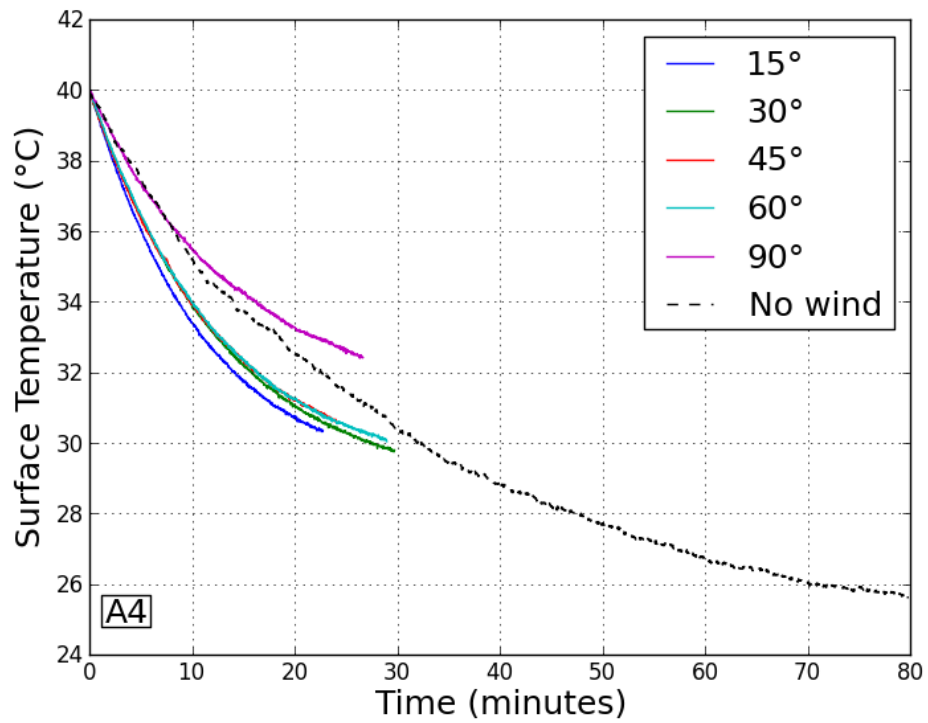

Figure C.27. Plot of surface temperature (in °C) vs. time (in minutes) curves for sample B0 for varying wind angles of 15°, 30°, 45°, 60°, 90° where the wind speed is kept fixed at 6 m/s and the no wind test case.

100

Figure C.28. Plot of surface temperature (in °C) vs. time (in minutes) curves for sample B1 for varying wind angles of 15°, 30°, 45°, 60°, 90° where the wind speed is kept fixed at 6 m/s and the no wind test case.
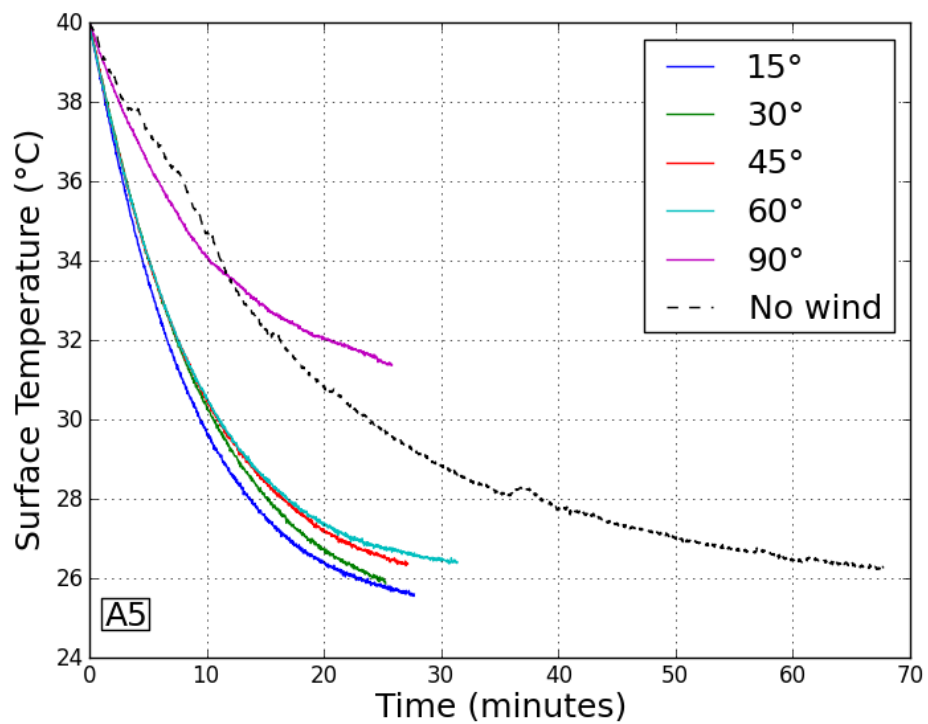

Figure C.29. Plot of surface temperature (in °C) vs. time (in minutes) curves for sample B2 for varying wind angles of 15°, 30°, 45°, 60°, 90° where the wind speed is kept fixed at 6 m/s and the no wind test case.
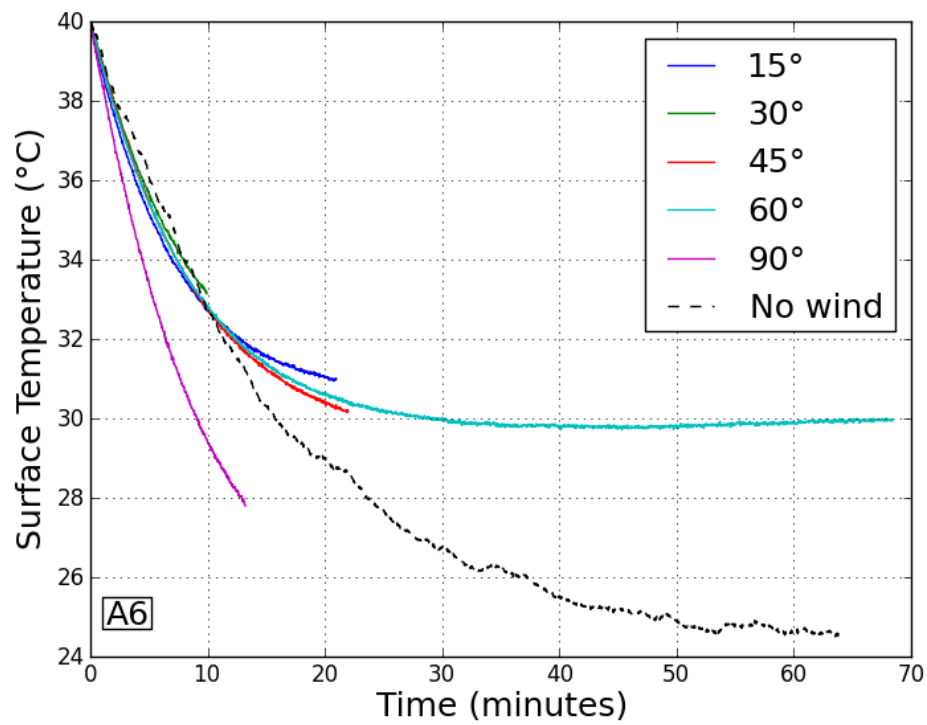
Figure C.30. Plot of surface temperature (in °C) vs. time (in minutes) curves for sample B3 for varying wind angles of 15°, 30°, 45°, 60°, 90° where the wind speed is kept fixed at 6 m/s and the no wind test case.

Figure C.31. Plot of surface temperature (in °C) vs. time (in minutes) curves for sample B4 for varying wind angles of 15°, 30°, 45°, 60°, 90° where the wind speed is kept fixed at 6 m/s and the no wind test case.
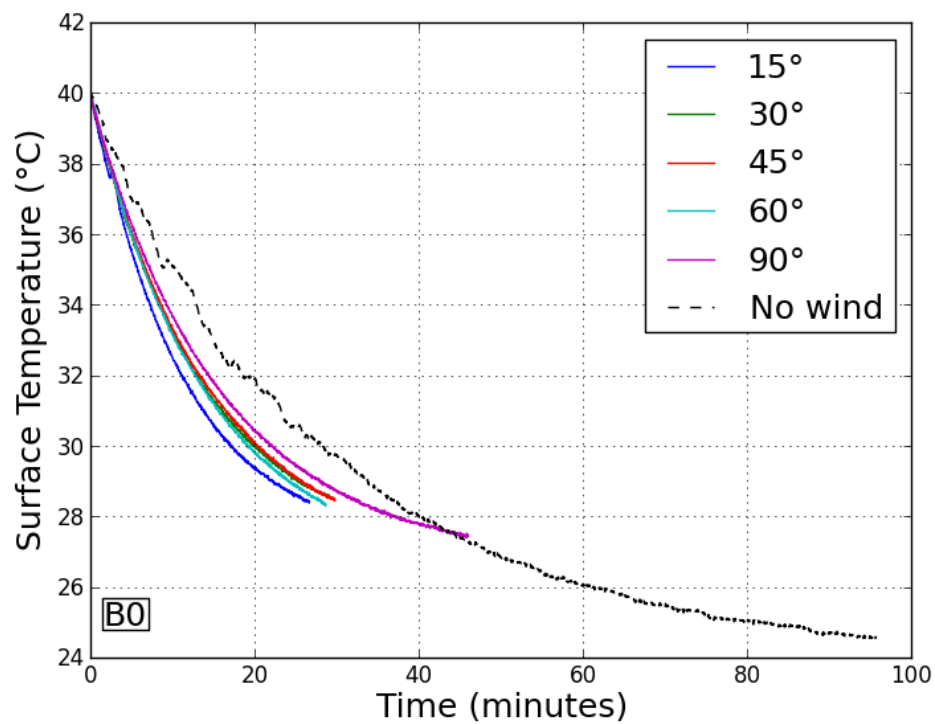
102

Figure C.32. Plot of surface temperature (in °C) vs. time (in minutes) curves for sample B5 for varying wind angles of 15°, 30°, 45°, 60°, 90° where the wind speed is kept fixed at 6 m/s and the no wind test case.
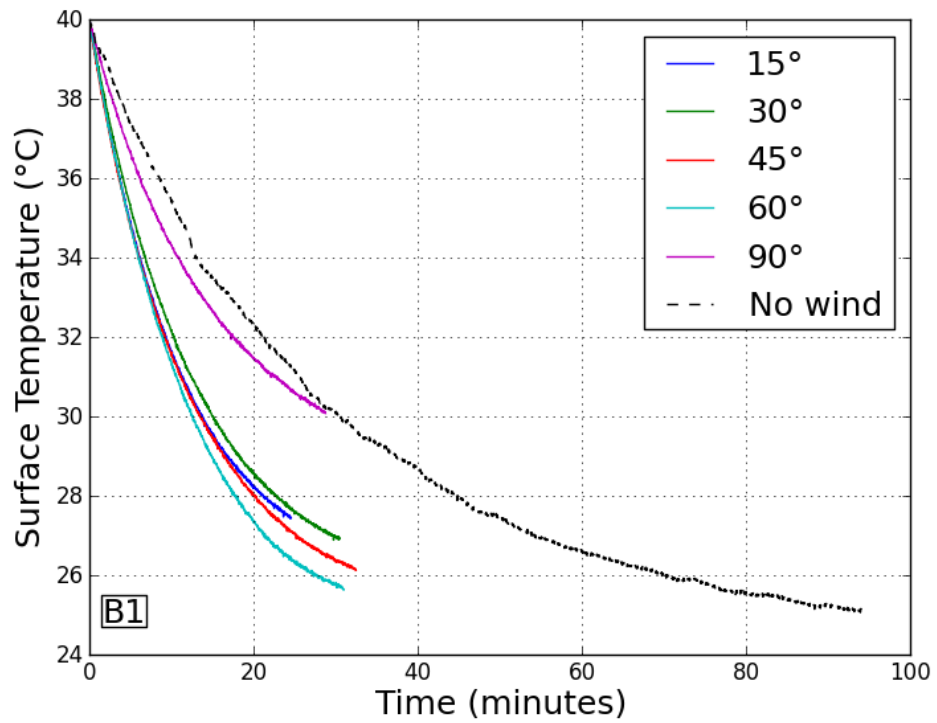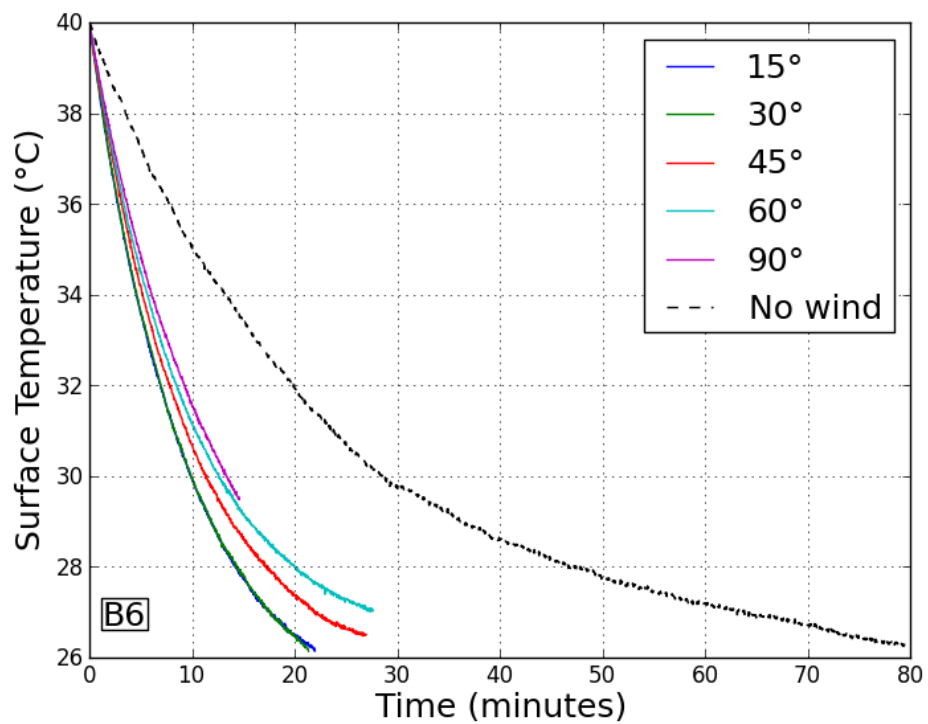

Figure C.33. Plot of surface temperature (in °C) vs. time (in minutes) curves for sample B6 for varying wind angles of 15°, 30°, 45°, 60°, 90° where the wind speed is kept fixed at 6 m/s and the no wind test case.

103
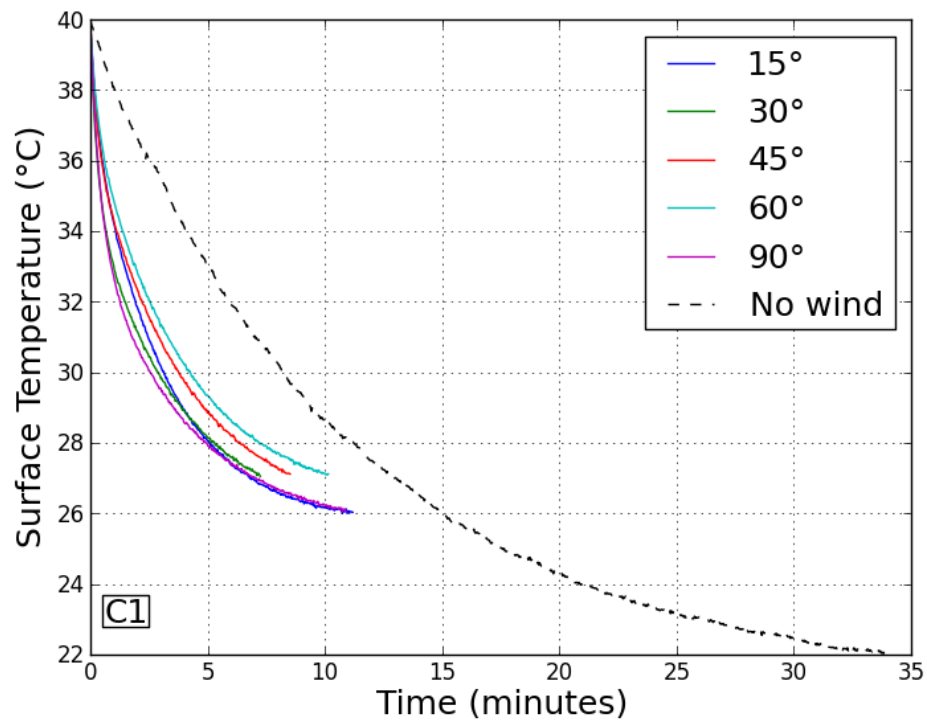
Figure C.34. Plot of surface temperature (in °C) vs. time (in minutes) curves for sample C1 for varying wind angles of 15°, 30°, 45°, 60°, 90° where the wind speed is kept fixed at 6 m/s and the no wind test case.
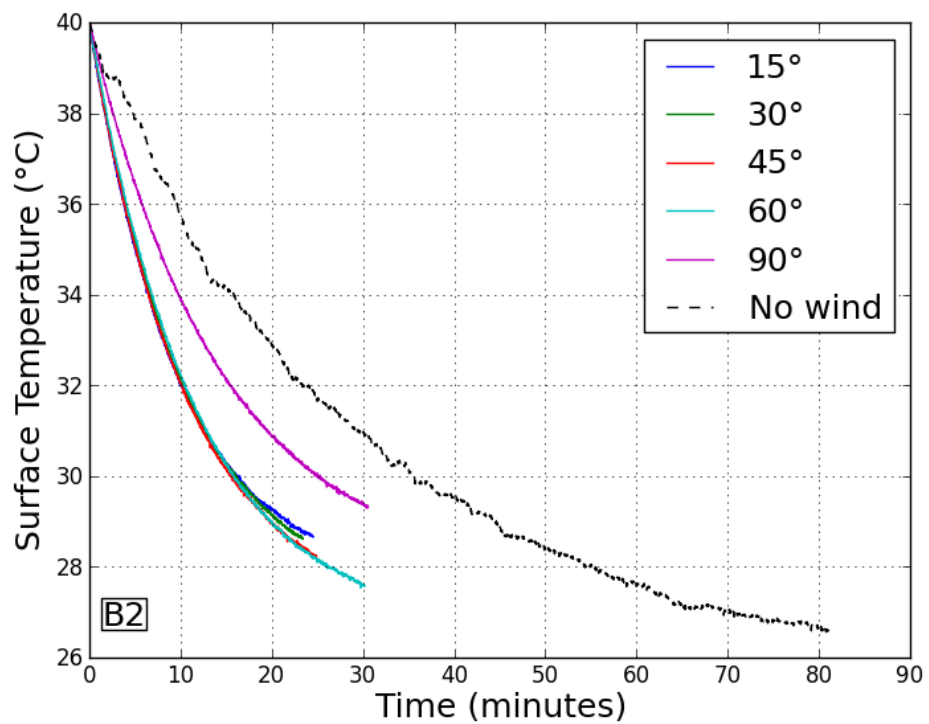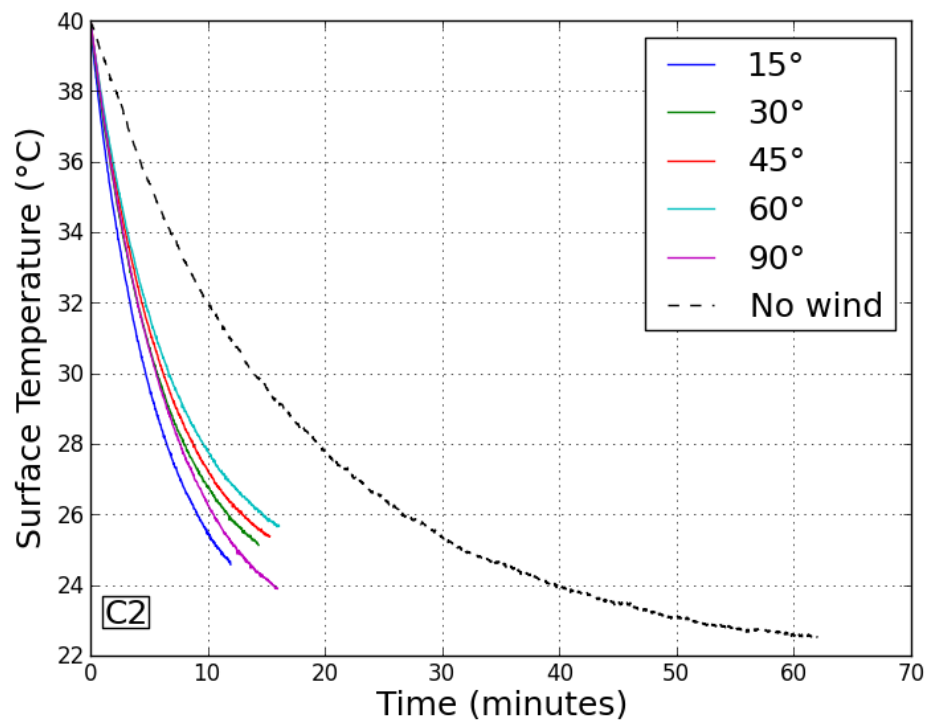

Figure C.35. Plot of surface temperature (in °C) vs. time (in minutes) curves for sample C2 for varying wind angles of 15°, 30°, 45°, 60°, 90° where the wind speed is kept fixed at 6 m/s and the no wind test case.
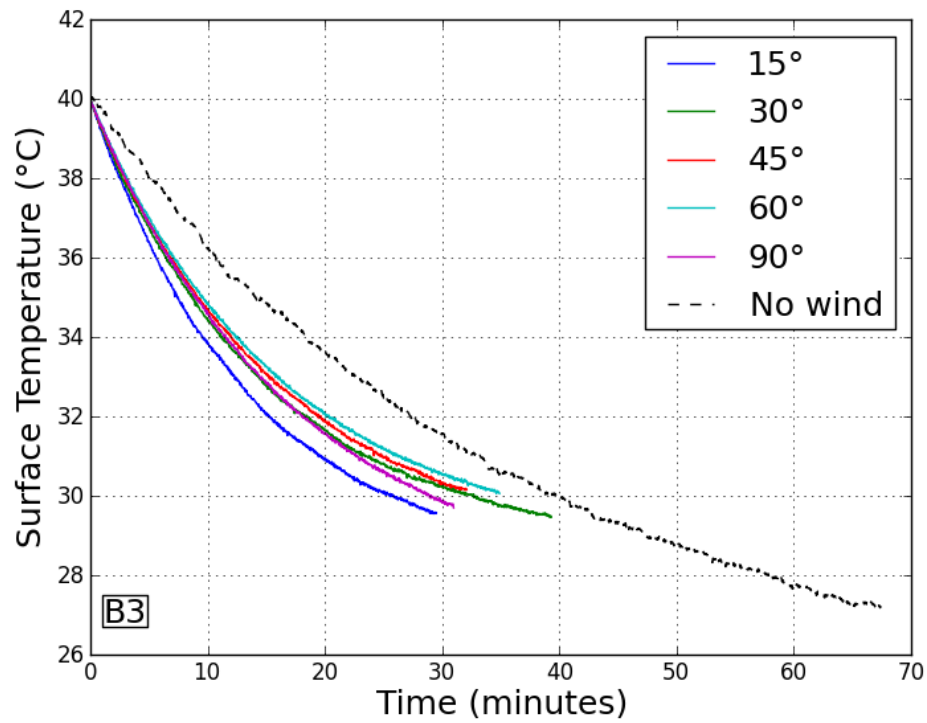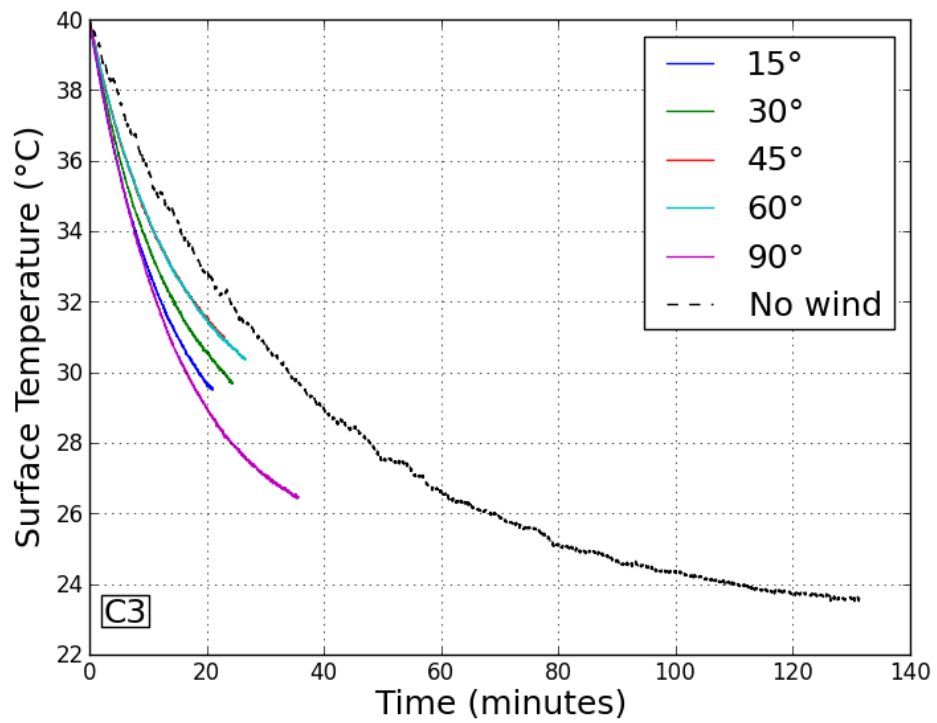
Figure C.36. Plot of surface temperature (in °C) vs. time (in minutes) curves for sample C3 for varying wind angles of 15°, 30°, 45°, 60°, 90° where the wind speed is kept fixed at 6 m/s and the no wind test case.
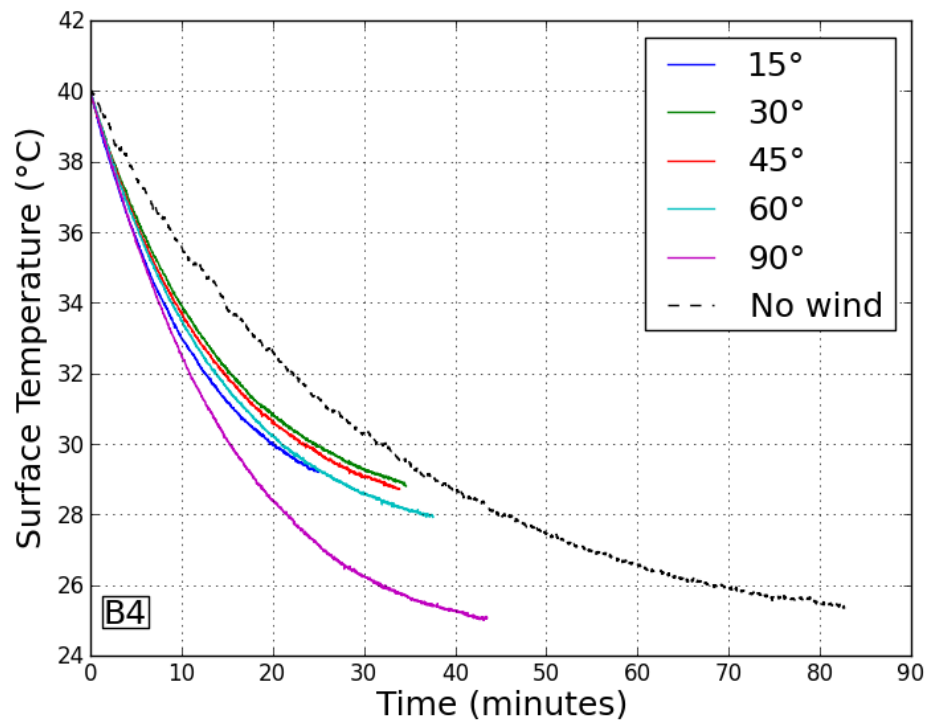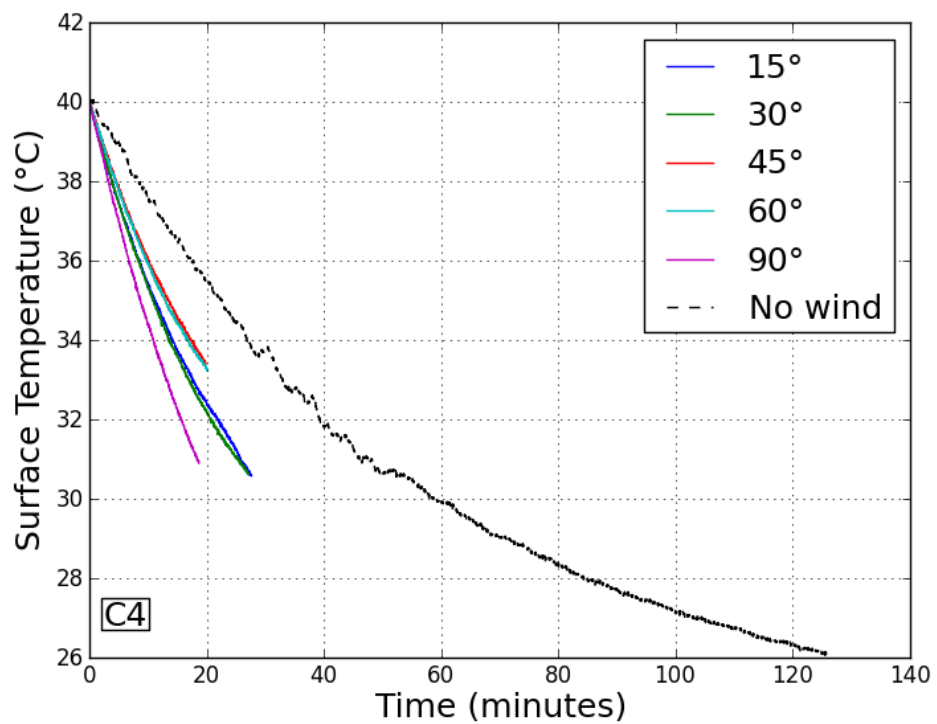

Figure C.37. Plot of surface temperature (in °C) vs. time (in minutes) curves for sample C4 for varying wind angles of 15°, 30°, 45°, 60°, 90° where the wind speed is kept fixed at 6 m/s and the no wind test case.
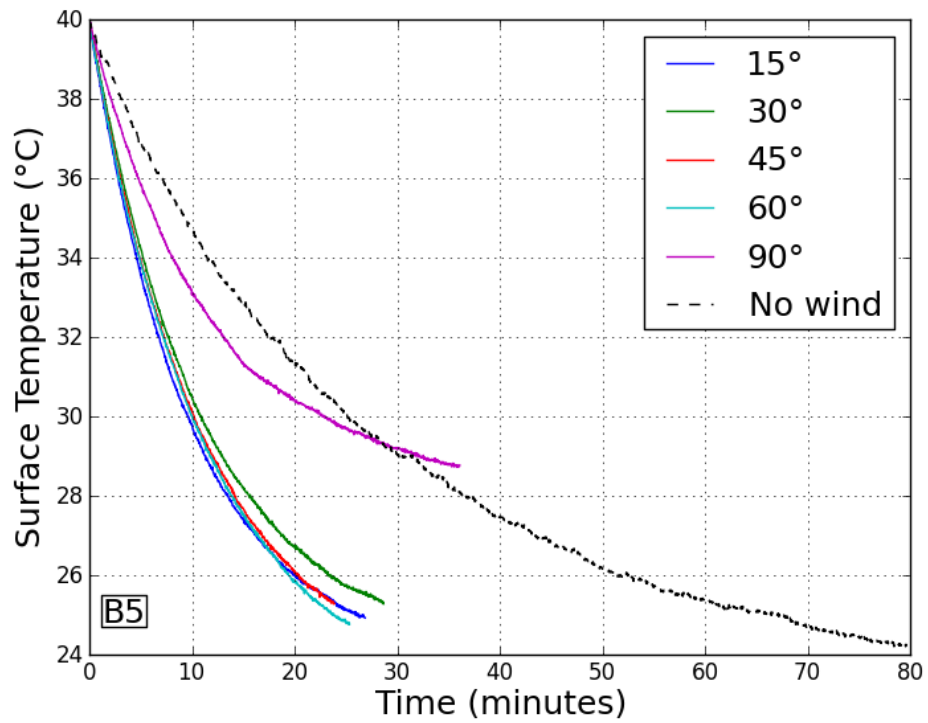
105
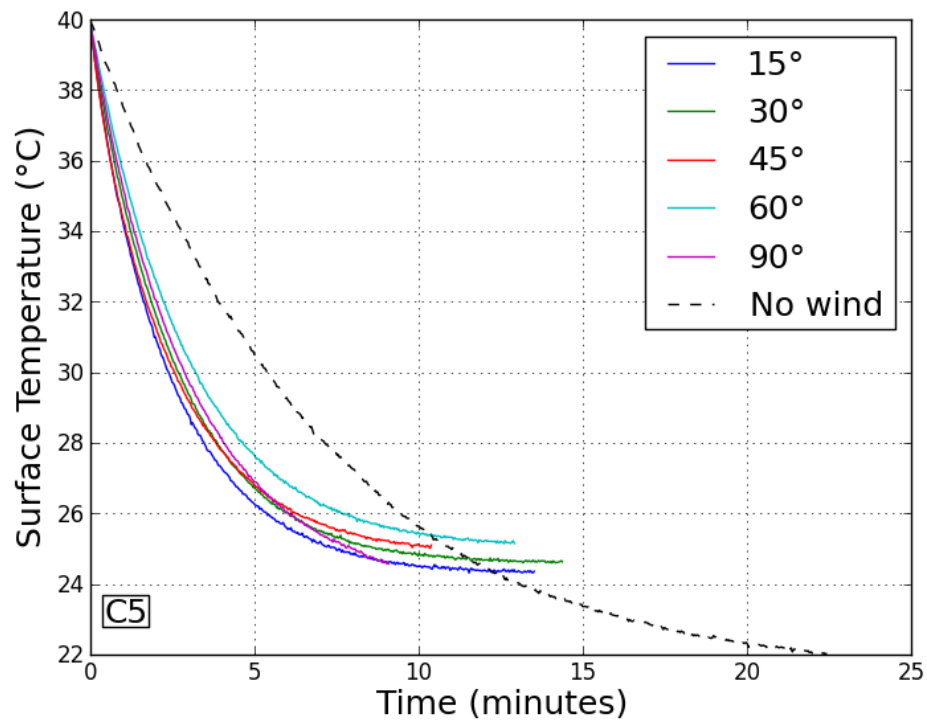
Figure C.38. Plot of surface temperature (in °C) vs. time (in minutes) curves for sample C5 for varying wind angles of 15°, 30°, 45°, 60°, 90° where the wind speed is kept fixed at 6 m/s and the no wind test case.

Table C.1. Surface texture integrated average convective heat transfer coefficients of sample of Experiment Sets A, B and C for no wind test case and wind speeds 2 m/s, 4 m/s and 6 m/s, where wind angle is 90°.

	No Wind	2 m/s	4 m/s	6 m/s
A0	8.74	10.31	15.04	16.46
A1	11.33	13.19	22.88	19.68
A2	10.3	13.8	17.58	15.22
A3	9.5	10.69	12.37	17.37
A4	8.64	11.09	17.66	18.95
A5	7.93	13.04	13.84	24.28
A6	10.21	10.77	15.86	19.14
B0	17.42	24.42	30.61	29.92
B1	17.67	22.2	29.59	37.38
B2	12.28	14.75	20.27	24.1
B3	13.67	17.36	24.87	27.1
B4	13.93	20.22	24.81	31.3
B5	14.83	18.45	29.54	39.77
B6	18.57	24.48	32.67	53.73
C1	13.59	48.23	49.74	152.06
C2	25.07	44.98	57.47	68.37
C3	14.15	22.66	34.26	35.12
C4	19.48	46.86	63.68	84.26
C5	15.39	23.83	31.32	35.92

Table C.2. Surface texture integrated average convective heat transfer coefficients of sample of Experiment Sets A, B and C for wind angles 15°, 30°, 45°, 60° and 90°, where wind speed is kept constant at 6 m/s.

	15°	30°	45°	60°	90°
A0	16.25	18.27	16.49	15.53	16.46
A1	28.4	31.64	24.34	25.25	19.68
A2	24.88	21.92	19.38	21.76	15.22
A3	20.3	19.39	19.1	17.92	17.37
A4	23.09	18.27	19.81	18.33	18.95
A5	21.96	19.6	20.93	22.93	24.28
A6	27.61	22.13	21.54	23.04	19.14
B0	43.93	36.03	42.29	38.8	31.31
B1	43.17	40.21	43.64	40.59	37.38
B2	40.05	35.59	35.03	28.71	24.1
B3	33.99	33.92	33.53	33.77	27.1
B4	41.14	33.2	32.73	32.15	31.3
B5	44.69	40.55	43.31	40.89	39.77
B6	53.89	54.83	47.16	44.17	53.73
C1	85.93	168.13	103.06	74.45	152.06
C2	80.76	73.49	75.14	65.41	68.37
C3	45.25	39.55	38.77	41.19	35.12
C4	86.99	67.97	100.13	96.83	84.26
C5	48.55	42.74	54.13	35.84	35.92

Table C.3. Surface texture integrated time constants of sample of Experiment Sets A, B and C for no wind test case and wind speeds 2 m/s, 4 m/s and 6 m/s, where wind angle is 90°.

	No Wind	2 m/s	4 m/s	6 m/s
A0	24.89	21.1	14.47	13.22
A1	18.79	16.14	9.31	10.82
A2	22.56	16.84	13.22	15.27
A3	20.45	18.17	15.71	11.18
A4	27.89	21.72	13.64	12.71
A5	23.72	14.43	13.6	7.75
A6	17.5	16.59	11.26	9.33
B0	27.55	19.65	15.67	16.04
B1	25.13	20	15.01	11.88
B2	26.73	22.26	16.2	13.62
B3	30.58	24.09	16.81	15.43
B4	31.55	21.73	17.71	14.04
B5	27.56	22.15	13.84	10.28
B6	23.51	17.83	13.36	8.13
C1	10.55	2.97	2.88	0.94
C2	16.65	9.28	7.26	6.11
C3	35.44	22.13	14.63	14.28
C4	53.65	22.3	16.41	12.4
C5	6.72	4.34	3.3	2.88

Table C.4. Surface texture integrated time constants of sample of Experiment Sets A, B and C for wind angles 15°, 30°, 45°, 60° and 90°, where wind speed is kept constant at 6 m/s.

	15°	30°	45°	60°	90°
A0	13.39	11.91	13.19	14.01	13.22
A1	7.5	6.73	8.75	8.43	10.82
A2	9.34	10.6	11.99	10.68	15.27
A3	9.57	10.02	10.17	10.84	11.18
A4	10.43	13.18	12.16	13.14	12.71
A5	8.57	9.6	8.99	8.21	7.75
A6	6.47	8.07	8.29	7.75	9.33
B0	10.92	13.32	11.35	12.37	15.33
B1	10.28	11.04	10.17	10.94	11.88
B2	8.2	9.22	9.37	11.43	13.62
B3	12.3	12.33	12.47	12.38	15.43
B4	10.68	13.24	13.42	13.67	14.04
B5	9.15	10.08	9.44	10	10.28
B6	8.1	7.96	9.26	9.88	8.13
C1	1.67	0.85	1.39	1.93	0.94
C2	5.17	5.68	5.56	6.38	6.11
C3	11.08	12.68	12.93	12.17	14.28
C4	12.01	15.37	10.44	10.79	12.4
C5	2.13	2.42	1.91	2.88	2.88

Figure C.39. Plot of surface texture integrated average convective heat transfer coefficients (in W/m²°C) vs. wind speed (in m/s) for samples of Experiment Set A.

Figure C.40. Plot of surface texture integrated time constants (in minutes) vs. wind speed (in m/s) for samples of Experiment Set A.

111

Figure C.41. Plot of surface texture integrated average convective heat transfer coefficients (in W/m²°C) vs. wind speed (in m/s) for samples of Experiment Set B.

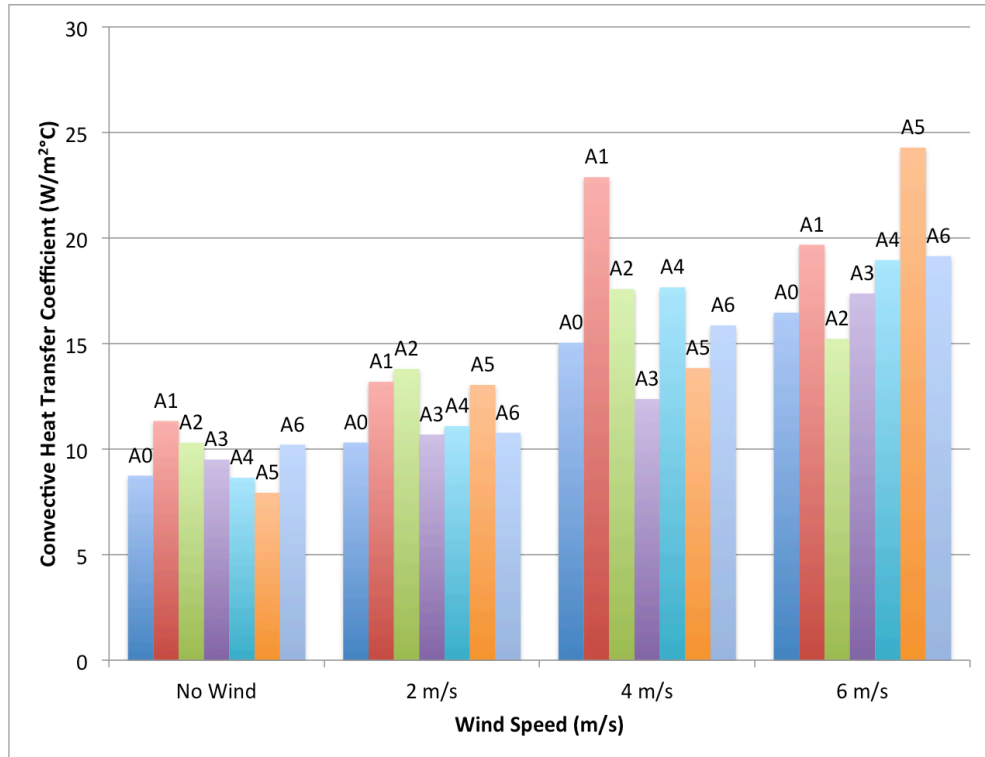Figure C.42. Plot of surface texture integrated time constants (in minutes) vs. wind speed (in m/s) for samples of Experiment Set B.

112
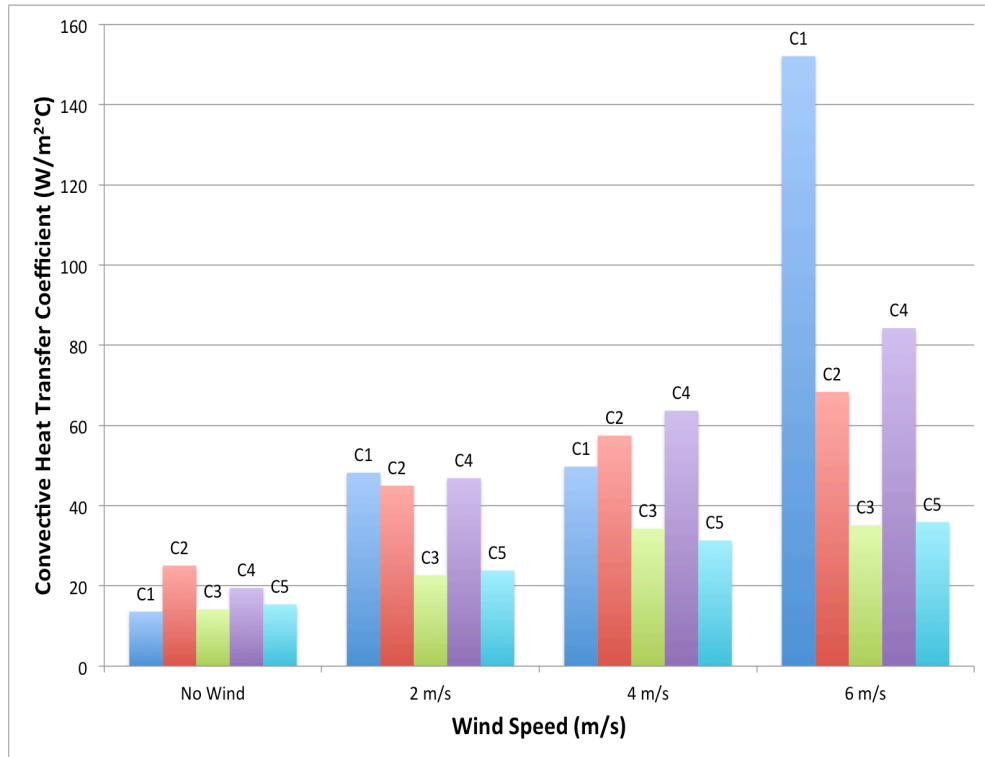
Figure C.43. Plot of surface texture integrated average convective heat transfer coefficients (in W/m^2°C) vs. wind speed (in m/s) for samples of Experiment Set C.
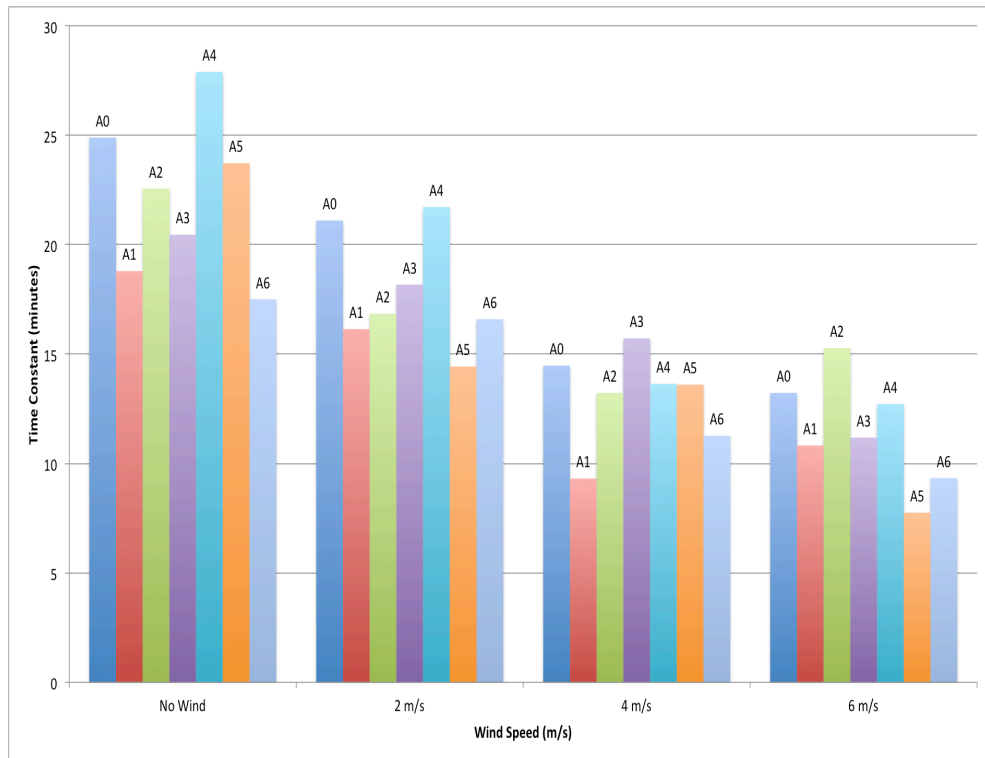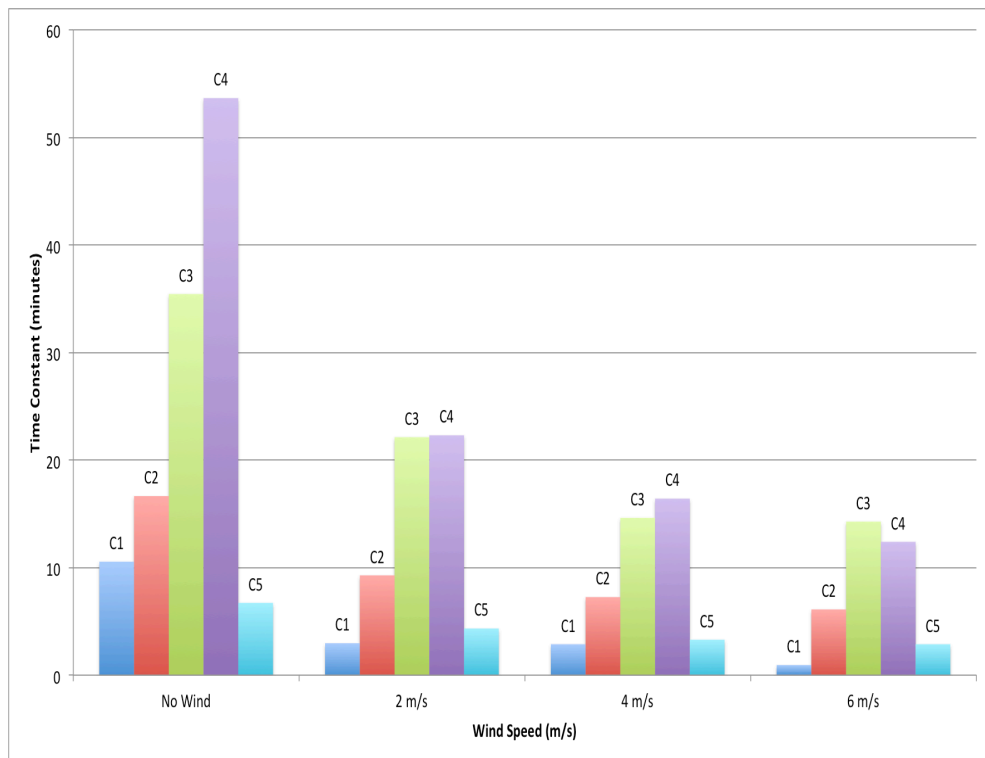

Figure C.44. Plot of surface texture integrated time constants (in minutes) vs. wind speed (in m/s) for samples of Experiment Set C.
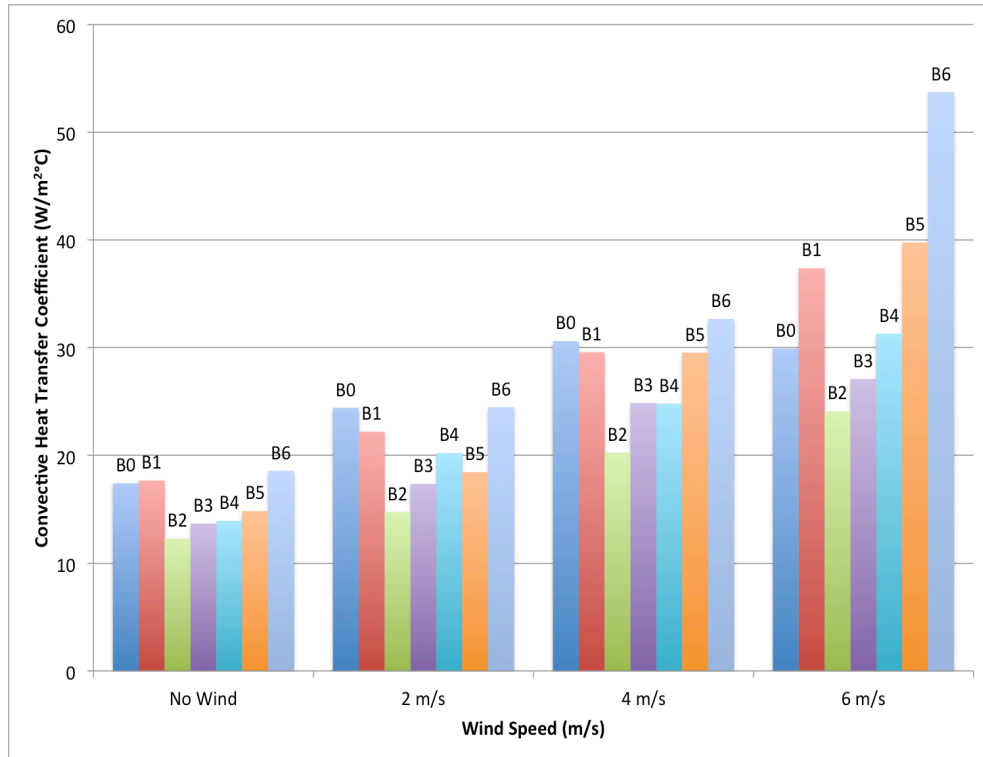
113
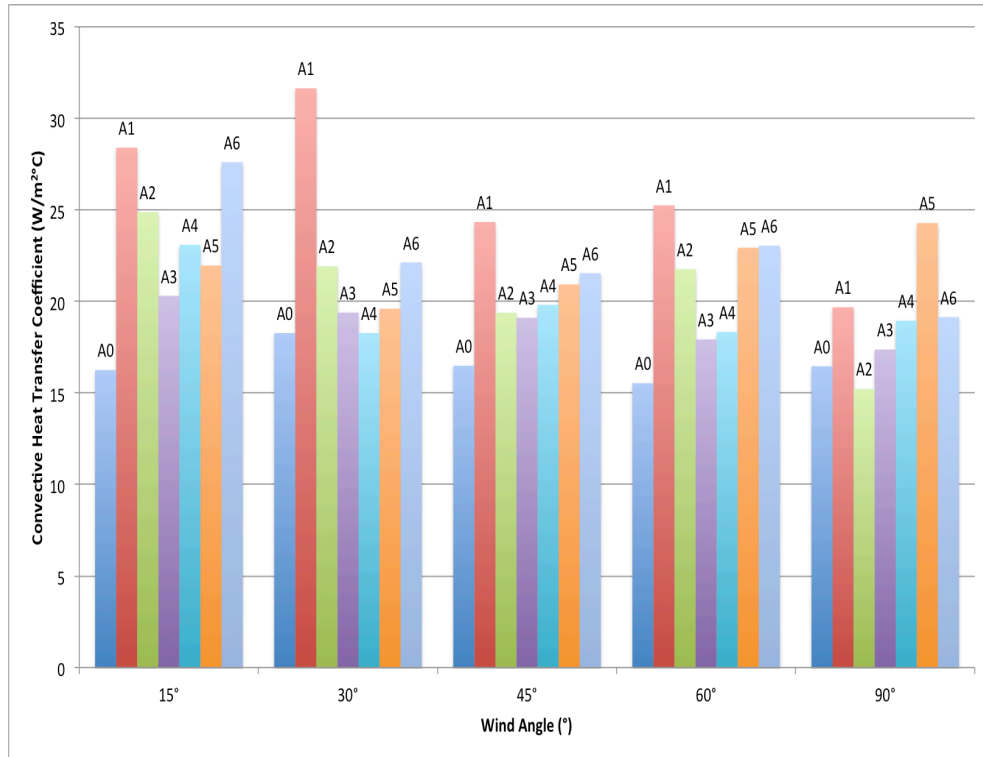
Figure C.45. Plot of surface texture integrated average convective heat transfer coefficients (in W/m²°C) vs. wind angle (in °) for samples of Experiment Set A.
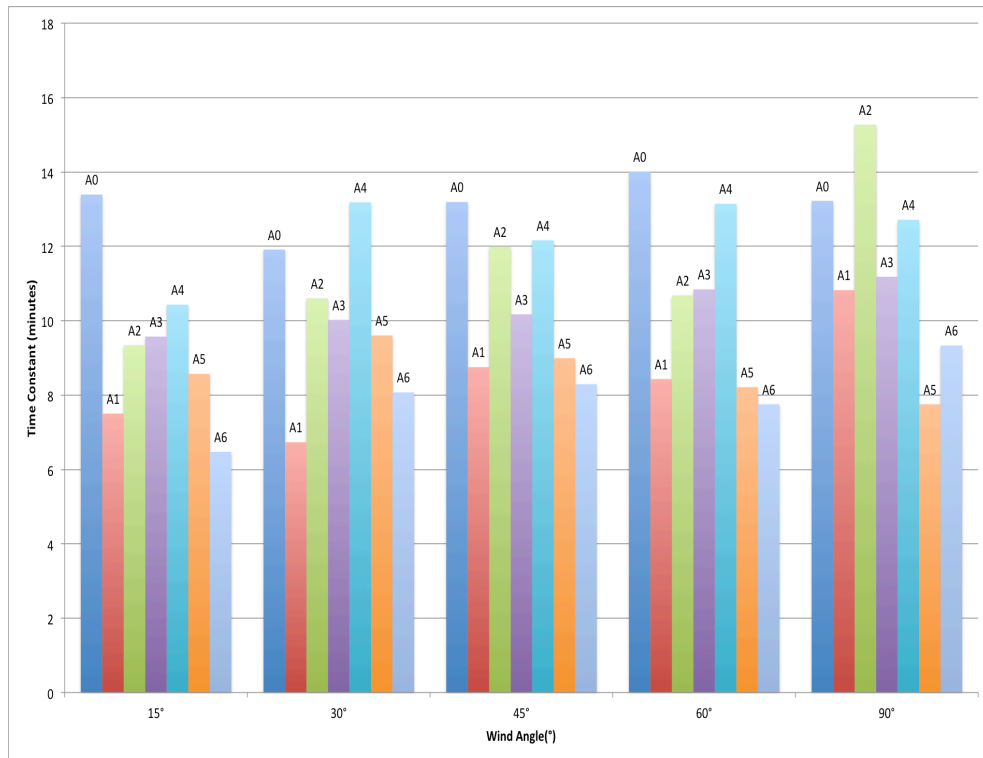
Figure C.46. Plot of surface texture integrated time constants (in minutes) vs. wind angle (in °) for samples of Experiment Set A.

114
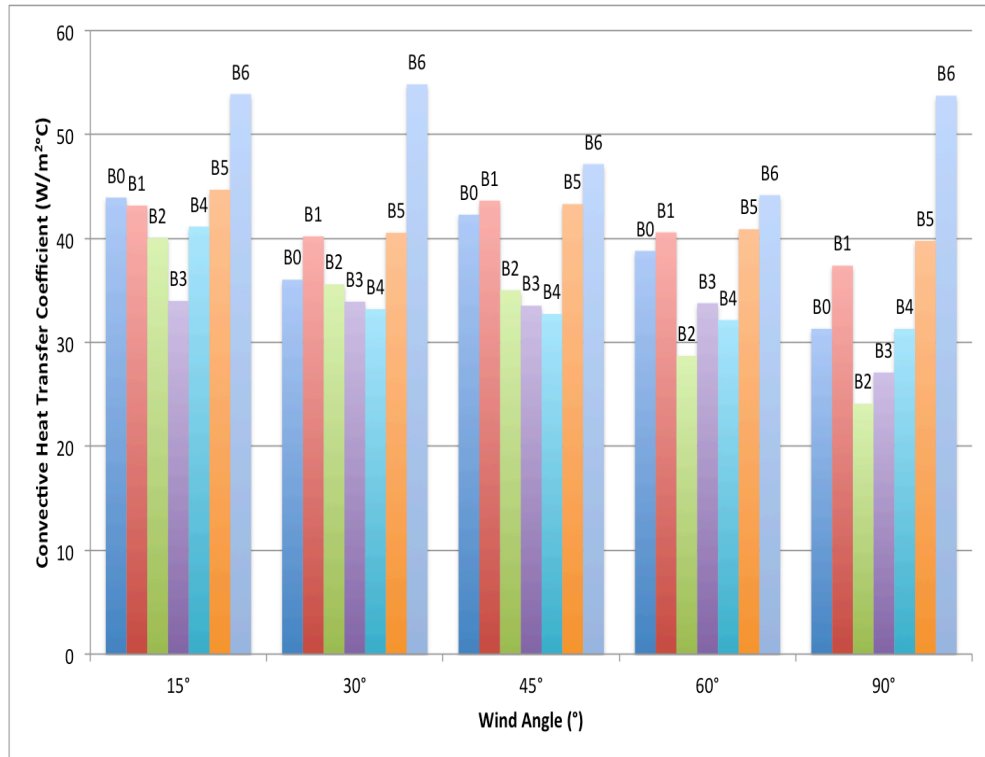
Figure C.47. Plot of surface texture integrated average convective heat transfer coefficients (in $W/m^2°C$) vs. wind angle (in °) for samples of Experiment Set B.
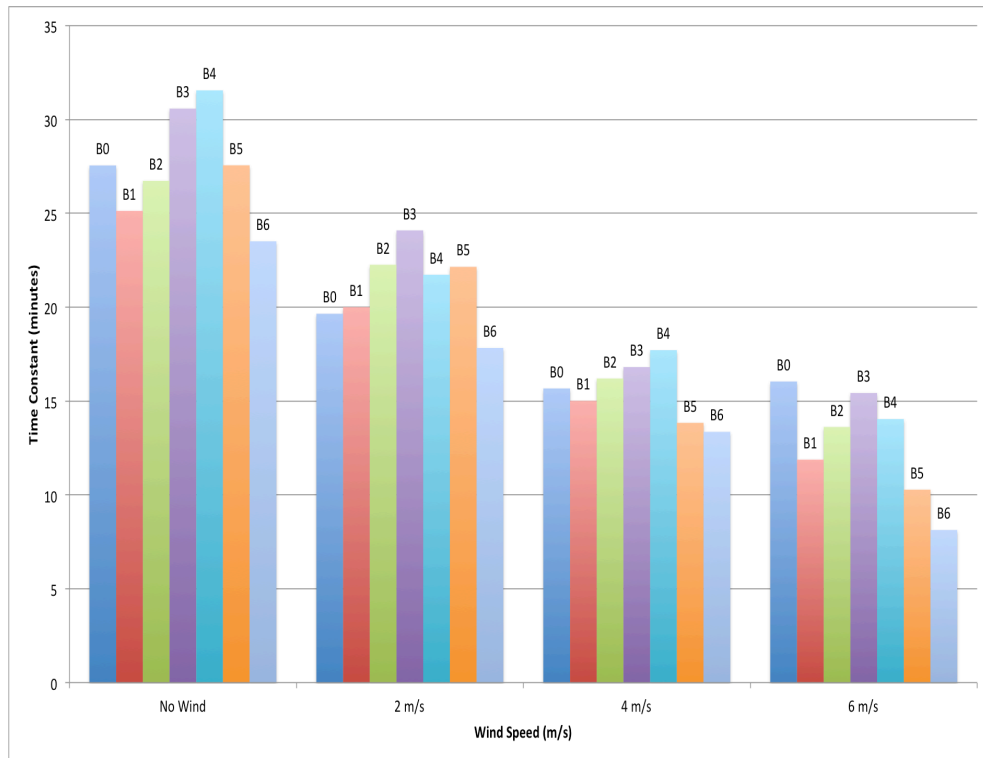

Figure C.48. Plot of surface texture integrated time constants (in minutes) vs. wind angle (in °) for samples of Experiment Set B.

115
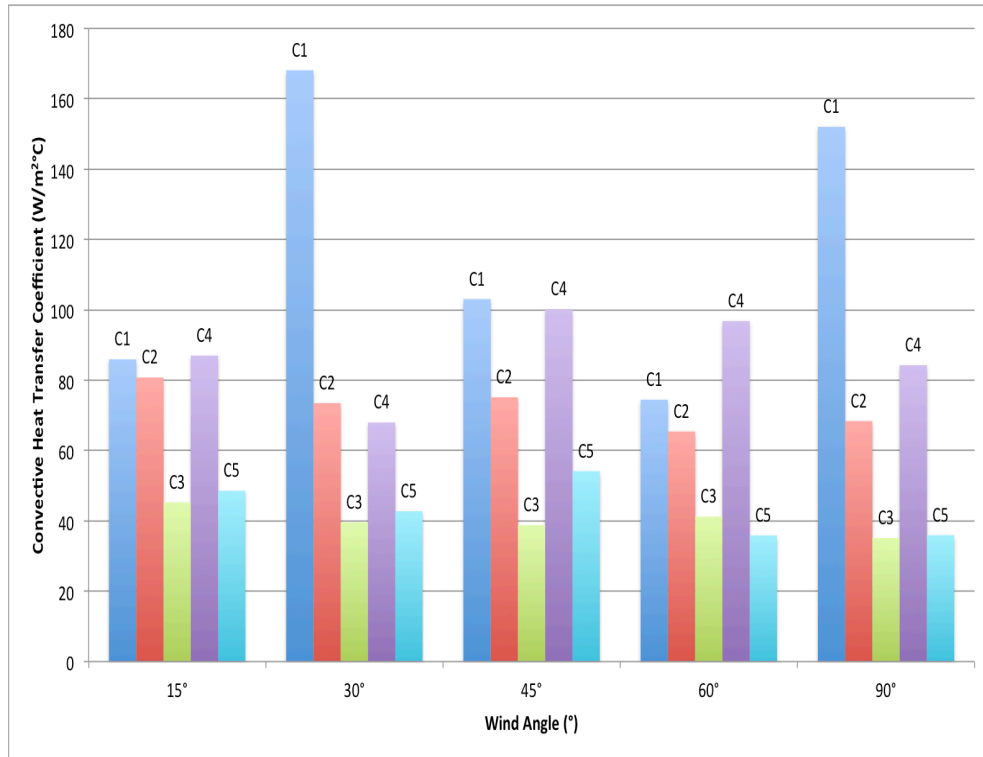
Figure C.49. Plot of surface texture integrated average convective heat transfer coefficients (in W/m^2°C) vs. wind angle (in °) for samples of Experiment Set C.
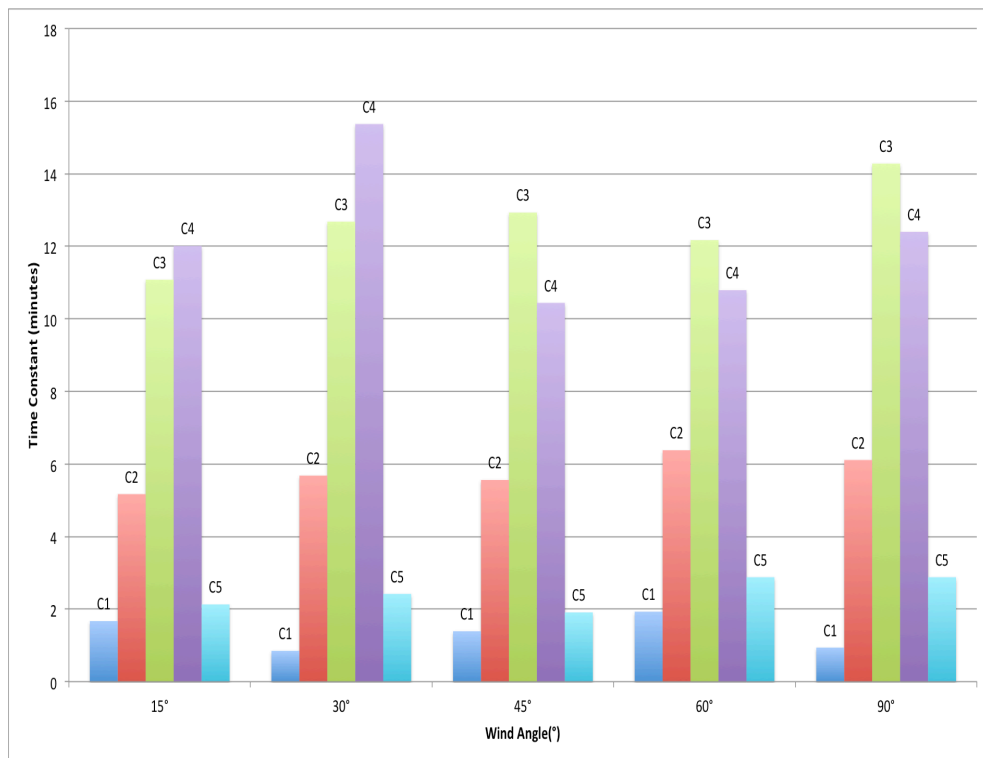
Figure C.50. Plot of surface texture integrated time constants (in minutes) vs. wind angle (in °) for samples of Experiment Set C.
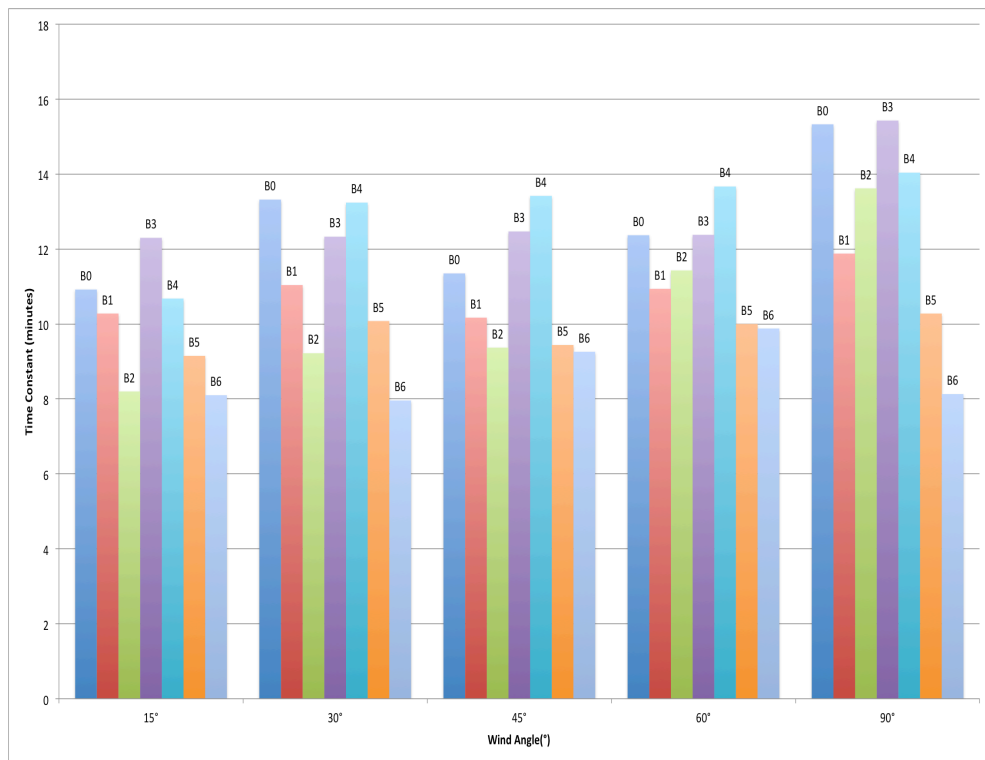
116

Table C.5. Environmental Test conditions for Experiment Set A.

Wind Angle – Wind Speed	A0	A1	A2	A3	A4	A5	A6
90° - No Wind							
AMB. TEMP. (°C)	25	25.5	27	24.5	25.5	26	24.5
HUMIDITY (%)	60	58	55	61	69	54	61
90° - 2 m/s							
AMB. TEMP. (°C)	25	28	29	32	32	31.5	24
HUMIDITY (%)	52	51	50	49	48	48	52
90° - 4 m/s							
AMB. TEMP. (°C)	25	30.5	28	31	32	28	25
HUMIDITY (%)	52	40	50	49	42	49	52
90° - 6 m/s							
AMB. TEMP. (°C)	25	29	27	31	32	32	24
HUMIDITY (%)	52	48	50	49	48	49	52
15° - 6 m/s							
AMB. TEMP. (°C)	25	31	27.5	29.5	29.5	25	30.5
HUMIDITY (%)	52	48	50	50	52	52	47
30° - 6 m/s							
AMB. TEMP. (°C)	26	31	25.5	28.5	29	25	30.5
HUMIDITY (%)	52	48	51	50	52	51	48
45°- 6 m/s							
AMB. TEMP. (°C)	26.5	30	25.5	29	29.5	26	29.5
HUMIDITY (%)	51	51	51	50	52	54	50
60° - 6 m/s							
AMB. TEMP. (°C)	26.5	30	28	29	29.5	26.5	30
HUMIDITY (%)	51	50	50	50	52	54	49

Table C.6. Environmental Test conditions for Experiment Set B.

Wind Angle – Wind Speed	B0	B1	B2	B3	B4	B5	B6
90° – No Wind							
AMB. TEMP. (°C)	24.5	25	26	26	25	24	26
HUMIDITY (%)	58	59	60	59	58	58	60
90° - 2 m/sec							
AMB. TEMP. (°C)	28	27	25.5	24	26.5	28	29
HUMIDITY (%)	57	54	62	62	59	54	46
90° - 4 m/sec							
AMB. TEMP. (°C)	27.5	29	28.5	29.5	25	28	29
HUMIDITY (%)	57	56	52	54	62	50	46
90° - 6 m/sec							
AMB. TEMP. (°C)	26.5	29.5	28.5	29	25	28.5	29
HUMIDITY (%)	57	54	51	54	64	50	45
15° - 6 m/sec							
AMB. TEMP. (°C)	28	27	28.5	29	28.5	25	26
HUMIDITY (%)	44	50	47	48	48	54	52
30° - 6 m/sec							
AMB. TEMP. (°C)	28	26.5	28.5	29.5	28.5	25	26
HUMIDITY (%)	44	50	48	45	47	54	52
45° - 6 m/sec							
AMB. TEMP. (°C)	28	26	27.5	30	28	25	26.6
HUMIDITY (%)	44	51	48	44	47	54	50
60° - 6 m/sec							
AMB. TEMP. (°C)	28	25.5	27.5	30	27.5	24.5	26.5
HUMIDITY (%)	44	52	50	44	48	54	49

Table C.7. Environmental Test conditions for Experiment Set C.

Wind Angle – Wind Speed	C1	C2	C3	C4	C5
90° - No Wind					
AMB. TEMP. (°C)	22	22.5	22.5	26	22
HUMIDITY (%)	57	56	55	58	56
90° - 2 m/s					
AMB. TEMP. (°C)	27	23	27.5	31	24
HUMIDITY (%)	53	60	50	55	58
90° - 4 m/s					
AMB. TEMP. (°C)	27	23	26	29.5	24
HUMIDITY (%)	53	61	54	62	58
90° - 6 m/s					
AMB. TEMP. (°C)	26	23	25.5	30	24.5
HUMIDITY (%)	57	62	58	60	55
15° - 6 m/s					
AMB. TEMP. (°C)	26	23.5	28	31	24
HUMIDITY (%)	54	61	49	51	58
30° - 6 m/s					
AMB. TEMP. (°C)	27	24.5	28.5	30	25
HUMIDITY (%)	54	59	48	48	58
45° - 6 m/s					
AMB. TEMP. (°C)	27	25	29.5	33	25
HUMIDITY (%)	54	58	48	48	58
60° - 6 m/s					
AMB. TEMP. (°C)	27	25	30	33	25
HUMIDITY (%)	53	58	48	45	58

CURRICULUM VITAE

PERSONAL INFORMATION

Surname, Name	: Öztürel, Necil
Nationality	: Turkish (TC)
Date and Place of Birth	: 9 June 1959, Ankara
Marital Status	: Married
Phone	: +90 532 272 52 21
Fax	: +90 312 210 22 91
Email	: necil.ozturel@proteko.net

EDUCATION

Degree	Institution	Year of Graduation
MS	HU Physics Engineering	1985
BS	METU Physics	1982
High School	TED Ankara College	1977

WORK EXPERIENCE

Year	Place	Enrollment
1994- Present	PROTEKO	Managing Partner
1993-1994	IBM	AIX Operation Manager
1991-1993	ORACLE	Regional Manager
1989-1991	SIEMENS-NIXDORF	Regional Manager
1987-1989	Honeywell-Bull	Chief Project Manager
1982-1987	TUBITAK Building Research Institute	Researcher

FOREIGN LANGUAGES

Advanced English, Fluent French

PUBLICATIONS

1. Öztürel, N. (1985) *Binalarda Güneş Enerjisi, Kullanımı ve Türkiyedeki Önemi.* Türkiye İnşaat Mühendisliği 8. Teknik Kongresi.
2. Ecevit, A., Zilan, R. & Öztürel, N. (2001) *Türkiye'de Pasif Yöntemle Güneş Enerjisi Kullanılarak Konut Isıtma Potansiyeli Ön Çalışması (Passive Solar House Heating Potential in Turkey-Preliminary Study).* Ulusal Enerji Verimliliği Kongresi ve Enerji Verimliliği Sergisi, 20.Enerji Tasarruf Haftası, Enerji ve Tabii Kaynaklar Bakanlığı, 17-19 Ocak 2001, Ankara.
3. Öztürel, N, Zilan, R. & Ecevit, A. *Türkiye'de Yenilebilir Enerji Kaynakları İçin İzlenmesi Gereken Strateji, Planlama, Politikalar ve Bunların Sosyal ve Siyasi Etkileri (The Proposed Strategy of Renewable Energy Sources, Planning, Policies and Their Social and Political Effects in Turkey).* Yenilebilir Enerji Kaynakları Sempozyumu, TMMOB Izmir Şubesi,18-20 Ocak 2001, İzmir

HOBBIES

Volleyball, Historical Maps, Scooters